Doctoral Dissertations 1896 - February 2014

1-1-1986

Chemical, structural, and electrical characterization of poly(p-phenylene vinylene)/

David R. Gagnon
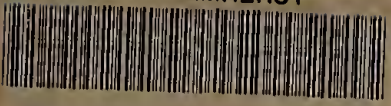*University of Massachusetts Amherst*

Recommended Citation

Gagnon, David R., "Chemical, structural, and electrical characterization of poly(p-phenylene vinylene)/" (1986). *Doctoral Dissertations 1896 - February 2014*. 708.
https://scholarworks.umass.edu/dissertations_1/708

Chemical, Structural, and Electrical
Characterization of Poly(p-Phenylene Vinylene)

A Dissertation Presented

by

DAVID R. GAGNON

Submitted to the Graduate School of the
University of Massachusetts in partial fulfillment
of the requirements for the degree of

DOCTOR OF PHILOSOPHY

September 1986

Polymer Science and Engineering

Chemical, Structural, and Electrical
Characterization of Poly(p-Phenylene Vinylene)

A Dissertation Presented
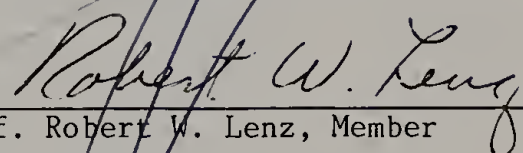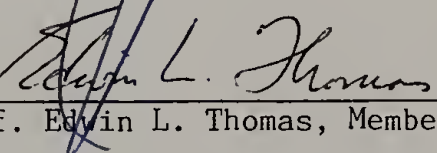
by

DAVID R. GAGNON

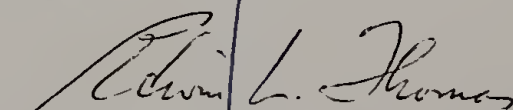Approved as to style and content by:

_____
Prof. Frank E. Karasz, Chairperson of Committee

_____
Prof. Robert W. Lenz, Member

_____
Prof. Edwin L. Thomas, Member

_____
Prof. Edwin L. Thomas, Head
Department of Polymer Science and Engineering

iii

DEDICATION

To my wonderful wife and friend, Brenda

and to our families.

ACKNOWLEDGEMENTS

other members of Dr. J. C. W. Chien's polyacetylene research group provided valuable experience. Other coworkers, integral to this research were: Dr. S. Antoun George, who synthesized most of the substituted polymers studied in the latter stages of this work; Dr. Thierry Granier, who performed the electron diffraction experiments and the unit cell calculations; Joe Machado, who also synthesized some of the PPV precursor polymer and whose collaboration led to many new ideas; and John Stenger-Smith who worked with me during the summer before officially joining our group.

In a project as interdisciplinary as this, I learned a great deal from discussions and collaborations with many of the other PSE students and post-docs too numerous to mention. The enthusiasm and atmosphere of fraternity of these colleagues made my work seem more like pleasure.

Funding for this work came primarily from the Air Force Office of Scientific Research, and was supplemented by a fellowship award from the Plastics Institute of America. Both of these sources are gratefully acknowledged.

I thank my parents, who taught me that nothing is out of reach with hard work and heart, and for always encouraging me to ask "why?". I also thank my wife's parents for their encouragement and support.

My most special thanks are reserved for my wife, Brenda, who made a herculean effort in typing this dissertation. There are no words to describe the strength and joy she has given me by her patience and understanding through the many nights I worked late, and by sharing in my successes and failures along the way. Her love and devotion has made this all worthwhile.

ABSTRACT

CHEMICAL, STRUCTURAL AND ELECTRICAL

CHARACTERIZATION OF POLY(P-PHENYLENE VINYLENE)

SEPTEMBER, 1986

DAVID R. GAGNON, B.A., SAINT ANSELM COLLEGE

M.S., UNIVERSITY OF MASSACHUSETTS, AMHERST

Ph.D., UNIVERSITY OF MASSACHUSETTS, AMHERST

Directed by: Professor Frank E. Karasz

Electrically conductive polymers, based upon highly conjugated
materials, have been the focus of an intensive research effort aimed
towards understanding the chemistry and physics of the conduction
process. One of the major impediments frustrating this study has been
the unprocessability of these morphologically heterogeneous conjugated
polymers. This dissertation work has utilized the preparation of
poly(p-phenylene vinylene), PPV, from a water soluble precursor
polymer, poly(p-xylene-α-dimethylsulfonium chloride) to obtain
homogeneous isotropic and oriented films. The objectives have been to
optimize the precursor synthesis, understand its conversion to PPV,
optimize the stretching process, characterize the molecular structure,
and study the conductivity of doped PPV as a function of the chemical
and molecular structure.

Synthetic optimization gave high molecular weight precursor
polymers which were cast into films prior to the thermal conversion to
PPV. This elimination reaction was characterized by elemental analysis
and TGA/MS which showed that quantitative conversion occurred above

TABLE OF CONTENTS

LIST OF TABLES

LIST OF FIGURES

CHAPTER I

INTRODUCTION

<u>Overview of Conducting Polymer Ideals and Realities</u>

Polymeric materials are generally characterized by their light weight, flexibility and highly insulative properties. Recently though, since the discovery of chemically modified polyacetylene,[1] a new class of polymers with high electrical conductivity has been the object of intensive investigation from both the scientific and technological perspectives. Evidence of the intensity of interest is the large number of review articles and books on this relatively new subject.[2-10] If perfected, conducting polymers could have a significant advantage over metals due to their preparation from relatively inexpensive and available feed stocks and their light weight.

Conducting polymers can be classified into two basic types; saturated backbone polymers with pendant groups which can form charge-transfer complexes by the reaction with suitable reagents, and conjugated backbone polymers which can be either oxidized or reduced with suitable reagents to create the charge carriers responsible for electrical conduction.

The term "dopant" is in common use in the conducting polymer literature and will be used throughout this text when referring to the oxidizing or reducing agent used to create charged species in

conducting polymers. This usage is not technically correct since the "dopant" remains in the polymer as an additional component, whereas the term was originally used to describe the substitutional replacement of atoms within crystalline semiconductor lattices such as silicone type semiconductors.

An example of the pendant class of conducting polymers is poly(2-vinylpyridine) reacted with iodine which forms the pyridinium iodide complex.[11] This complex can then undergo an electronic exchange reaction with neighboring uncomplexed pyridine units to provide the charge carrier. This is analogous to the mechanism of charge transport in low molecular weight charge transfer salts of tetrathiofulvalene and tetracyanoquinodimethane.[12] Other examples of charge transfer type conducting polymers are shown in Figure 1.1.

The focus of this dissertation is poly(p-phenylene vinylene), PPV, which is a member of the conjugated conducting polymer class. The reaction of conjugated polymers with an oxidant results in a delocalized positive charge residing on the polymer backbone and is commonly called p-doping. Conversely, reaction with a reducing agent results in a delocalized negative charge and is called n-doping.

Conjugated polymers can be further subdivided into those, like polyacetylene, with resonance structures that have equivalent energies (degenerate ground states) and those, like PPV and other aromatic conjugated polymers, that have resonance structures which are nonequivalent in energy (non-degenerate ground states). The primary difference between these two types is that both resonance structures of polyacetylene can coexist on a single chain supporting a neutral

3

Figure 1.1.   Examples of some polymeric charge-transfer type

conducting polymers.

METALLOMACROCYCLES (MMC)
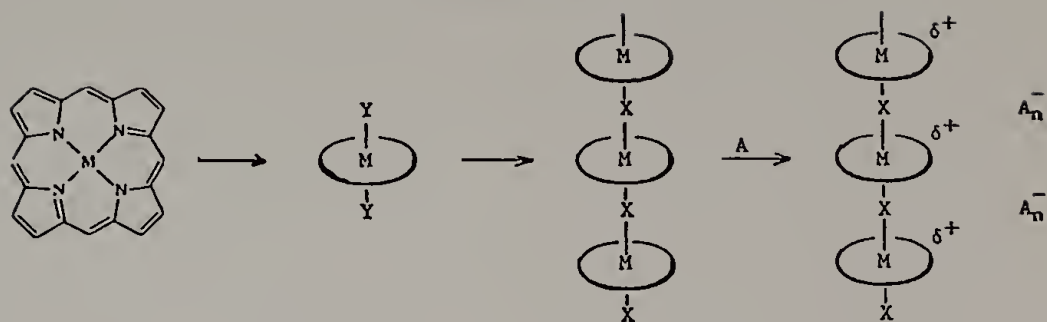
PENDANT COMPLEXATION

Poly(2-vinylpyridine)   (PVP)
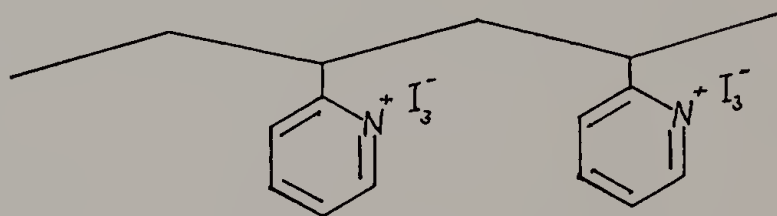
Poly(N-vinylcarbazole)   (PN-VC)
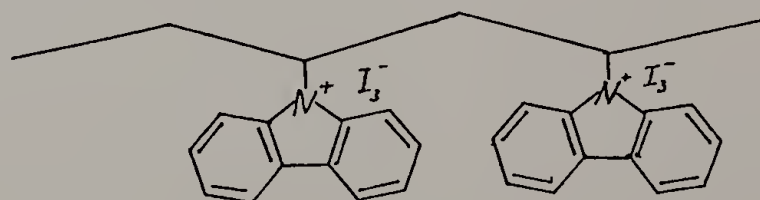
radical called a soliton at the boundary between them which may
contribute to the observed electrical properties.[9] In non-degenerate type conjugated polymers, neutral radicals are not supported under normal conditions, and thus are not important to the electrical properties. The doping process actually creates charged radicals called polarons. However, as the concentration of the charged radicals increases, the radicals combine to form a doubly charged carrier called a bipolaron.[10] Examples of some common conjugated conducting polymers, their resonance structures, along with the method of their synthesis and their resulting physical form are shown in Figure 1.2.

One of the major debates in the field of conducting polymers is the mechanism by which the delocalized charges propagate through the polymer matrix under an applied electric potential. The most simple answer is that the charge propagates along the conjugated chain through delocalization. However, it is obvious that an individual polymer chain does not extend over the macroscopic dimensions of the samples whose conductivities are measured, and that inevitably there will be chemical and conformational defects which will interrupt conjugation. Thus, a certain contribution from the interchain hopping of charge carriers must be invoked to explain the high macroscopic conductivities measured. The question is: to what relative extent do the intrachain and interchain transport mechanisms contribute to the overall conductivity?

To answer this question and to enable utilization of conducting polymers in devices such as batteries, solar cells, sensors, and semiconductors requires a detailed understanding of the chemistry of

Figure 1.2. Examples of some conjugated polymers showing their resonance structures, including the method of synthesis and the resulting physical form.

SYNTHESIS & FORM

Poly (acetylene)   vapor/film

(PA)
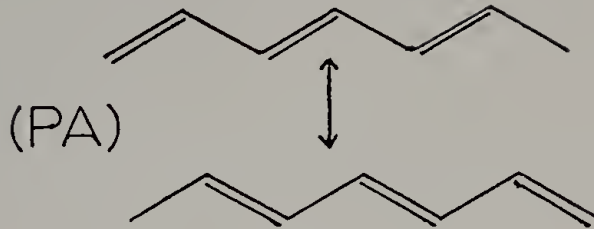
Poly (p-phenylene)   sol'n/powder

(PPP)
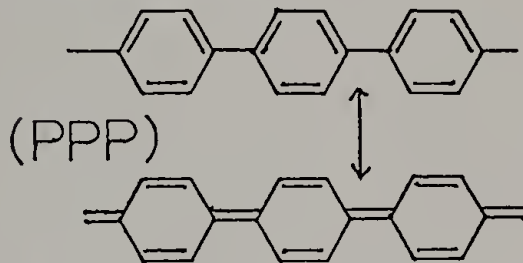
Poly (pyrrole)   e-chem/film

(PPy)
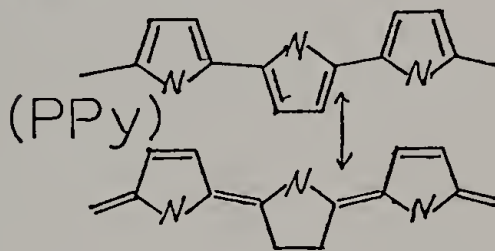
Poly (p-phenylene vinylene)   sol'n/powder
                                          precursor/film

(PPV)
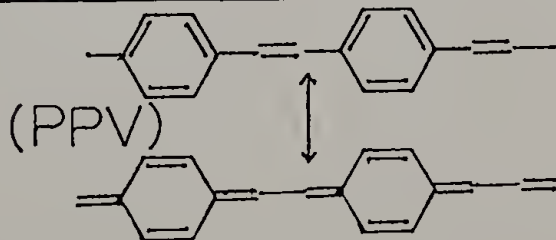
the parent polymer, the doping reaction, and the morphological and crystalline structure of the undoped and doped polymer. In terms of these studies, the ideal conducting polymer system would have a known, simple homogeneous chemical and morphological structure which could be perturbed chemically and morphologically in order to understand the conductivity structure-property relationships. Also, a simple molecular structure would facilitate molecular orbital calculations of the expected electronic energy levels of the system. Practical criteria to aid applications of these materials would include material strength and flexibility, easy and inexpensive synthesis and processing, and long term environmental stability. High electrical conductivity would only be important in applications which require large currents, but most envisioned applications would not require conductivities higher than that presently found with common semiconductors.

The realities of the microstructure and properties of known conducting polymers are the reason for the continued debate about the conduction mechanism and about other questions. The debate stems from the fact that there are a number of serious problems with the conducting polymers known to date. The most severe limitation from the applications standpoint is that the highly reactive nature of these chemically modified polymers gives them quite poor stability to the atmosphere. Another limitation is that since polymers, such as polyacetylene and PPV, depend upon a highly conjugated and rigid backbone for their reactivity and conduction properties, they are insoluble, infusible, and intractable and thus cannot be processed

into any form or shape other than that initially synthesized. Compounding this situation is that in order to solve the stability problem, the chemical and physical structure of the material must be fully understood; but this understanding is thwarted by the unprocessibility and the highly complicated morphology of conjugated conducting polymers as they have classically been prepared.

Objectives

This dissertation research explored an approach for the synthesis and processing of the highly conjugated conducting polymer PPV, which was synthesized from a water soluble, high molecular weight precursor polymer. This route enabled the preparation of both densely packed amorphous and highly molecularly oriented films of PPV, and allowed the study of conductivity as a function of systematic morphological variation for the first time. The synthetic versatility offered by this system also permitted the study of various PPV derivatives and analogs. The objectives of this research and the experimental techniques to be used were as follows:

1) Optimize the synthesis of the precursor polymer in order to obtain consistently high molecular weight, which is necessary for cast film integrity and subsequent uniaxial orientation.

2) Study the elimination reaction of the precursor

polymer using thermogravimetry, mass spectroscopy,

ultraviolet/visible and infrared spectrophotometry,

differential scanning calorimetry and elemental

analysis in order to determine the best conditions

for performing the orientation of the precursor

films and for completing the elimination to give

PPV quantitatively.

3) React the PPV films with various dopants and measure

the resulting conductivity using the usual four-probe

technique to learn about the reactivity of PPV

and to determine the best dopant for further studies

of structure/conductivity relationships.

4) Measure the conductivity of doped PPV as a

function of elimination degree (i.e., this is

roughly proportional to conjugation length) to

determine the effect of conjugation length on

conductivity.

5) Examine the morphology and crystallographic structure

of PPV films as a function of orientation using

polarized infrared spectrophotometry, and x-ray

and electron diffraction.

6) Measure the conductivity of doped oriented PPV

as a function of the draw ratio, measuring both

parallel and perpendicular to the draw direction

in order to probe the charge transport mechanism.

7) Prepare and dope various analogs of PPV, including
PPV with substituents on the phenyl ring and PPV
analogs with a different aromatic unit such as
1,4- or 2,6- naphthalene units.

Dissertation Organization

The above objectives form the basis for the organization of this
dissertation. Chapter II presents a review of the basic concepts and
literature pertinent to conducting polymers with an emphasis on
pointing out the importance of being able to rationally control
conducting polymer morphology. Chapter III includes a description of
the synthetic and experimental methods. Chapter IV concentrates on the
chemistry of the PPV precursor synthesis along with a detailed
discussion of a proposed polymerization mechanism, and of the
elimination mechanisms involved in the thermal conversion of the
precursor to PPV. Chapter V concerns the application of the
elimination variables to the stretching process of the precursor
polymer and presents the results of crystallographic and morphological
characterization of the oriented PPV films as a function of the draw
ratio. Chapter VI is a discussion of the chemistry of the doping
process and the resulting conductivity as a function of the degree of
conversion of the precursor to PPV, and of the degree of molecular
orientation of stretched PPV. Chapter VII is a compilaton of
preliminary results on the study of the chemistry and electrical

properties of various analogs of PPV and Chapter VIII summarizes the above results in the light of the initial objectives and then concludes with suggestions for the future work necessary to more fully understand the structure-property relationships in conducting polymers.

CHAPTER II

LITERATURE REVIEW

Conducting Polymer Concepts

Conductivity

Conductivity is calculated from the measured bulk resistance of a

sample. For a rectangular sample the conductivity, σ, is just

$\sigma = \frac{1}{R} (\frac{\ell}{w \times t})$; where R is the measured resistance, ℓ is the length

between the electrodes and (w x t) is the film's cross-sectional area.

On a molecular level conductivity is defined as $\sigma = nq\mu$; where n is the

number of carriers of charge q, and μ is the mobility of the carriers.

The units of conductivity are reported in $Ohm^{-1}cm^{-1}$ or more recently in

the identical units of Siemens per cm, $S\ cm^{-1}$. The chemistry of these

reactions (i.e., the polymer reactivity towards the dopant and the

subsequent charge stability) is determined primarily by the electronic

structure of the conjugated polymer. The mobility, on the other hand,

is affected both by the extent of electronic delocalization and by the

molecular structure and morphology. The magnitude of the

conductivities measured for the examples listed in Figures 1.1 and 1.2

are displayed along with the conductivities of other common materials

for reference in Figure 2.1. The lower bound on the conductivity

ranges in Figure 2.1 is that of the undoped polymer. Mid-range values

are obtained by partial doping. The shaded area in the bar graph of

the polyacetylene and PPV ranges reflect conductivity enhancement

Figure 2.1. Range of conductivities exhibited by the conducting

polymers shown in Figure 1.1 and 1.2 compared with

some common materials. (See text).

SILVER, COPPER
IRON
METALS — BISMUTH
10^6
10^4
10^2
In Sb
1
GERMANIUM
10^{-2}
SEMI-CONDUCTORS
10^{-4}
SILICON
10^{-6}
SILVER BROMIDE
10^{-8}
GLASS
10^{-10}
DNA
10^{-12}
INSULATORS
DIAMOND
10^{-14}
SULFUR
10^{-16}
QUARTZ
10^{-18}
$\Omega^{-1} cm^{-1}$

MMC   PVP   PN-VC   PA   PPP   PPy   PPV

10^6
10^4
10^2
1
10^{-2}
10^{-4}
10^{-6}
10^{-8}
10^{-10}
10^{-12}
10^{-14}
10^{-16}
10^{-18}
$\Omega^{-1} cm^{-1}$

= Increase in σ due to stretch
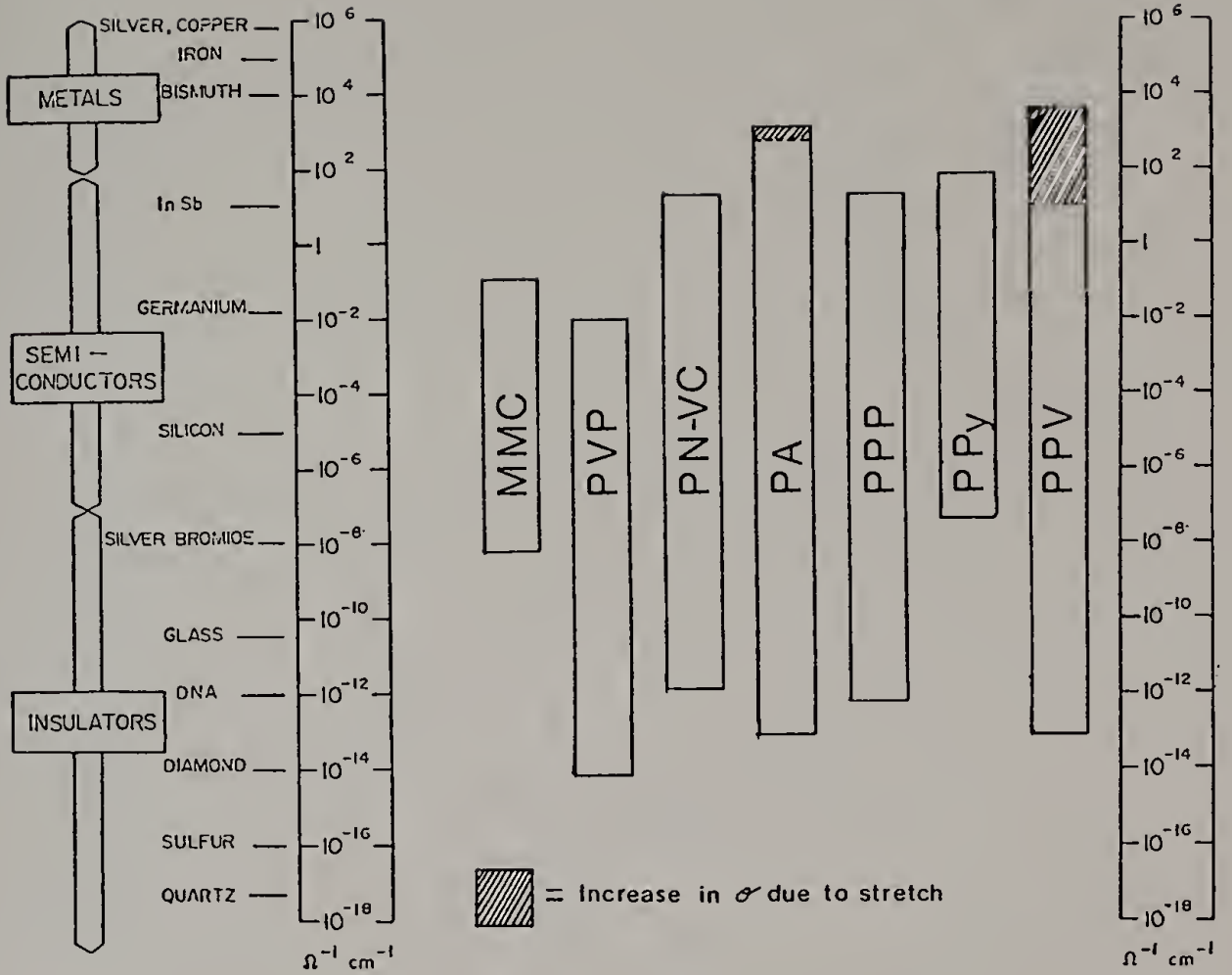
due to stretching of the undoped polymer prior to doping. This effect is of profound importance in conduction mechanism studies, and is one of the major topics of this dissertation.

Charge Transport

There are two schools of thought on how a charge moves through the molecules of a conducting polymer. One school proposes that the conjugation is only necessary to stabilize the charge created by the doping reaction, and that charge transport occurs only through hopping between alternating stacks of charged and neutral molecules.[13] This is in analogy to the charge transport mechanism in stacks of low-molecular weight organic charge transfer salts such as TTF-TCNQ complexes. In this model it is assumed that the charge is prevented from traveling along the polymer backbone due to the pinning effect of the dopant counter-ion and due to the high energy associated with the bond length change (lattice distortion) of the charged sequence relative to that of the neutral sequence.[14] Evidence for this theory comes from studies of the weak dependence of the conductivity on the degree of polymerization. Specifically cation-radical salts of ter-[15] and quater-phenyl are used as models for poly(p-phenylene)[16] in which the conductivity is relatively insensitive to the chain length. This theory also predicts that the conductivity should increase with crystallinity or pressure due to higher interchain interaction. To date, experiments on undoped poly(p-phenylene) give conflicting evidence; on the one hand increasing pressure does not measurably change the conductivity;[17] while on the other hand, increasing

crystallinity induced by annealing causes an increase in conductivity
by a factor of about 3.[18]   It is critical to note, however, that
these studies were performed on pressed pellets of powders, and not on
materials with long range order.

The second school proposes that charge transport does occur most
easily along the polymer backbone through charge delocalization and
that the role of the counterion is primarily only to provide overall
electrical neutrality.[19-21]   Of course it is recognized that
individual polymer chains do not extend from one end of a bulk sample
to the other, and that chemical and conformational defects in the
conjugated structure are present, preventing infinitely long conjugated
sequences. Therefore, some kind of interchain charge transport
mechanism must be invoked; but this interchain mechanism would be the
charge mobility limiting process rather than the only charge transport
mechanism (Figure 2.2). If this theory is valid, then there should be
a significant increase in conductivity measured parallel to the
orientation direction, $\sigma_{//}$, in materials with uniaxially oriented
conjugated chains, and a decrease in the conductivity measured
perpendicular to the orientation direction, $\sigma_{\perp}$, thus giving a high
conductivity anisotropy defined as: $\sigma_{//} / \sigma_{\perp} = \sigma^*$.

Conducting Polymer Morphologies

Probably the best example of the processing and morphological
limitations of conducting polymers is polyacetylene, PA, as prepared by
the standard Shirakawa technique.[22,23]   The chemical structure of PA
is deceivingly simple, but the synthesis results in polyacetylene

Figure 2.2. Model for charge carrier transport, showing paths
of conduction for parallel conductivity, $\sigma_{/\!/}$, and
perpendicular conductivity, $\sigma_{\perp}$.

chain end or sp³ carbon · carrier · conjugated chain · dopant · $\sigma_{//}$ · $\sigma_\perp$
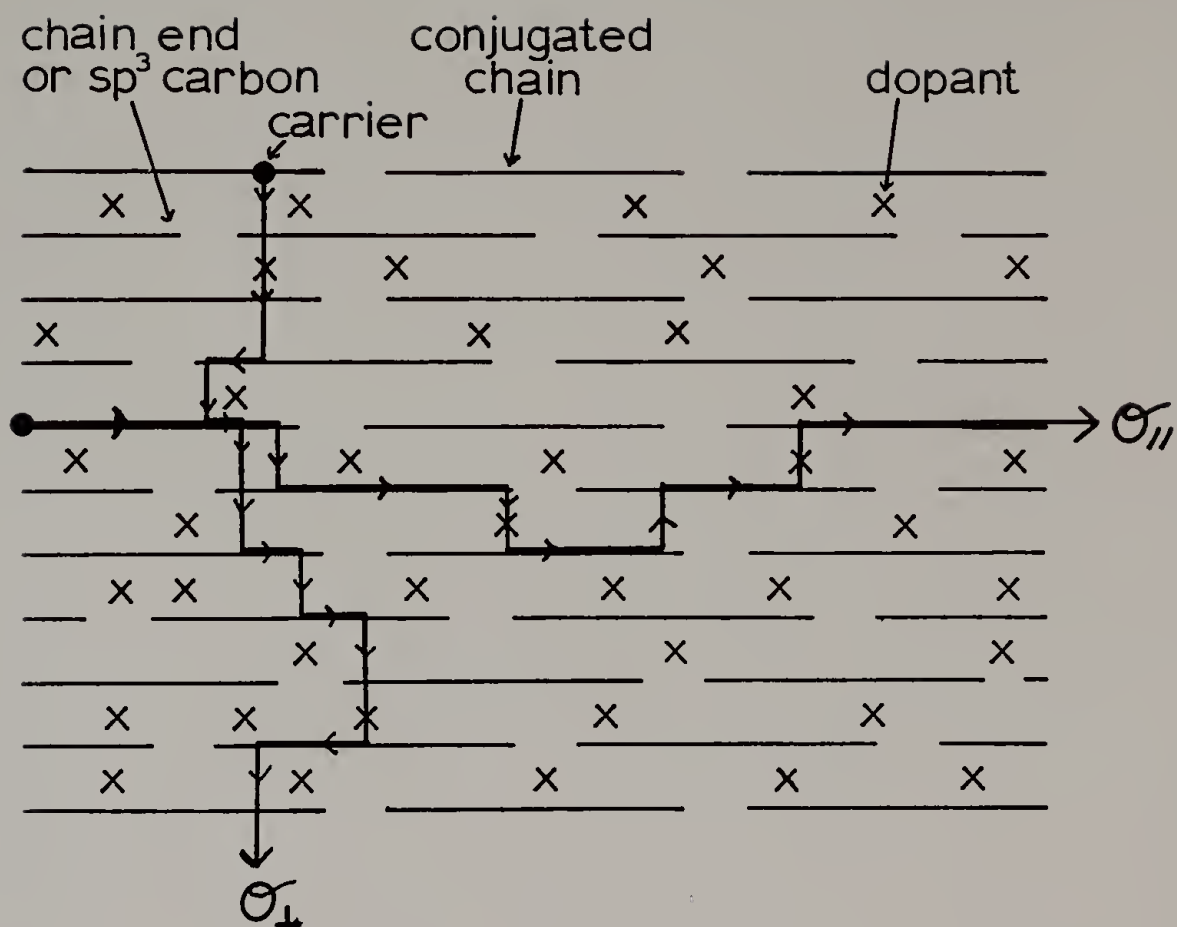
films which are comprised of a loose complex network of randomly
oriented semicrystalline fibrils approximately 200 Å in diameter,[24]
(Figure 2.3). Within the fibril, the polymer chains are preferentially
aligned in the fibril direction, but the molecular structure at the
fibril/fibril junctions is considerably more complicated and unknown.
Since conductivity measurements can only be made with these films on a
macroscopic scale, an interpretation of the conduction mechanism at the
molecular level is ambiguous at best.

Other conducting polymers are generally synthesized directly either
by solution or electrochemical techniques. Direct solution
polymerization of poly(p-phenylene),[25,26] poly(p-phenylene
vinylene),[27,28] and other conjugated polymers leads only to powders
of a low degree of polymerization due to the insolubility of these
stiff conjugated polymer chains. Hence, conductivity measurements must
be made on pellets of the compressed powder. The added resistance of
powder grain/grain boundaries are necessarily included in the
conductivity measurement and lead to a similar interpretive ambiguity
as with the fibril/fibril junctions in PA.

Electrochemical polymerization of poly(pyrrole) and poly(thiophene)
films directly onto an electrode surface has the advantage of
simultaneously doping to high conductivity as the polymerization
proceeds, but again there is a significant grainy or fibrillar nature
to the resulting films, especially with thick films.[29,30] In all of
the above procedures, the resulting polymer cannot be processed. Thus
no variation of microstructure, which is necessary for understanding
and optimizing electronic charge transport,[31] can be performed.

Figure 2.3. Transmission electron micrograph of Shirakawa

polyacetylene film.

←200nm→
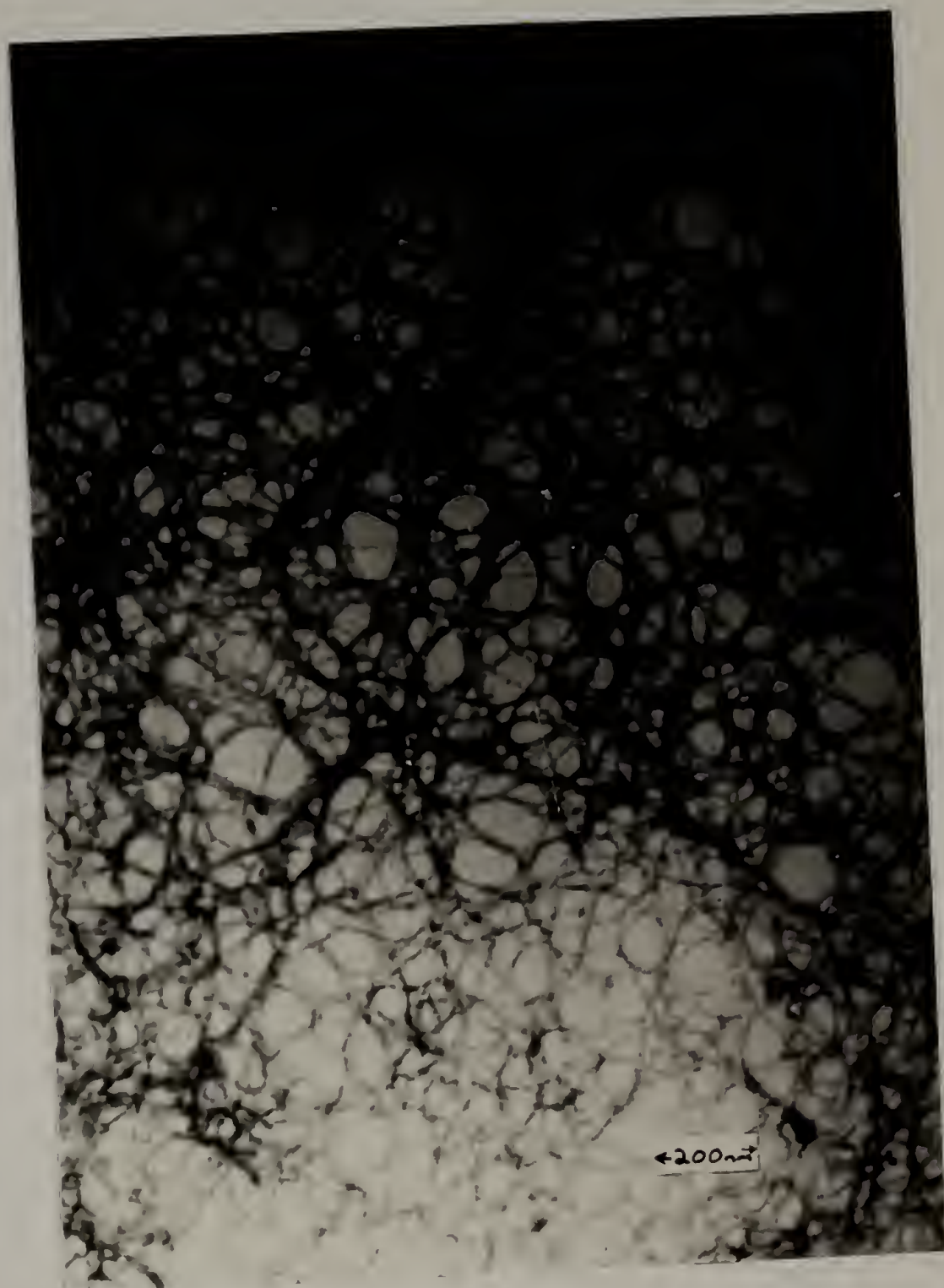
Orientation of Polyacetylene

Stretching of Shirakawa Polyacetylene

The first attempts to orient polyacetylene came shortly after the discovery in 1977 that it could be doped to high conductivity.[19] Initial studies employed uniaxial elongation of Shirakawa polyacetylene to draw ratios of up to three times the initial length.[19,31,32] It must be emphasized that these experiments only caused the alignment of the fibrils of the nascent PA network, and the molecular orientation within the fibrils was virtually unchanged. Only moderate electrical anisotropies were recorded: $\sigma_{/\!/}/\sigma_{\perp} \simeq 16$, however there was a significant increase in the absolute parallel conductivity from a value of 250 S/cm to approximately 2500 S/cm. One of the problems with the results of these experiments, was that densification of these porous films was not taken into account in conductivity calculations and that the morphology still consisted of a fibrillar network. Qualitatively though, the quasi-one dimensionality of conduction in doped conjugated polymers was demonstrated.

Shear Flow Polymerization of Polyacetylene

A novel shear flow technique for preparing oriented PA was used by Meyer in 1981.[33,34] His procedure employed the usual Shirakawa chemistry, but instead of polymerizing in a quiescent system, the acetylene gas was bubbled into a vessel containing the catalyst solution in a 3mm space between a rotating teflon drum (4000rpm) and a cylindrical glass stator. The result was a highly oriented, fibrous

film of PA deposited on the glass stator which displayed a large

optical anisotropy. Transmission electron microscopy showed a lamellar

type structure within the fibrils (i.e., alternating crystalline and

amorphous regions); this probably accounted for the rather weak

electrical anisotropy of the SbF_5 doped samples: $\sigma_{//}/\sigma_{\perp} \simeq 6.$[35]

Chien et al. used another type of shear flow technique by growing PA

whiskers onto a catalyst coated teflon stir bar spinning at

approximately 800 rpm.[25] Electron diffraction confirmed the high

orientation, but electrical measurements were not reported due to the

extremely small size of the whiskers.

Epitaxial Polymerization of Polyacetylene

Still another route to synthesize oriented Shirakawa PA was devised

by Woerner et al.[37,38] and by Ozaki et al.[39,40] These groups

performed the polymerization of acetylene gas onto a catalyst treated

surface of crystalline biphenyl or benzene. As the PA formed, it

crystallized epitaxially onto the substrate thus creating oriented PA

regions of areal dimensions ranging from approximately $0.25 - 16\ mm^2$

with a thickness ranging from 400-3000 Å thick. The PA orientation

decreased with increasing distance in the thickness direction from the

substrate. Selected area electron diffraction and polarized optical

microscopy demonstrated the high molecular orientation especially for

thin films. Only the benzene substrate produced oriented PA areas

large enough for electrical characterization, and low anisotropies on

the order of $\sigma_{//}/\sigma_{\perp} \simeq 3.2$ were measured for 400 Å thick samples.[39]

Precursor Route to Polyacetylene

Edwards and Feast, in 1980, were the first to utilize a precursor route to obtain a doped conducting polymer.[41] In their procedure (Figure 2.4), a high molecular weight[42] precursor (soluble in common organic solvents) to polyacetylene was synthesized by the metathesis of 7,8-bis(trifluoromethyl)tricyclo[4,2,2,0^{2,5}]deca-3,7,9-triene, I, which was cast, and then converted to polyacetylene by the thermal elimination of 1,2-bis(trifluoromethyl)benzene, IV. This was a significant breakthrough in polyacetylene chemistry simply because it gave the first non-fibrillar, fully dense films of PA. Initial attempts to dope the films with vaporous iodine were unsuccessful due to slow iodine diffusion into the dense films, however doping with a dilute iodine solution gave a conductivity comparable to Shirakawa PA of approximately 200 S/cm.[43] Since Edwards' and Feast's discovery, a number of groups have begun to study this material from the standpoints of the thermal elimination reaction[44-46] and the optical and electrical properties.[47,48]

In 1984 White and Bott reported that while preparing electron microscopy samples, via casting of the precursor directly onto the microscope grids before thermally eliminating the precursor to PA, the film which was between grid bars became highly oriented due to the volume decrease associated with the loss of the 1,2-bis(trifluoro-methyl)benzene.[49] Shortly after this report, Leising published the preparation of macroscopic fibers of oriented PA made by removing the solvent from the precursor solution contained in a capillary fitted with a needle to initiate fiber growth.[50] It was from these

41
Figure 2.4. Precursor synthesis route to polyacetylene.

I

$\xrightarrow{\text{WCl}_6 : \text{Ph}_4\text{Sn}}$

II

Δ

III

$+$

IV
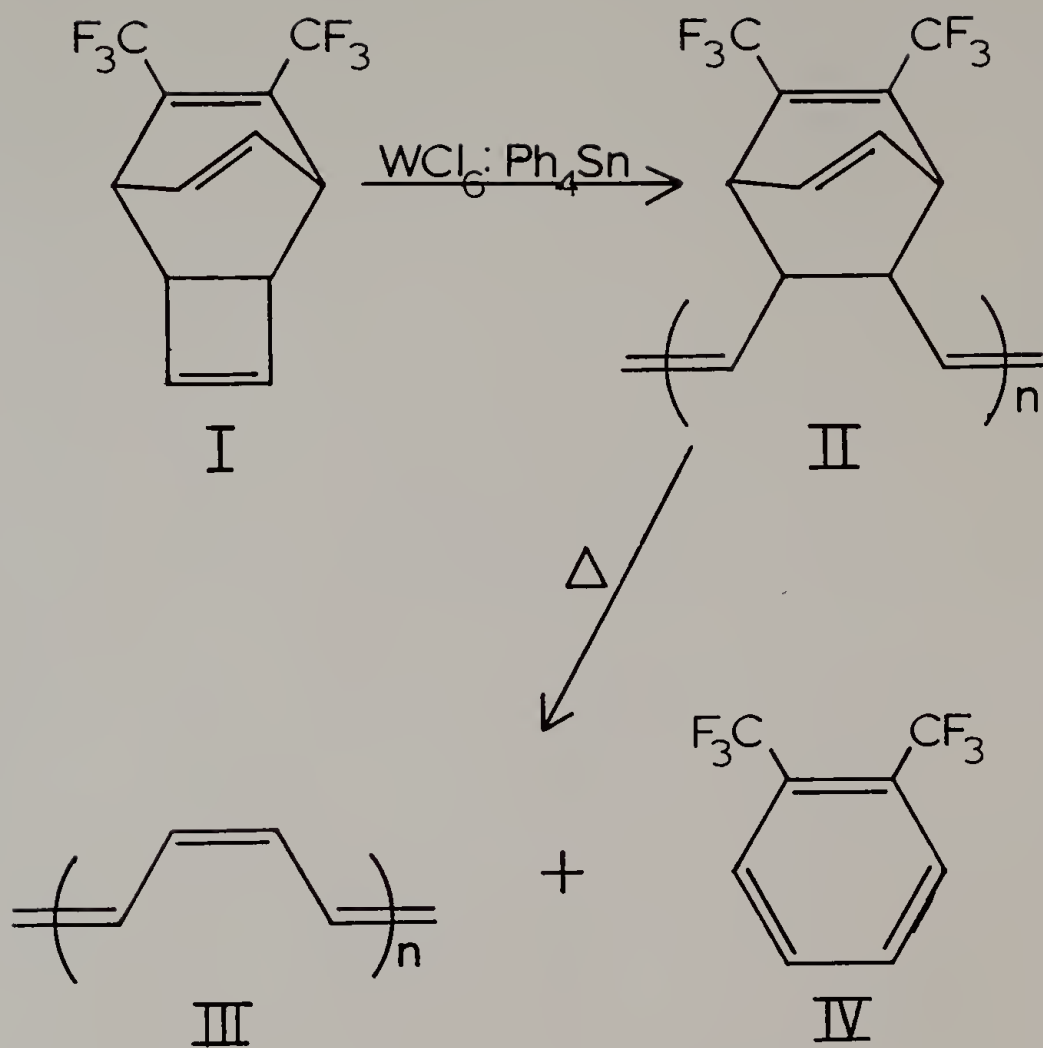
experiments that Leising recognized that during the elimination of the

volatile product of the precursor, the films became plastic and could

be stretched to give dense packed films with a high degree of molecular

order.[51]   Bott et al. also discovered that a concentrated precursor

solution kept at room temperature for 24 hours would form a gel which

could be stretched, dried and thermally converted to oriented PA.[52]

The orientation protocol of Leising was the most useful one for

preparing polyacetylene samples that could be studied in terms of their

anisotropic optical and electrical properties. Although these workers

were apparently unaware of Wessling's earlier work on the precursor

route to PPV,[52] Leising's procedure utilized the same concept. These

oriented PA films were highly crystalline and were characterized by

x-ray diffraction measurements as having a monoclinic unit cell with

the c-axis parallel to the stretching direction and the a and b axes of

the crystallites oriented randomly about the c-axis. Polarized

infrared absorbance measurements clearly demonstrated the molecular

nature of the orientation and gave a refractive index ratio $n_{/\!/}/n_{\perp}$ of

about 5. Polarized uv/vis absorption spectra also showed that

the $\pi \rightarrow \pi^*$ transition (band gap) measured parallel to the stretch

direction was at an energy about 0.3eV lower than that measured

perpendicular to the stretch direction, thus the electronic

delocalization had one dimensional character.[54]

Electrical conductivity measurements were also highly anisotropic.

Undoped oriented PA showed an anisotropy $\sigma_{/\!/}/\sigma_{\perp}$ of about 100, but

contrary to intuition, initial measurements of the temperature

dependence of conductivity indicated that the activation energy of

parallel conduction (approximately 0.26eV) was higher than that for

perpendicular conduction (approximately 0.17eV). Iodine doped,

oriented PA, $(CHI_{0.09})_x$ also showed an anisotropy of approximately 100,

but in this case the apparent activation energies were virtually

equal. Although no reason was presented to explain this data,

apparently the delocalized charges on the chains contribute to the

decrease of intrachain and activation energy.

Poly(p-Phenylene Vinylene)

PPV Oligomers

The Wittig[27] and dehydrohalogenation[28] syntheses of PPV shown

in Figure 2.5 yielded only powders with degrees of polymerization less

than about 11. Even with this limitation, the versatility of these

reactions for preparing many derivatives of oligo-PPV (i.e., with

substituents on either the phenyl group or the vinyl group) has led to

a considerable amount of research on the spectral and electrical

properties of pressed pellets of undoped and doped PPV.[55]

In the undoped state, PPV and its derivatives fall within the

$\sigma < 10^{-9}$ S/cm range. However, Wnek et al. demonstrated that reaction

of pressed PPV powders with the strong electron acceptor, arsenic

pentafluoride, AsF_5, resulted in an increase of 13 orders of magnitude

in conductivity to approximately 3 S/cm.[56] Various analogs of PPV

(i.e., with extended vinylene units or with methoxy substitution on the

phenyl ring) could also be doped, but not to as high a conductivity as

PPV itself.[57-59] In the case of the 2,5-dimethoxy-PPV, the side

Figure 2.5. Wittig[21] and dehydrohalogenation[28] synthetic methods for obtaining oligomeric powders of PPV.

WITTIG SYNTHESIS

$$Ph_3\overset{+}{P}-CH_2-\!\!\langle\bigcirc\rangle\!\!-CH_2-\overset{+}{P}Ph_3 \quad + \quad OHC-\!\!\langle\bigcirc\rangle\!\!-CHO$$
$$Cl^- \qquad\qquad\qquad Cl^-$$

$$\Big\downarrow \text{LiOEt / EtOH}$$

$$OHC-\!\Big(\!\langle\bigcirc\rangle\!-C\!=\!C\Big)_x\!\langle\bigcirc\rangle\!-CHO$$
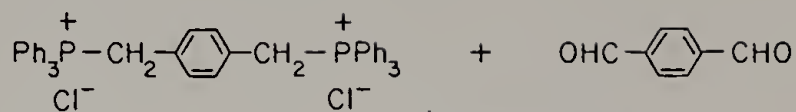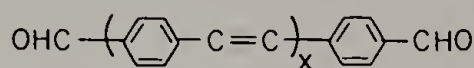
$$\text{Reflux} \Big\downarrow \text{I}_2/\text{Toluene}$$

$$\text{TRANS PPV OLIGOMER } \quad DP \cong 4\rightarrow9$$

DEHYDROHALOGENATION SYNTHESIS

$$ClCH_2-\!\langle\bigcirc\rangle\!-CH_2Cl \xrightarrow[\text{DMF}]{\text{NaH}} H_3C-\Big(\!\langle\bigcirc\rangle\!-C\!=\!C\Big)_x\Big(\!\langle\bigcirc\rangle\!-\overset{Cl}{\underset{}{C}H}-CH_2\Big)_Y\!\langle\bigcirc\rangle\!-CH_2Cl$$

$$\xrightarrow[\text{3hrs}]{300°C} CH_3-\Big(\!\langle\bigcirc\rangle\!-C\!=\!C\Big)_x\!\langle\bigcirc\rangle\!-CH_2Cl \qquad DP \cong 11$$
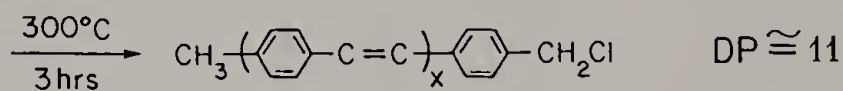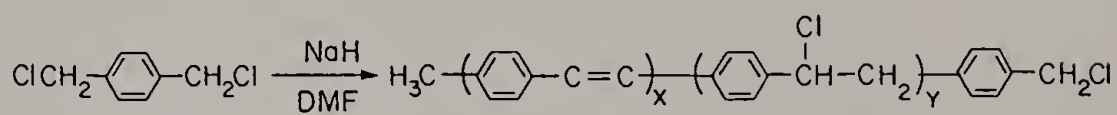
reaction of the AsF_5 dopant with the oxygen of the methoxy substituent was invoked to explain the inability to obtain a conductivity higher than 10^{-4} S/cm. It was expected that this polymer would have at least as high a conductivity as PPV, due to the cation stabilizing effect of the electron donating methoxy group.[60] There may be another explanation of the low conductivity which is based upon the fact that bulky side groups such as the methoxy group may impair molecular packing, thus interchain charge transport could be hindered. However, with these pressed powders, a detailed structural analysis is impossible, and so the separation of the effects of backbone electronic structure and molecular packing structure could not be performed. The separation of electronic and morphological variables would be critical for the unambiguous interpretation of the conductivity as a function of dopant concentration and of temperature.

Precursor Route To PPV

The precursor route to PPV was first reported by Wessling and Zimmerman, in a patent by the Dow Chemical Company in 1968,[53] and by Kanbe also in 1986.[61] The synthesis, outlined in Figure 2.6, began with the conversion of α,α'-dichloro-p-xylene (V) to the bis-sulfonium salt monomer, p-phenylenedimethylene-bis(dimethylsulfonium chloride), VI, using an eight time excess of dimethylsulfide followed by precipitation in 0°C acetone and vacuum drying of the white crystalline powder, (yield > 95%). The polymerization was carried out by rapidly mixing equal volumes of deoxygenated 0.5 M aqueous solutions of monomer and base at < 0°C. (It should be noted that Wessling's patent

Figure 2.6. Sulfonium precursor route for obtaining high molecular
weight films of PPV.[62]
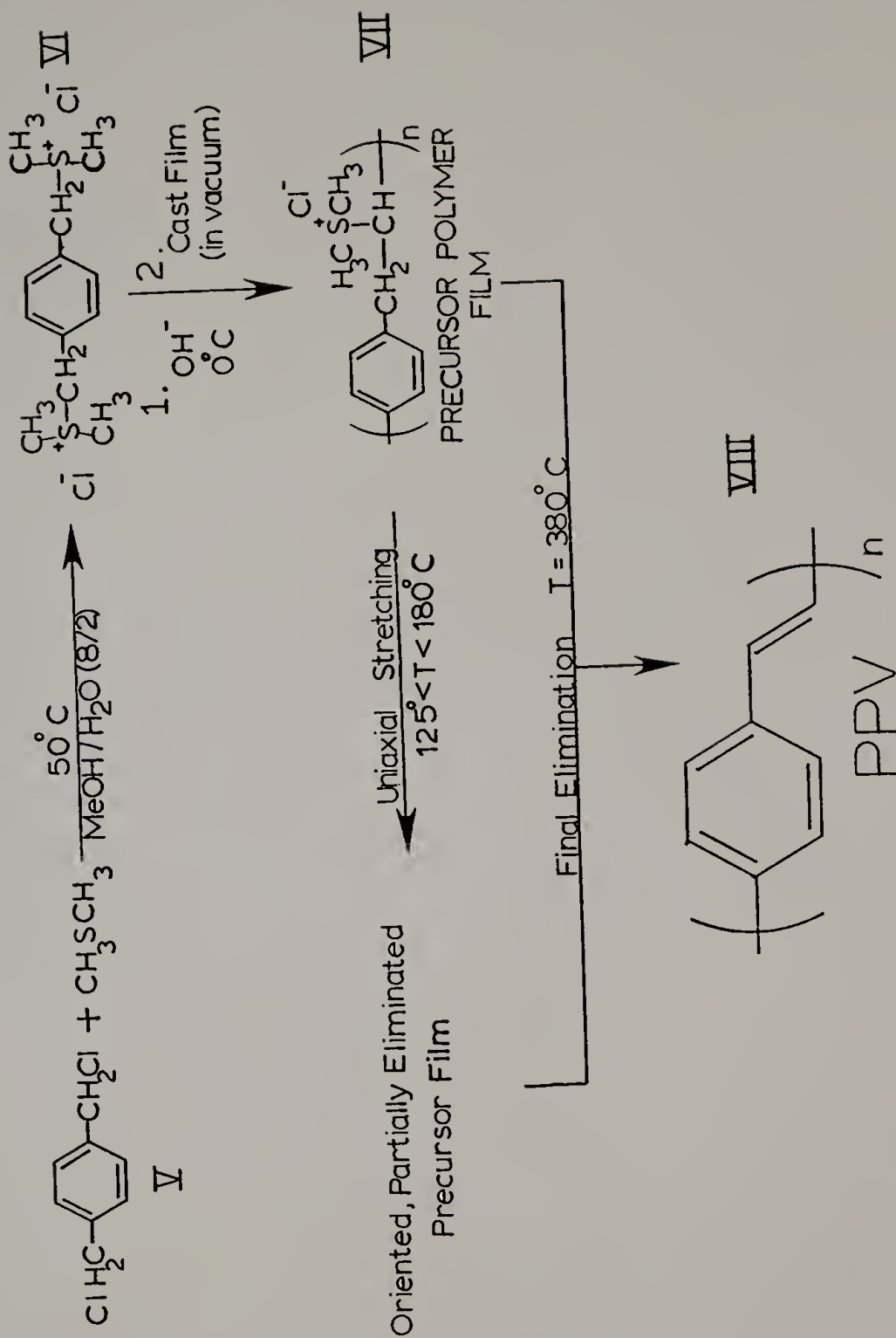
FIGURE 1: Synthesis and Processing of PPV

specifies equinormal solutions of base and monomer, however results in

our laboratory have shown that this high base concentration induced the

premature elimination of the sulfonium pendant group of the precursor

polymer giving only a yellow insoluble and infusible powder of PPV

which was essentially useless for further processing).[62]   This

precursor polymer solution was then neutralized to a pH ≃ 6.5 with

dilute HCl followed by dialysis against deionized water to remove the

low molecular weight salts and unreacted monomer. The dialyzed

solution could then be vacuum cast to form clear, strong, freestanding

films of the precursor polymer (VII), poly(p-xylene-α-dimethyl-

sulfonium chloride). Finally, the precursor film was heated to

approximately 380°C in vacuum or inert atmosphere to eliminate Me_2S and

HCl to form dense packed, amorphous films of PPV (VIII).

The distinct advantage of this precursor route for performing

structure/property studies of conducting PPV is that during the thermal

elimination reaction, the diffusing volatiles act as a plasticizer and

enable stretching of the films to up to 15 times their initial

length.[62]   Such highly stretched films display a pronounced molecular

orientation as determined from polarized infrared absorbance, optical

anisotropy and x-ray diffraction. Furthermore, after reaction with

dopants, the oriented films display a significant electrical

anisotropy; that is, the conductivity is increased in the stretch

direction with increasing draw ratio ($\lambda = \frac{\ell}{\ell_o}$) and is decreased

slightly perpendicular to the stretch direction.[64]   Thus, the

precursor route to PPV has now made it possible to investigate the

microstructure of unoriented and oriented PPV films without the

ambiguity inherent in studies of powdered or fibrillar samples, and to relate these findings to the electronic properties.

The synthetic versatility of the sulfonium precursor route to PPV also makes it relatively easy to prepare various analogs of PPV. These analogs include a range of groups substituted on the phenyl ring of the PPV backbone, and the replacement of the phenyl ring with other aromatic moieties. Figure 2.7 shows some of the PPV analogs which have been prepared by this route.

Figure 2.7. Analogs of PPV prepared by the sulfonium precursor
route.

$R = OCH_3, OC_2H_3, CH_3, Br$
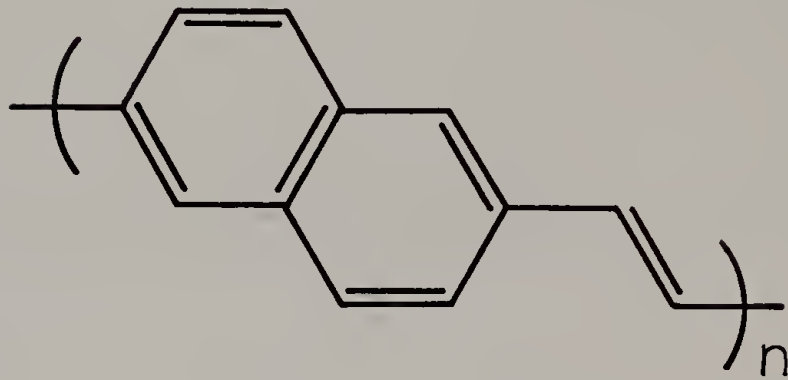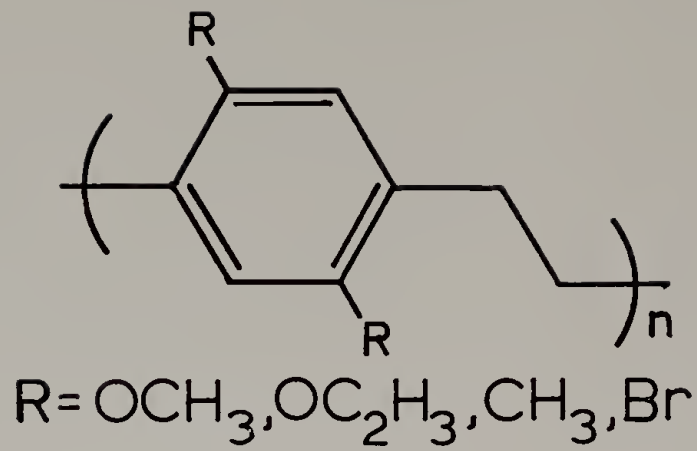
Poly (2,6-Naphthalene Vinylene)
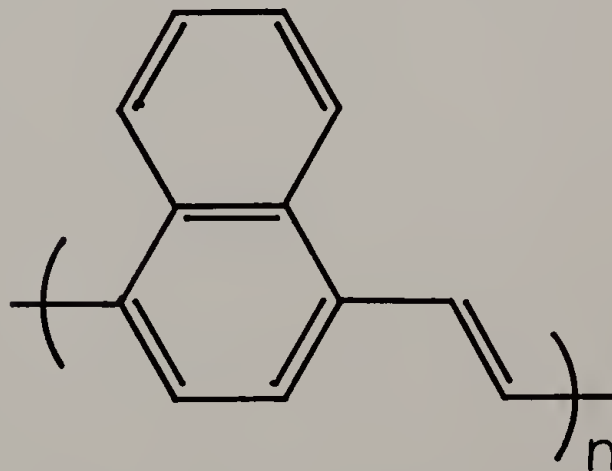
Poly (1,4-Naphthalene Vinylene)

CHAPTER III

EXPERIMENTAL METHODS

The discussion of the synthetic techniques and the experimental equipment and methods in this chapter is organized according to the chronology of the preparation of the final doped polymer. That is, the chapter begins with the synthesis of the monomer and the precursor polymer utilizing an optimized version of Wessling's method, followed by a discussion of the processing protocol used to obtain oriented PPV films and the methods of structural characterization. The chapter concludes with a description of the conductivity measuring apparatus including the vacuum line techniques required to handle the highly reactive dopants, with particular attention being paid to the detailing of the necessary precautions.

Synthesis

Typical Bis(Sulfonium) Monomer Synthesis

8.9 grams (0.051 mole) of α,α'-dichloro-p-xylene (Aldrich Chemical Co.) was added to a 250 ml three neck round bottom flask fitted with a nitrogen purge, an oil bubbler output, and a water cooled condenser. 48.0 ml of methanol and 10 ml of water were added as the solvent (the water was found to help the reaction go to completion by increasing the solubility of the sulfonium salt product). 11.2 ml (9.5 grams) of dimethyl sulfide(0.153 moles) (98%, Aldrich Chemical Co.) was then

added to the flask along with a magnetic stir bar and the system was flushed with nitrogen for 20 minutes. (NOTE: To obtain high yields, it was important to use at least a 50% excess of dimethyl sulfide. Also, although dimethyl sulfide is not considered hazardous, an efficient hood should be used for this reaction due to its strong, offensive odor.) The round bottomed flask was then partially immersed in an oil bath mounted above a stirring hotplate equipped with a temperature controller set to 50°C. After the initial 20 minute nitrogen flush, the heat was turned on and the reaction system was kept at 50°C overnight.

The p-xylene-bis(dimethylsulfonium chloride) monomer was isolated by concentration of the reaction mixture with a "Roto-vap" apparatus in the hood which removed the solvent and excess dimethyl sulfide leaving an oily concentrate. A minimum amount of methanol (< 8 ml) was added to break-up the oil prior to dropwise precipitation into 1 liter of 0°C acetone stirred with a magnetic stir-bar contained in a 2 liter beaker in an ice bath. The precipitate (light green in color) collected on the walls of the beaker after about 30 minutes of stirring. The acetone was decanted as much as possible and the monomer which was still dispersed in the acetone, was collected by vacuum filtration. Most of the monomer was collected in a vial by scraping it off of the beaker wall. The wet monomer was placed into a vacuum desiccator (with the vial covers off) and pumped on for ca. 3 days until the monomer powder became loose and fluffy (i.e., no clumps remained). At this point, the color had changed from light green to a pure snow white powder which was extremely hydroscopic. This powder had a melting

range of 150-152°C, whereas if it was not dried sufficiently it would

decompose without melting at ∿ 110°C. Typically, yields of > 90% were

obtained and seemed to be limited primarily by the care taken during

the concentration, precipitation and separation steps. Scale-up of

this reaction, by about 4 times the amounts above, has been

accomplished a number of times without difficulty. The main difficulty

with scale-up is the large amount of acetone needed for precipitation,

therefore precipitation was done in batches.

Precursor Polymer Synthesis

The sulfonium precursor polymer was synthesized by rapidly mixing

equal volumes of equimolar aqueous monomer and base solutions as

follows. 17.28 grams (0.06 moles) of the bis(sulfonium) monomer was

dissolved in 150 ml deionized water in a 500 ml 3-neck flask, which

included a stir-bar, resulting in a 0.4 M solution. In a separate

vessel, 2.4 grams NaOH was dissolved in 150 ml deionized water

(0.4 M). This base solution was cooled to -10°C in a rock salt/ice

bath and then added to a 200 ml addition funnel which was stoppered

with a septum and fitted to the center neck of the 3-neck flask, which

was then immersed in the ice bath. This apparatus assembly is shown in

Figure 3.1. To remove dissolved oxygen, prepurified nitrogen was

bubbled through both solutions for 15 minutes. This time gave the

monomer solution time to cool to about -5°C without too much warming of

the base solution. An oil bubbler was fitted to the third neck as a

nitrogen outlet.

Figure 3.1. Apparatus assembly for sulfonium precursor synthesis.

N₂

Bubbler

Base Solution

Monomer Solution 0° C
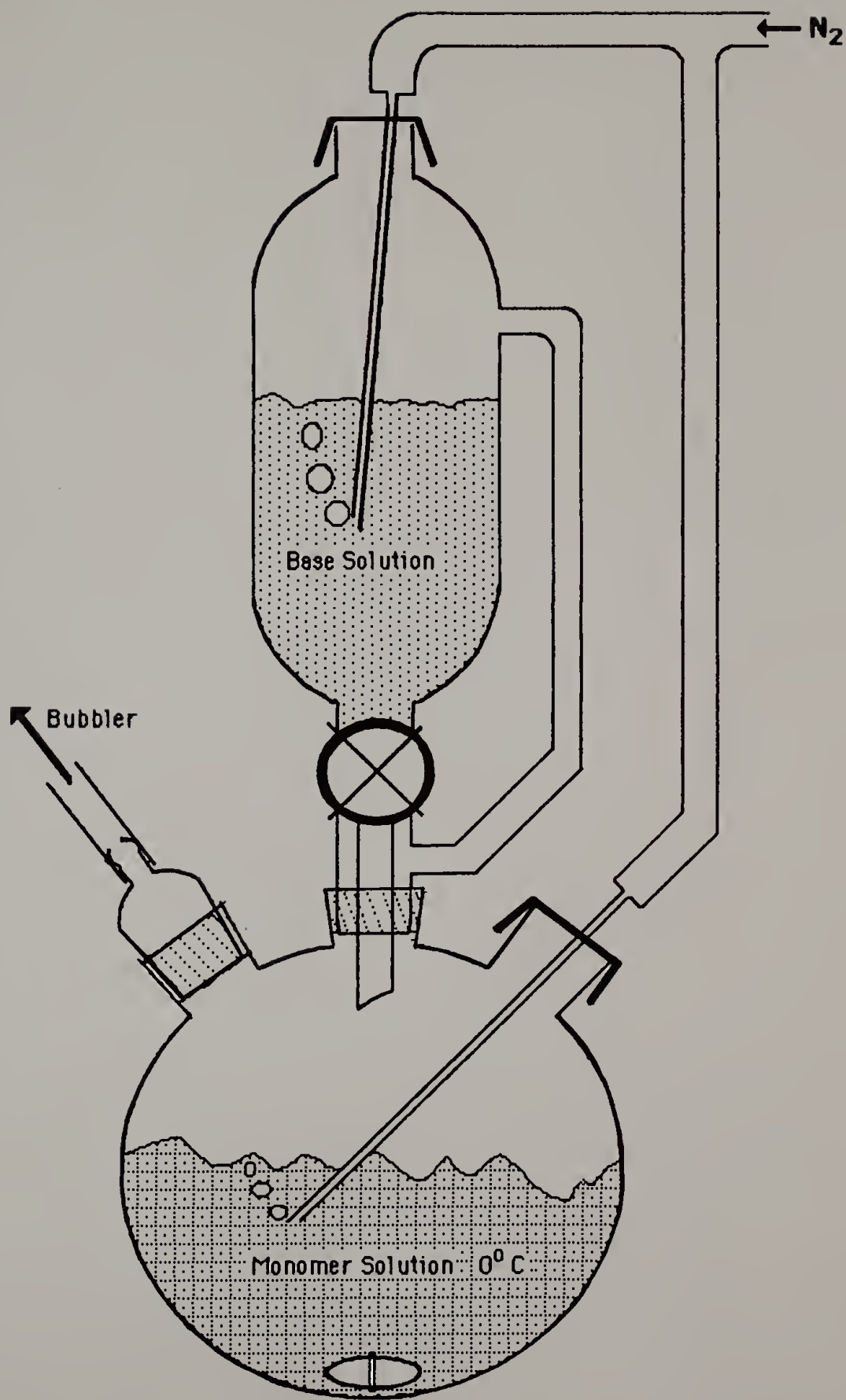
Once the system had been cooled and purged, the base solution was added to the monomer solution as quickly as possible with vigorous stirring. This mixing gave final reagent concentrations of 0.2 M. The viscosity of the solution increased rapidly over the first 10 minutes and stirring became more difficult. The polymerization was allowed to proceed for about 40 minutes. One indication of a successful reaction was the ability for the solution to visibly fluoresce when a hand held broad band UV source was used to illuminate it. Presumably the fluorescence was due to a small concentration of unsaturated PPV units formed by the base induced elimination of the precursor polymer.

The reaction was stopped by neutralizing the unreacted base with dilute HCl to a pH of 6.5. The neutralization was done quite slowly (over 30-60 minutes) due to the slow kinetics observed in these viscous solutions.

Final purification of the aqueous sulfonium precursor polyelectrolyte was accomplished by dialyzing against deionized water for about 3 days using Spectra/Por 3 cellulose membrane tubing with a reported molecular weight cut off of ca. 3500 daltons. Dialysis removed low molecular weight impurities including residual monomer, sulfonium elimination products, and the neutralization product, NaCl. The end point of dialysis was determined by the reversal in the osmotic pressure (i.e., when the volume of the polyelectrolyte solution in the dialysis tube began to increase). The yield of precursor polymer was about 20-25%.

This procedure was quite easy to perform as long as the following precautions were taken. 1) It was critical to begin with very dry, fresh monomer and to weigh it out immediately after removal from the vacuum desiccator, because with time the sulfonium monomer would degrade back to the starting materials. If the monomer was wet, the apparent weight of monomer would be higher than the actual, thus the final base to monomer stoichiometry would have an excess of base. Excess base caused unwanted premature formation of PPV units in the precursor polymer, thus turning the solution yellow and severely decreasing the precursor polymer solubility. 2) This polymerization could be scaled up successfully only if adequate stirring could be maintained. 3) If the final concentration of reactants was higher than about 0.3 M, the solution would be too viscous to stir and a gel rapidly formed. The resulting solution inhomogeneity means that partial volumes of the solution, high in base concentration, would prematurely eliminate resulting in a virtually insoluble gel. 4) If oxygen was not completely removed initially from the monomer and base solutions (i.e., by inadequate flushing), the polymer would be of low molecular weight and could not be cast into strong coherent films.

<div align="center">

Precursor Polymer Processing

</div>

Casting

Glass casting dishes were fashioned by fusing 2 inch long sections of 2 to 6 inch diameter glass tubing to a circular piece of optically flat plate glass. It was necessary to pretreat the glass surface to

prevent the cast film from sticking. The procedure employed was adapted from similar procedures used to prevent protein adsorption to glass. The dish was soaked for at least 1 hour in a 2.0 M NaOH base bath followed by rinsing with 1 N HCl and deionized water to leave Si-OH groups on the glass surface. After drying in a 110°C oven and cooling, a small amount ($\sim$ 5 ml) dichlorodimethylsilane, Cl_2Me_2Si, was poured into the dish and swirled to coat the glass, and the excess was disposed of by evaporation in the hood. (CAUTION: Dichlorodimethyl-silane reacts instantly with atmospheric moisture to release HCl gas, therefore this treatment must be done in the hood and thick rubber gloves must be worn.) Especially on humid days, the dichlordimethyl-silane also reacts with atmospheric moisture which leaves an oily residue in the dish. This oil could be removed by rinsing the dish consecutively with THF, acetone and distilled water. This treatment results in a methylated surface of low surface energy from which the vacuum cast precursor polymer films could easily be removed.

The thickness of the films could be controlled by the initial amount of solution added to the casting dish which was then placed in a vacuum desiccator. A large volume liquid nitrogen vacuum trap was used to collect the evaporated water. In order to obtain films of even thickness, the final stage of casting was carried out using a cartesian diver at a vacuum of $\sim$ 1 torr, rather than using the full $< 10^{-2}$ torr produced by the vacuum pump. The cast films were colorless to light green depending upon the amount of time the film was kept under vacuum after removal of the water solvent. Typically, films of 10-20 μm were desired for further stretching, elimination, and doping processes.

Film Stretching

Film samples to be uniaxially drawn were cut from the cast films into pieces measuring about 1.3 cm x 5 cm. An indelible fine-point felt pen was used to place marks 3 mm apart along the film length for draw ratio measurement. Although the films are strong to tensile stress, they tear easily, so it was important to cut the pieces cleanly so as not to provide any sites for tear initiation. The films could only be stretched during thermal elimination, when the volatile elimination products diffuse through the film to plasticize it. Thus, if the film was too thick (i.e., > 15 μm thick) voids would form in the film because the volatiles were being produced faster than they could diffuse out of the film. Conversely, if the films were less than 5 μm thick they lacked the strength to be drawn effectively.

A zone heating apparatus, shown in Figure 3.2, was constructed by wrapping two glass slides, separated by 2 mm Teflon$^{®}$ spacers, with resistive "Ni-Chrome" heating wire to form a heat zone about 2.5 cm long and 3 cm wide. The wire was affixed to the ends of the slides using Sauereisen #29 low expansion refractory cement. Power was supplied to the heater wire using a Variac, and the temperature was monitored by placing a thermocouple near the sample at the center of the heat zone.

The film was placed in the heat zone at room temperature before turning on the Variac power, which was set empirically so that the temperature increased quickly until a temperature of about 90°C and then increased slowly to about 160°C. When the temperature reached about 110°C the film softened and could be stretched by hand to the

Figure 3.2. Zone heating apparatus for stretching precursor films.

Variac

150° C

Digital Thermometer

Ni-Chrome Wire

Precursor Film

Neck

Zone Heater
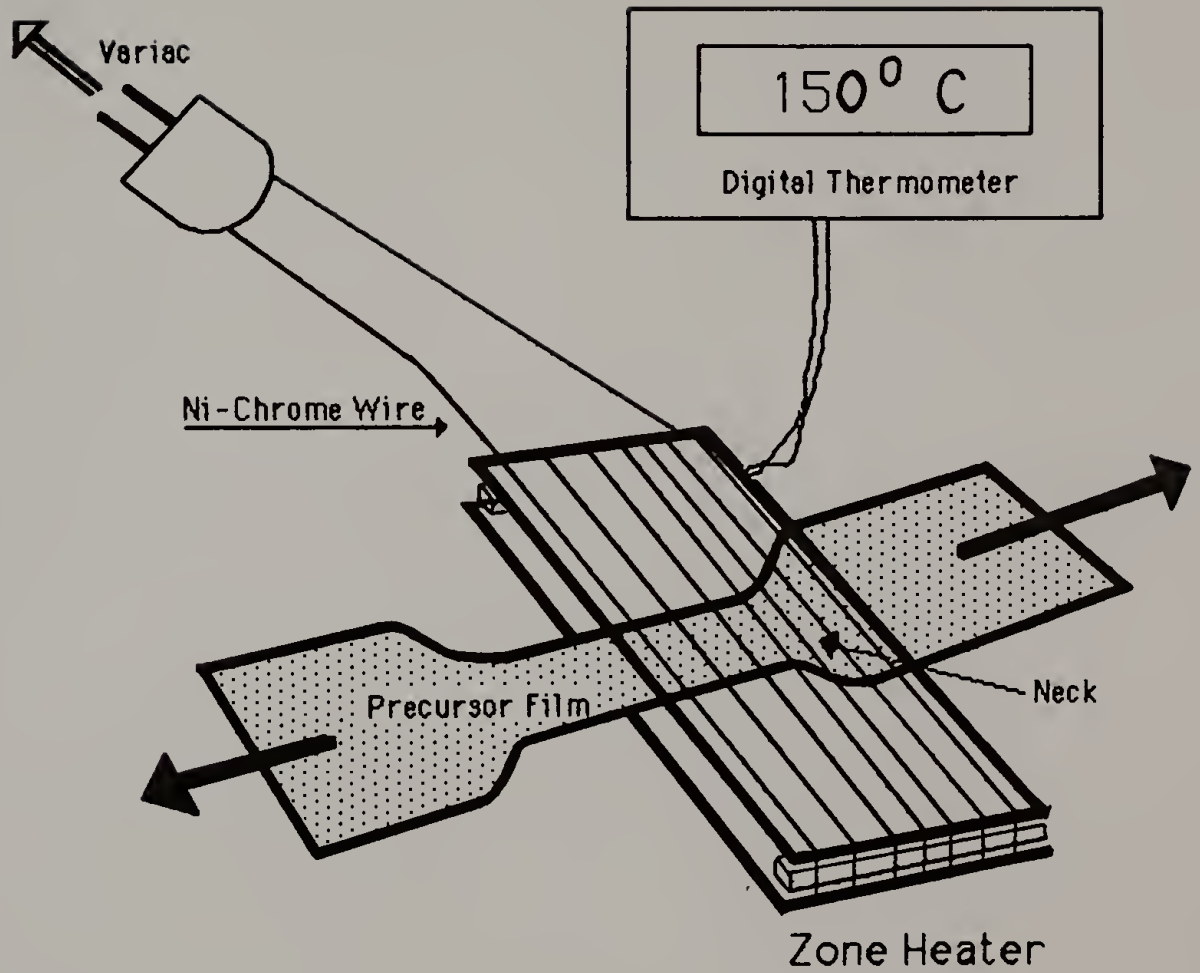
desired draw ratio. The neck which formed with stretching was kept in the heat zone during the stretching. When the neck had propagated to the end of the film, the film was repositioned to place the other half of the neck in the heat zone and that end of the film was stretched. The film was then moved back and forth through the heat zone until the approximate desired draw ratio was attained uniformly. The distance between the ink spots was measured and the draw ratio, λ, was calculated by dividing the final spot spacing by the initial spacing (i.e, $\lambda = \dfrac{\ell}{\ell_o}$).

Thermal Elimination of Precursor Films

Apparatus

Once the precursor film had been processed into the desired form (i.e., as an isotropic cast film, or as an oriented film) it was converted to PPV by the thermal elimination of the sulfonium moiety in vacuum. The elimination apparatus was constructed by wrapping the outside of a 2.5 cm ID x 12.5 cm long pyrex tube (sealed at one end and fitted with a #25 o-ring flange at the other) with resistive "Ni-Chrome" wire and affixed with Sauereisen #29 low-expansion refractory cement. Power was supplied with a Variac and the temperatue was controlled with an Omega model #4001K digital temperature controller. In order to prevent the films from curling during the heating, they were sandwiched between two pieces of Teflon® separated by a Teflon® spacer and then the sandwich was inserted into the tube. The tube was attached to a vacuum line via a cap made of a #25 o-ring

flange and a ball joint compatible with the vacuum line opening. An 0-3 Teflon® stopcock was also provided in the cap to maintain the vacuum after elimination was complete. The vacuum line was used with the forepump only (i.e. the diffusion pump was bypassed). After pumping on the sample for at least 1 hour to remove oxygen, the heater was turned on and the elimination was performed at 365°C for 4 hours to effect complete conversion to PPV, or was performed at lower temperatures to effect partial elimination.

Characterization

Initial characterization of the effectiveness of the thermal conversion process of the precursor film to PPV was performed using elemental analysis (University of Massachusetts Microanalytical Laboratory). The most sensitive measure of conversion was the residual sulfur content. For complete elimination, no sulfur was detectable (< 0.1 wt %). No other direct analytical method was found to be sensitive to high degrees of conversion. For example, infrared spectroscopy (Perkin Elmer IR-283) was not sensitive to the detection of sulfur-carbon bonds, and the ultraviolet visible absorption spectrum (Beckman DV-7) was insensitive to the increase in conjugation length induced by elimination beyond a conjugation length of about 6 [65] units.

Indirect characterization of the elimination process was performed by thermogravimetric analysis, TGA, (Perkin Elmer TGS-2) and differential scanning calorimetry, DSC, (Perkin Elmer DSC-2). With these techniques it was only possible to learn at which temperatures

the thermal reactions occurred. More detailed information about the chemical nature of the eliminated components was obtained using thermogravimetry coupled with mass spectral, MS, analysis. These analyses were performed using a TGA made from a Cahn microbalance with the vaporous elimination products being characterized by a Granville Research Finnigan 200 Quadrapole MS by Dr. E. Grant Jones at Systems Research Laboratories, Inc. of Dayton, Ohio. A 3 mg sample was mounted in the balance and the entire system was evacuated to $\sim 10^{-6}$ torr. When the vacuum had stabilized, the temperature was increased at a rate of 3°C/min over a temperature range of 25°C to 600°C.

Structural Characterization of Oriented PPV

Crystallographic structure, molecular orientation, and the crystallite size perpendicular to the draw direction, were determined using x-ray diffraction, electron diffraction, and polarized infrared dichroism.

d-Spacings

X-ray diffraction. Initial semiquantitative molecular structure characterization was accomplished by flat film Statton x-ray diffraction using nickel filtered CuK_{α} radiation ($\lambda = 1.5418$ Å). A schematic of the Statton configuration and the measured distances discussed below are shown in Figure 3.3. Calibration of the sample to film distance was done by dusting the sample with NaF, NaCl, or Al_2O_3 standards whose crystallographic d-spacings are well known. The

66

Figure 3.3. Schematic of the Statton flat film x-ray diffraction

camera. See text for explanation of labelled distances

shown.
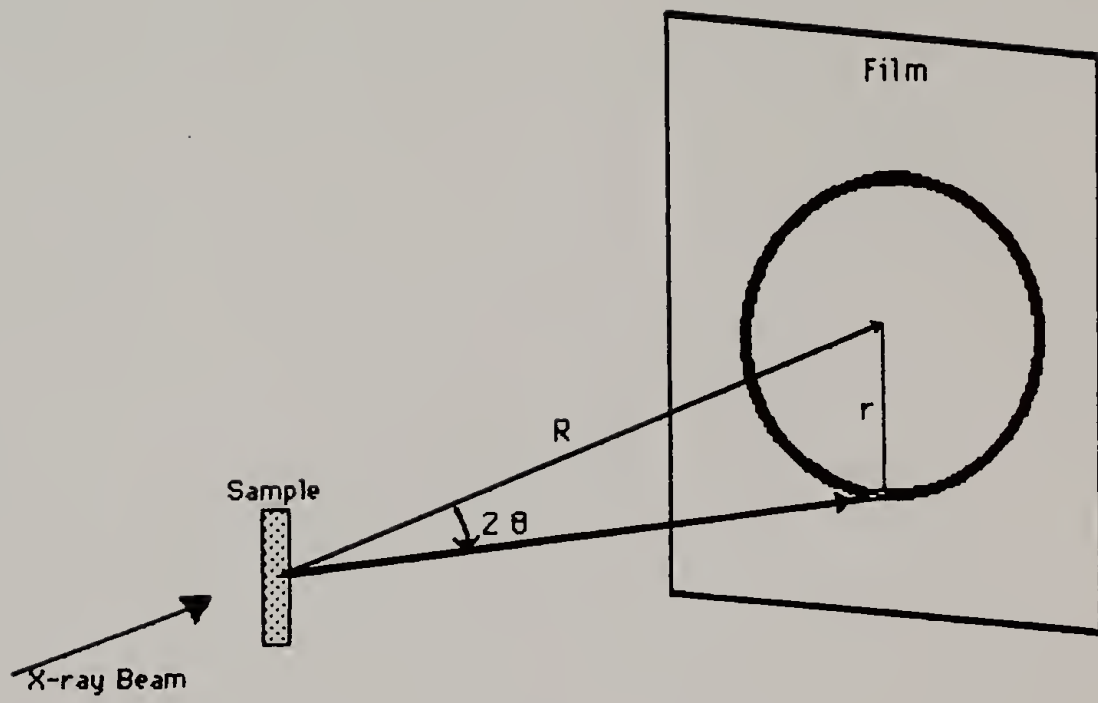
specimen to film distance, R, was calculated from the measured radial
distance of the standard's reflection ring on the film, r, and the
known d-spacing, d, using Bragg's Law:

$$n\lambda = 2 \, d \, \sin\theta \qquad (3.1)$$

$$\text{where } \tan(2\theta) = \frac{r}{R} \, . \qquad (3.2)$$

Once R was known then the measured r's from the PPV reflections were
used to calculate the d-spacings for PPV. A comparator on a light
table was used to measure r to an accuracy of $\pm$ 0.5 mm giving
d-spacings to $\pm$ 0.2 Å.

More accurate measurements were made using a Siemen's D-500 x-ray
diffractometer again using nickel filtered CuK_α radiation with a
0.15 mm receiving slit width. Results were given in terms of
diffracted intensity as a function of the Bragg angle, θ, from which
the d-spacing could be calculated directly from Bragg's Law.

Electron diffraction. The x-ray diffraction analysis of the
d-spacings was severely limited by the low intensity of the reflections
due to thin (< 10 μm) samples. Electron diffraction, ED, which
requires samples < 1000 Å thick, did not suffer from this problem.
Thus, ED was found to be the most useful to analyze the PPV reflections
for the calculation of a crystallographic unit cell of highly oriented
PPV specimens. These experiments were performed by Dr. Thierry Granier
with a JEOL 100-CX Scanning Transmission Electron Microscope. Thin
specimens were prepared by mechanical fibrillation of a highly oriented
PPV film having a draw ratio of 14.8. Diffraction patterns were made
using an incident beam voltage of 100 KeV and were recorded on Kodak
S0163 film. The camera length, R, was calibrated using the reflections

from gold which was sputter coated to a thickness of $\sim$ 100 $\overset{o}{A}$ on the PPV

specimen prior to analysis. The value of the reflection spacing, r, on

the film was measured using an Optronics International Photoscan P1000

microdensitometer by Dr. Wade W. Adams and Mr. Joseph O'Brien at the

Air Force Wright Aeronautical Laboratory, Polymer Branch, Dayton, Ohio.

Molecular Orientation

X-ray diffraction. The degree of molecular orientation for draw

ratios varying from 1 to 8.3 was calculated from the measurement of the

diffracted intensity of the first equatorial reflection as a function

of the azimuthal angle from the equator using the Hermans orientation

function, f,

$$f_{x-ray} = \frac{1}{2}(3 <\cos^2\emptyset> -1) \tag{3.3}$$

with $<\cos^2\emptyset>$ approximated by $\cos^2<\emptyset>$, where $<\emptyset>$ was determined by

measuring the full azimuthal angular width at half the maximum

intensity (FWHM), after subtraction of background intensity. The FWHM

method was chosen because the relatively weak diffracted intensity from

the thin samples (< 10 μm) prevented the determination of the exact

line shape needed to perform the more rigorous calculation of

$<\cos^2\emptyset>$[67] by

$$<\cos^2\emptyset> = \frac{\int_{o}^{\pi/2} I(\emptyset) \cos^2\emptyset \sin\emptyset \, d\emptyset}{\int_{o}^{\pi/2} I(\emptyset) \sin\emptyset \, d\emptyset} \tag{3.4}$$

Infrared dichroism. The Hermans molecular orientation function can

also be calculated by measuring the dichroic ratio, D, of the

absorbance of infrared radiation polarized parallel and perpendicular to the draw direction using $D = A_{/\!/}/A_{\perp}$ and

$$f_{IR} = \frac{D-1}{D-2} \left(\frac{D_o+2}{D_o-1}\right) \qquad (3.5)$$

where $D_o = 2 \cot^2 \alpha$, and α is the angle that the bond vibration transition moment makes with the chosen frame of reference.[68] In this case, the vinyl C–H out of plane bending mode at 963 cm^{-1} was chosen because its vibrational transition moment should be nearly perpendicular to the chain axis direction, and because the transition is not overlapped with neighboring transitions. Thus, if the frame of reference is also chosen to be perpendicular to the chain orientation direction, then α should be close to zero and

$$f_{IR} \simeq (D-1)/(D+2). \qquad (3.6)$$

Thus f_{IR} provides a measure of the orientation of the C–H bending transition moment perpendicular to the stretch direction and should be a good approximation of the chain axis orientation with the stretch direction.

To perform the dichroism measurements an IBM IR-30S Fourier transform infrared spectrophotometer was fitted with a Perkin-Elmer model #0186-0240 gold wire grid polarizer on a AgBr crystal which was placed between the source and the sample in a rotable mount. To reduce the effect of instrumental vertical polarization of the IR beam, the PPV sample was mounted with its stretch direction at 45° to the vertical, and the polarizer directions used were -45° to vertical (90° to the sample stretch direction) and 45° to vertical (0° to the sample stretch direction).

Crystallite Size

The crystallite size transverse to the orientation direction was calculated by a Scherrer analysis of the diffraction width, β, of the first non-overlapped, equatorial reflection using D-500 diffractometer scans of intensity versus Bragg angle, θ.[67] Again the angular FWHM method was used to estimate the peak breadth, $\Delta\theta$, which was converted to radian units to give the experimental diffraction width, β_{exp}. To correct for instrumental broadening, the β_{std} of a standard, hexamethylenetetramine, which is known to have large crystallite sizes was measured.[69] A corrected β was calculated assuming a Gaussian line shape from $\beta_{corr} = (\beta_{exp}^2 - \beta_{std}^2)^{\frac{1}{2}}$. The average crystallite size, t, is related to β_{corr} by

$$t = \frac{K \lambda}{\beta_{corr} \cos \theta} \tag{3.7}$$

where K is the Scherrer constant reported to be equal to 0.89 by Bragg, and 0.94 by Scherrer. The value of K depends upon the type of reflection studied. A K value of 1.84 has been reported by Warren[70] for systems with one dimensionally disordered sheet-like crystal structures such as graphite. As will be discussed in Chapter V, this graphitic structure may have some similarities to the axial registrational disorder of oriented PPV. But, since Warren's value was determined for spherically averaged reflections from powder patterns, it was not directly applicable to PPV. And, since the primary purpose of the present study was to probe the change to t with the draw ratio, which is not affected by the choice of K, a value of 0.94 was used.

Doping and Electrical Characterization

The principle dopant used to impart high conductivity to PPV was arsenic pentafluoride, AsF_5, vapor. AsF_5 is an extremely powerful oxidizing agent and poison, thus specialized equipment and particular care were required in its handling. All doping and handling of AsF_5 was performed using a high vacuum line in a hood. Doped PPV was also quite reactive; that is, the conductivity of doped PPV deteriorated rapidly if exposed to the atmosphere, thus all handling of doped PPV was done under high vacuum or inert environmental conditions. The specialized glassware required for these operations was made by the University of Massachusetts glassblowing shop.

71

Vacuum Lines

The vacuum line used for AsF_5 handling was constructed of Pyrex glass fitted with Teflon® stopcocks and consisted of a primary manifold made of 25 mm diameter glass tubing attached to a secondary low volume manifold made from 8 mm glass tubing which could be isolated by the use of 0-3 mm stopcocks, and is shown in Figure 3.4. The primary manifold was designed to allow the introduction of an inert gas (argon) through a 0-5 mm stopcock at one end. Vacuum could be established down to a pressure of $< 10^{-5}$ torr by the use of a mercury diffusion pump flanked by liquid nitrogen traps, and a Welch Duo-Seal model 1400 forepump. A mercury manometer was also attached to the primary manifold. Glass vessels for AsF_5 storage, doping, etc. could be mounted on the vacuum line through the 18/9 ball socket joint ports attached to the

Figure 3.4. High vacuum line apparatus.

Ar →

Manometer

Vacuum

Primary manifold
Secondary manifold
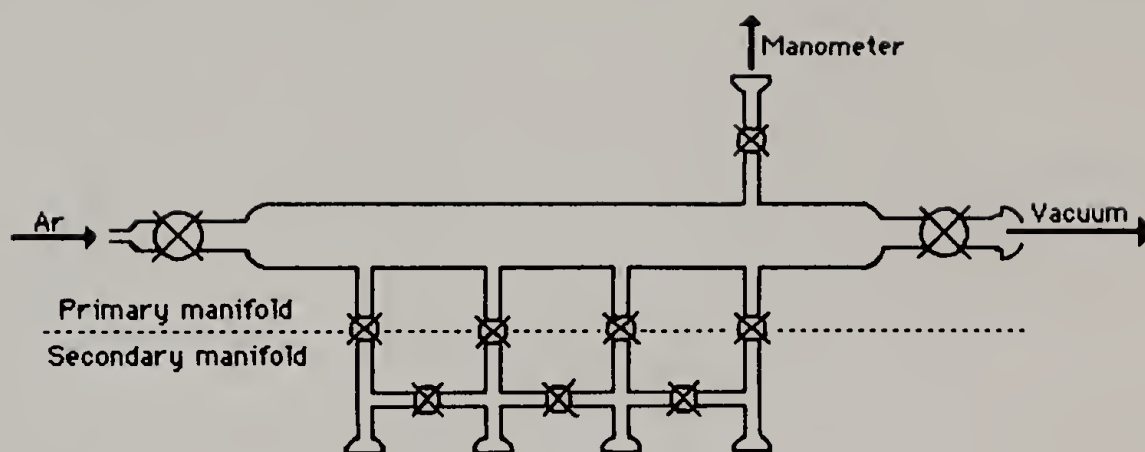
⊗ = Stopcock

⊥ = 18/9 Socket Joint

⇒ = 28/12 Ball Joint

secondary manifold. The vacuum was measured with an Edwards Penning 8 vacuum gauge. Routine qualitative measurement of the vacuum was done using a high frequency discharge Tesla coil (Fisher model BD-10 leak detector) which ionizes gases in the vacuum line and causes a bluish glow if the pressure exceeds about 10^{-4} torr. AsF_5 manipulation was only performed when the vacuum was tested to be less than 10^{-4} torr.

Arsenic Pentafluoride Storage and Purification

A 1 liter gas bulb shown in Figure 3.5 was used to contain the AsF_5 to be used on the vacuum line. Initial filling of the bulb was accomplished by mounting a lecture bottle of AsF_5 (Ozark Mahoning Company) to the vacuum line via a lecture bottle top made of a 316 stainless steel valve fused to pyrex glass tubing fitted with an 18/9 ball joint. After evacuation and repeated flame drying of the gas bulb and the lecture bottle top, the stopcock to the vacuum pump was closed, and the lecture bottle was opened carefully to fill the vacuum line and the gas bulb with AsF_5 to a pressure of about 500 torr as measured with the manometer. The lecture bottle valve was then closed and the AsF_5 in the line was condensed into the cold finger of the gas bulb with liquid nitrogen. (CAUTION: The valve of the lecture bottle must be opened using two wrenches torqued in opposite directions. Extreme care must be used to prevent applying any stress to the glass connnecting tube. This operation is by far the most dangerous of the AsF_5 handling steps, because if the connecting tube is broken, the entire volume of the lecture bottle can escape.)

Figure 3.5.   AsF$_5$ gas storage bulb.

Vacuum Line
Sub-Manifold

Stopcock

Teflon®
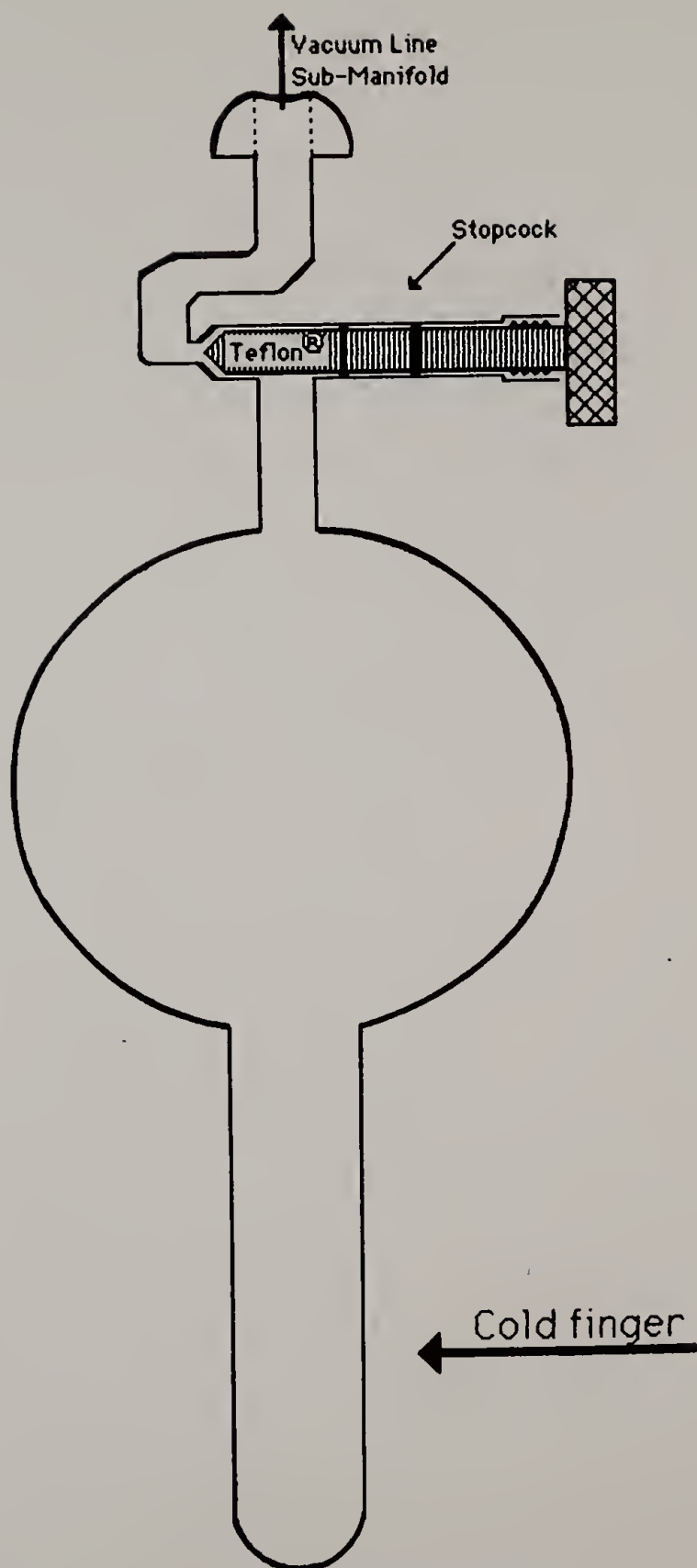
Cold finger

After filling the gas bulb, the AsF_5 was purified by freezing it into the cold finger with liquid nitrogen followed by opening the bulb stopcock to the vacuum line until all vapors had been removed as tested with the Tesla coil. The bulb stopcock was then closed and the AsF_5 was allowed to thaw back to a gas. This freeze, pump, thaw routine was repeated until no Tesla glow could be seen after freezing. Further removal of other volatiles such as SiF_4 and CF_4 could be accomplished by freeze, pump, thaw cycles at $-131°C$ using a pentane slush bath for cooling. After this treatment, no HF or AsF_3 could be detected.[72]

Four-Probe Apparatus and Sample Mounting

Conductivity measurements and doping of PPV samples were simultaneously performed in the apparatus shown in Figure 3.6. Conductivity was measured using a four-probe configuration by attaching four platinum electrodes across the width of a rectangular piece of the PPV film (cut to about 15 mm x 5 mm) using a conductive colloidal graphite adhesive (Electrodag 502). Four-Probe resistance measurements were made using a Data Precision model 2590 digital multimeter.

A simplified schematic of the four-probe resistance measurement, as performed by the meter, is shown at the top of Figure 3.6. A current, I, is passed through the sample via the outer two probes and through a standard of known resistance, R_r. The magnitude of the current, I, is calculated with Ohm's Law by measuring the voltage drop, V_r, across the standard resistor as $I = V_r/R_r$. The voltage drop, V_s, between the inner two probes is then used to calculate the sample resistance R_s as $R_s = V_s/I$. The advantage of the four-probe measurement is that no

Figure 3.6. Four-probe apparatus for simultaneous doping reactions

and conductivity measurements. Four-probe measurement

circuit is shown at the top of the figure.

$$R_S = \frac{V_S}{V_R} R_S$$

to vacuum line

Teflon stopcock

FETFE
O-ring

glass
pin

sample

copper
wire

Electrodag

mercury

sample
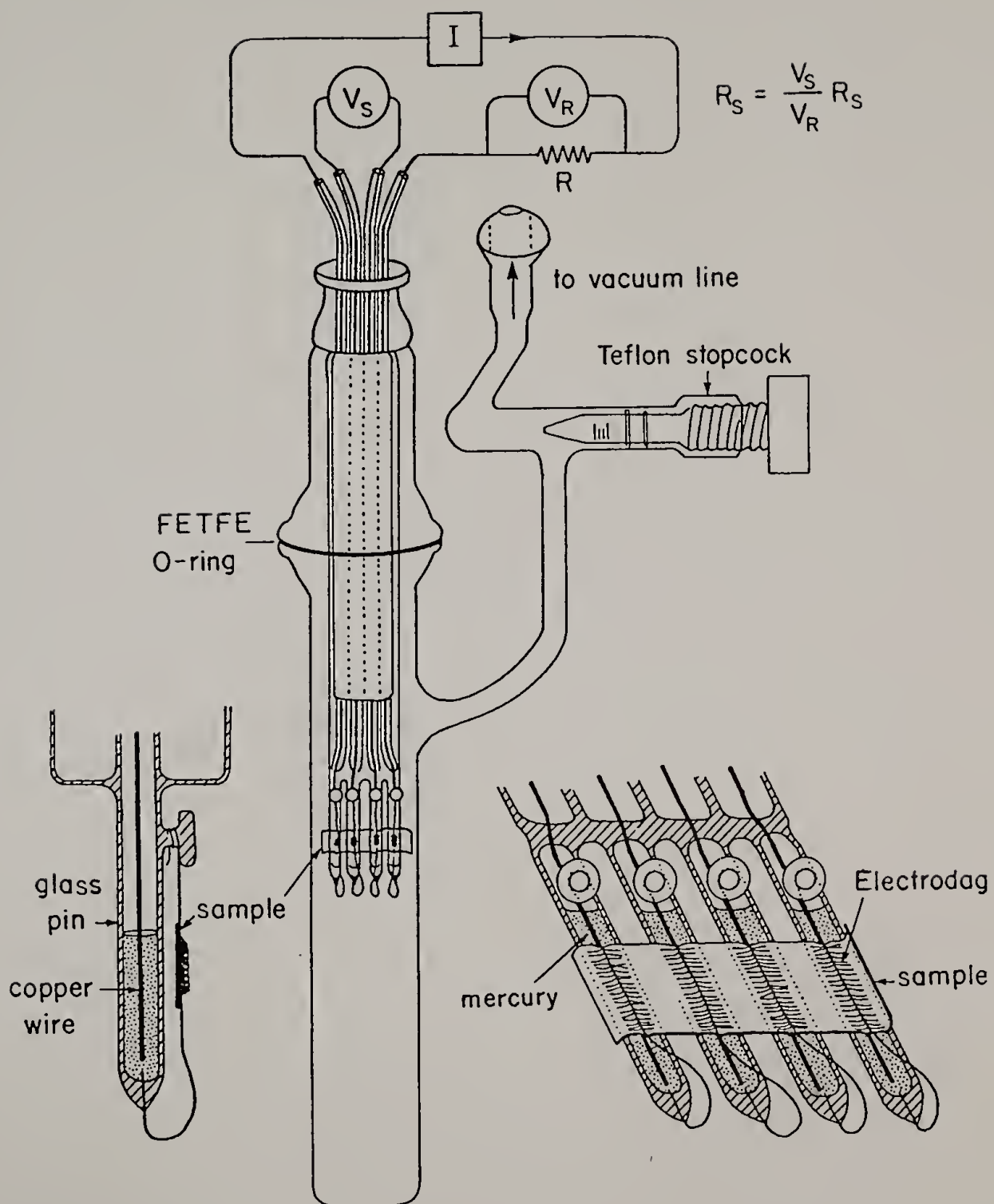
current is passed through the Electrodag contacts of the inner two electrodes during the V_s measurement, thus the contact resistance of the Electrodag is not added to the measured R_s.[73] Initial measurements of the resistance of undoped PPV samples were made with only the inner two probes using a Hewlett Packard model #4329A high resistance meter. The resistance of undoped PPV was in the 10^{11} Ω range, thus the inclusion of the small contact resistance (~ 100 Ω) was insignificant.

Conductivity, σ, was calculated by normalizing R_s by the sample dimensions between the two inner probes as $\sigma = \frac{1}{R} (\frac{\ell}{w \cdot t})$. The film width, w, and the length between the inner two electrodes, ℓ, varied from sample to sample averaging about 4 mm each and was measured with a calibrated magnifying loupe to $\pm$ 0.02 mm. The film thickness, t, averaged about 0.01 mm (10 μm) and was measured to $\pm$ 0.002 mm with a micrometer (this was the largest source of error).

Measurements of the conductivity of oriented PPV films were made on samples mounted with the stretch direction either parallel, $\sigma_{/\!/}$, or perpendicular, $\sigma_{\perp}$, to the electrode separation direction. The ratio of $\sigma_{/\!/}$ to $\sigma_{\perp}$ is the conductivity anisotropy, σ^*.

Arsenic Pentafluoride Doping Procedure

After mounting the film sample, the four-probe vessel was attached to the vacuum line secondary manifold, evacuated, and flame dried. To insure complete evacuation, the vessel was kept open to the vacuum line overnight. The vapor pressure of AsF_5 was maintained at 50 torr by immersing the cold finger of the gas bulb in a methanol bath contained

in a large dewar cooled to $-90^{\circ}C$ by the heat transfer coil (type-FV) of a Neslab Cryocool CC-100II immersion cooler. Prior to introduction of AsF_5 into the four-probe, the secondary manifold was isolated from the primary manifold by closing the 0-3 stopcocks. With the four-probe stopcock closed, the AsF_5 gas bulb stopcock was opened to allow AsF_5 to fill the secondary manifold for about 10 minutes, giving the AsF_5 a chance to react with any adsorbed impurities on the inner glass surface of the secondary manifold. The four-probe stopcock was then opened, allowing AsF_5 to react with the PPV. The secondary manifold was kept isolated, and the four-probe and gas bulb stopcocks were kept open. With this open system doping method, the side products of the doping reaction (AsF_3) and any impurities on the four-probe vessel walls were continuously cryogenically removed into the cold finger of the gas bulb.

The sample resistance was monitored during the doping process and was recorded as a function of time. Typically, samples were doped continuously for up to 5 weeks until no decrease in resistance was noted over a 2 day period indicating that the maximum conductivity had been achieved. At this point doping was terminated by cryogenically removing the AsF_5 back into the gas bulb using liquid nitrogen. The four-probe vessel was then opened to the vacuum line, and the resistance was monitored for 1-2 days until constant. This final resistance was then used to calculate the final conductivity. The dopant concentration in the PPV film was measured by adding an additional pre-weighed PPV sample to the four-probe vessel before AsF_5

introduction. This film was then weighed again after doping to determine weight uptake.

Procedure for Other Dopants

Acid doping. Acid doping of PPV was accomplished by passing the vapors of sulfuric acid or perchloric acid (both Fisher reagent grade) across mounted PPV films using a four-probe vessel with a #10 o-ring flange built into the lower portion of the vessel wall. The acid, contained in a 250 ml round bottom bulb which was fitted with a 0-3 mm Teflon[®] stopcock opening to a #10 o-ring flange and a gas inlet also with an 0-3 mm stopcock was degassed by the freeze-pump-thaw technique. The acid bulb was attached to the four-probe vessel using a FETFE o-ring. The other opening of the four-probe was connected to vacuum line via a solvent trap and with the acid stopcock closed the system was evacuated. This apparatus is shown in Figure 3.7. Acid vapor was cryogenically forced across the sample, after closing the trap stopcock to the line, by opening the acid stopcock to the four-probe and immersing the trap in liquid nitrogen. (CAUTION: Perchloric acid must be handled with care because it can induce spontaneous combustion of organic materials. Perchloric acid doped polyacetylene has also been reported to be explosive.[74])

Sodium naphthalide. A 1.0 M sodium napthalide solution in THF was prepared in a 250 ml round bottom bulb of the same type as was used for the acids above. 6.4 grams (0.5 moles) of naphthalene (Aldrich Chemical Co.) was added to the flask under a flow of dry nitrogen, after the flask had been thoroughly dried by evacuation and flaming.

Figure 3.7. Apparatus for protonic acid doping of films mounted in the four-probe vessel.

Vacuum Line
Sub-Manifold

Trap

Liquid nitrogen

Dewar

Sample

4-Probe Vessel

Acid
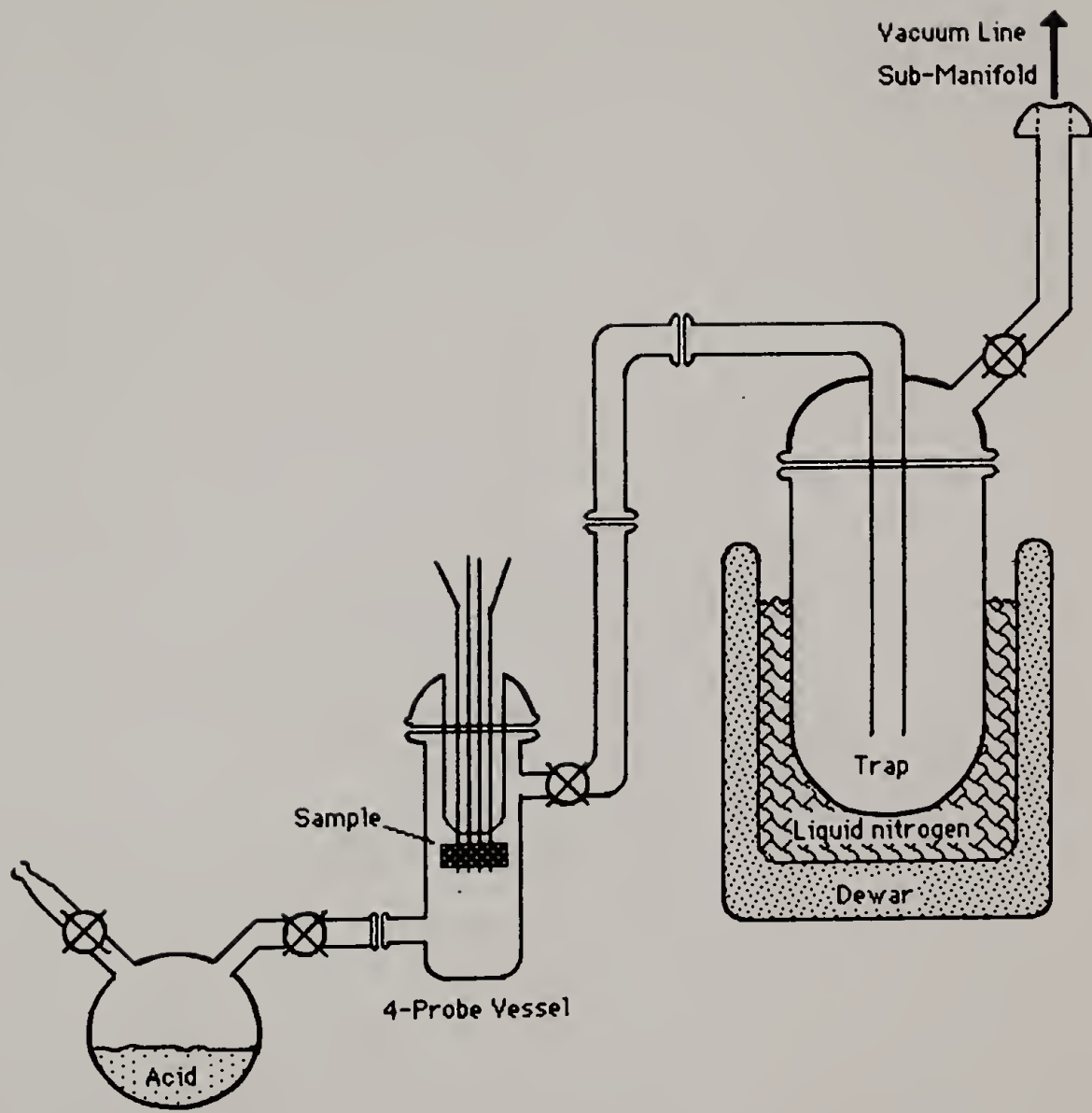
50 ml of anhydrous THF, prepared by distillation over potassium acetophenone, was added to the flask under inert conditions dissolving the naphthalene. An excess (> 1.2 grams) of sodium metal was freshly cut under paraffin oil and washed with pentane and added to the solution, which turned bright green indicating that the sodium naphthalide complex had been formed.

After freeze-pump-thaw degassing of this solution, the bulb was attached to the four-probe, and with the bulb stopcock closed, the four-probe was evacuated. The four-probe stopcock to the vacuum line was closed and the four-probe and bulb were removed from the line. The bulb stopcock was then opened and the sodium naphthalide solution was poured into the four-probe until the solution just covered the mounted film. Doping was allowed to proceed for 2 hours. The solution was then poured back into the bulb. (Cooling the bulb with liquid nitrogen helped to create a THF vapor pressure difference which aided this transfer.) Pure THF was then cryogenically distilled from the bulb back into the four-probe using liquid nitrogen, and the four-probe and sample were washed. The THF was then poured back into the bulb. This washing was repeated until the green color of the THF in the four-probe disappeared. The bulb was closed, the four-probe was opened to vacuum, and resistance was measured. (NOTE: Partial degradation of the Electrodag contact was observed due to the THF. To circumvent this problem, platinum wire electrodes could be cast into the film and then soldered to the existing four-probe electrodes instead of Electrodag mounting.)

Temperature Dependent Conductivity Measurements

Conductivity was measured over a temperature range of 80°K to 300°K using doped PPV samples mounted in an Air Products LT-3-110 Liquid Transfer Heli-Tran system cooled by liquid nitrogen and a APD-E model #3700 Digital Temperature Indicator/Controller.

The doped samples of these experiments were prepared by adding an extra piece of the desired PPV film to the four-probe vessel prior to doping. The doped sample was removed from the four-probe and mounted on the Heli-Tran conductivity probe in a Vacuum Atmospheres DLX-001-SG dry-box which used a HE-493 dri train to purify the argon atmosphere to H_2O and O_2 levels of < 1 ppm. The PPV sample was mounted in contact with the sapphire crystal of the Heli-Tran probe which provided thermal contact with the controlled temperature source. After mounting, the Heli-Tran probe was sealed prior to removal from the dry box and then evacuated to a vacuum of better than 10^{-5} torr. The cooling of the probe was then initiated by starting the liquid nitrogen flow until a stable temperature of $\sim 80^\circ$K was attained. The resistance was then measured and the indicator/controller was turned on to begin a slow warm up to each desired temperature. Readings were taken at 4° intervals after the temperature had stablized to $\pm 0.1^\circ$K.

The resistance measured was actually the parallel combination of the resistance of the sapphire ($6 \times 10^{10} \Omega$) and the sample. Thus the measured resistance is related to the true sample resistance by

$$R_{PPV} = \left[\frac{1}{R_{measured}} - \frac{1}{R_{sapphire}} \right]^{-1}. \qquad (3.8)$$

However, only highly doped PPV samples were used, which had an 80°K

resistance of $< 10^4 \ \Omega$, thus this correction was negligible.

CHAPTER IV

PPV SYNTHESIS AND ELIMINATION CHEMISTRY

The polymerization of p-xylene-bis(dimethylsulfonium chloride), is

an unusual reaction because the actual monomer is not the bis(sulfonium

salt) but is the reaction product of the bis(sulfonium salt) and a

molar equivalent of base. This chapter begins with a brief discussion

of the monomer synthesis and its optimization, followed by a proposal

for the mechanism of polymerization. A discussion of the difficulties

associated with the characterization of the molecular weight is next,

along with the results that were obtained.

In order to optimize the final conversion of the precursor

sulfonium polyelectrolyte to PPV and to understand the processes

occurring during the stretching of the precursor films, a detailed

study of the thermal elimination reaction which yields PPV was

undertaken by a variety of characterization techniques. The chapter

concludes with a description of the morphology of the unstretched PPV

films.

Sulfonium Salt Syntheses

General Considerations

Sulfonium salts were first discovered by Ofele in 1864 when he

obtained triethylsulfonium iodide by the reaction of diethylsulfide and

ethyl iodide.[75]   Since this time, much more work has been done in the

area of sulfonium salt synthesis and reactivity and is the subject of numerous reviews.[76-82] A dialkylsulfide reacts with an alkyl halide via SN_2 nucleophilic substitution.

$$R^1_2S + R^2X \rightarrow R^1_2R^2S^+ X^- \tag{4.1}$$
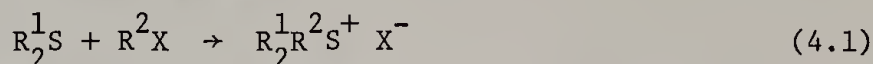
The reaction proceeds easily with primary alkyl halides, usually under mild (room temperature) conditions with the rate of reaction being increased by the use of polar solvents that stabilize the transition state and the resulting salt, which are both more polar than the starting materials. Alkyl iodides are the most reactive, with reactivity decreasing as the length of the alkyl group is increased. Activated primary alkyl halides such as allyl,[83] benzyl,[83,84] α-halocarbonyl,[85,86] and arylthiomethyl[87] chlorides and bromides are often used.

An important factor to keep in mind is that sulfonium salt formation is reversible; that is, the halide can dealkylate the sulfonium to regenerate a dialkylsulfide and an alkyl halide.[82] A possible problem arises because it is more favorable for the alkyl halide generated in this reverse step to react with the alkylsulfide to result in the lowest molecular weight sulfonium salt (i.e., Equation 4.2).[88]

$$(CH_3)_2S + C_2H_5I \rightleftharpoons (CH_3)_2C_2H_5S^+I^- \rightleftharpoons CH_3SC_2H_5 + CH_3I \tag{4.2}$$
$$(CH_3)_2S + CH_3I \rightleftharpoons (CH_3)_3S^+I^-$$
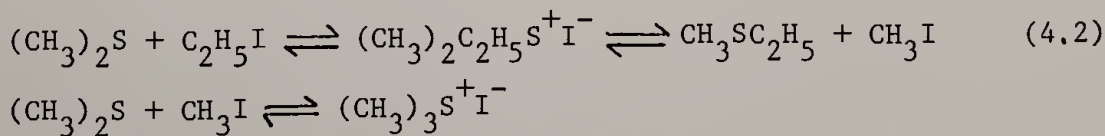
This is especially true when the high molecular weight alkyl substituent has limited solubility in the solvent. Alkyl scrambling of this nature can be avoided when necessary, by reacting an alkylating

agent containing a non-nucleophilic counterion, such as triethyloxonium tetrafluoroborate, with the appropriate sulfide (Equation 4.3).

$$(CH_3)_2S + (C_2H_5)_3O^+ \ BF_4^- \rightarrow (CH_3)_2S^+C_2H_5 \ BF_4^- + (C_2H_5)_2O \qquad (4.3)$$
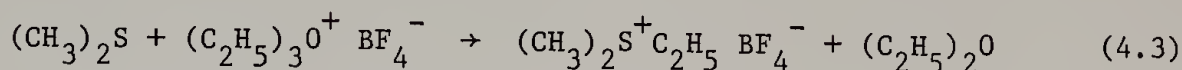
With most sulfonium salt syntheses, an excess of dialkyl sulfide is used to drive the reaction towards the sulfonium salt side of the reaction. Under these conditions, however, the chance for direct alkyl exchange of the sulfonium salt alkyl groups to the sulfide forming a new salt and sulfide is possible. This reaction occurs by an SN_2 attack on the sulfonium alkyl by the sulfide. The primary driving force for this reaction is the relief of steric strain in the sulfonium salt moiety, with the basicity of the sulfide playing a secondary role.[88] This is an important reaction in systems where the sulfonium group contains two or three bulky alkyl groups such as t-butyl or benzyl groups. But, when only one of the sulfonium alkyls is a bulky group, the initial strain is not very high and the rate of alkyl exchange is almost insignificant. For example, a benzyldimethyl-sulfonium salt, such as in the PPV precursor polymer, does not have much steric strain and would not be expected to lose a methyl group to dimethylsulfide because there is little driving force.

PPV Monomer Synthesis

The monomer chosen for polymerization to the PPV precursor polymer was synthesized by the reaction of α,α'-dichloro-p-xylene, (I), with excess dimethylsulfide which yields p-xylene-bis(dimethylsulfonium chloride), (II), (Figure 4.1). This choice was based upon the earlier

79

Figure 4.1. Synthesis of <u>bis</u>(sulfonium) monomer.

$$Cl\text{-}CH_2 \overset{}{\underset{}{\bigcirc}} CH_2\text{-}Cl \ + \ CH_3SCH_3$$

(excess)

I

$$\downarrow \ 50°C \quad MeOH$$

$$CH_3\overset{+}{\underset{CH_3}{S}}\text{-}CH_2 \overset{^-Cl}{\underset{}{\bigcirc}} CH_2\text{-}\overset{+}{\underset{CH_3}{S}}\overset{CH_3}{\underset{CH_3}{}}$$

^-Cl

II

(XSC)
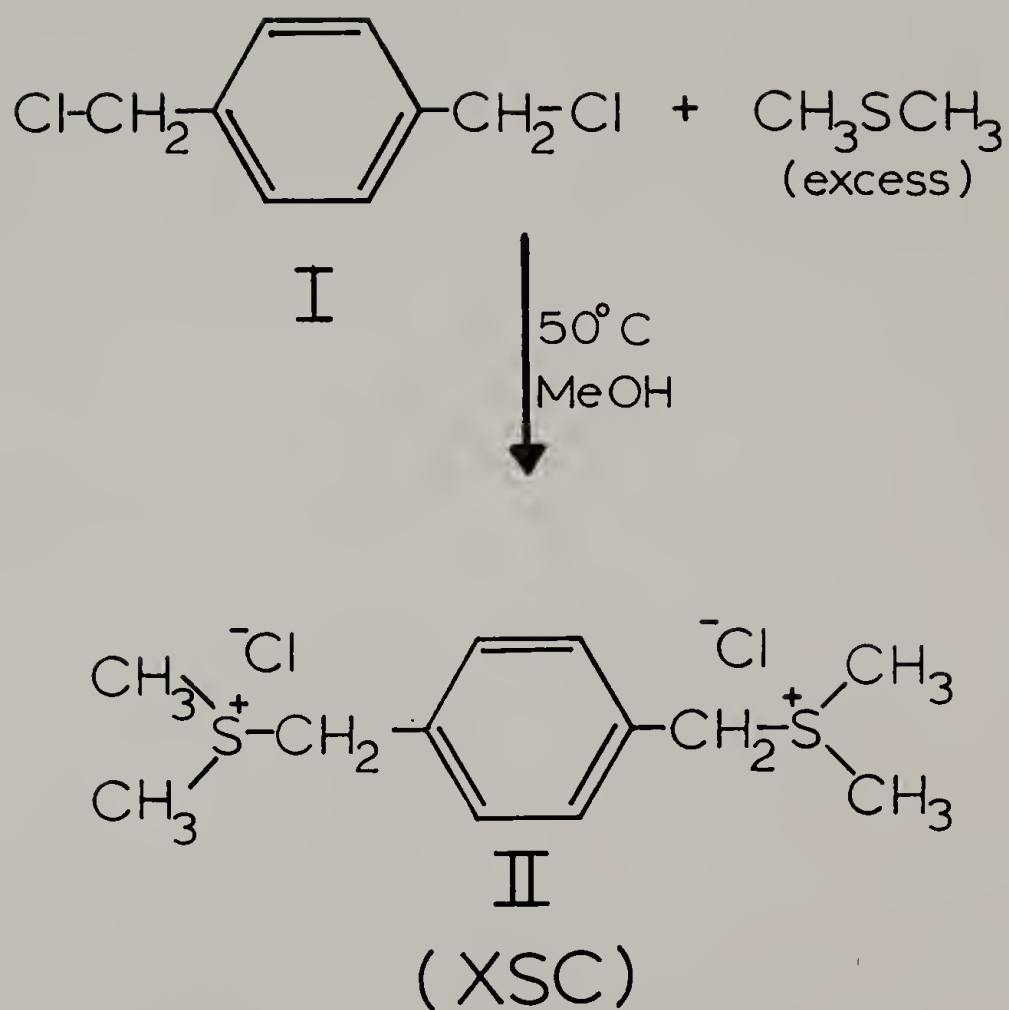
work of Wessling and Zimmerman,[53] and of Kanbe and Okawara.[61] Kanbe

and Okawara used nearly the same monomer as above except that the

chloride was replaced with a tetrafluoroborate counterion. It was

difficult to evaluate the usefulness of Kanbe's tetrafluoroborate

monomer for the precursor formation because the conditions they used

were designed to obtain a powder of PPV directly. The work of Wessling

and Zimmerman, however, clearly demonstrated that the p-xylene-

bis(dimethylsulfonium chloride), XSC, was at least one of the better

choices for precursor synthesis. The product obtained by Wessling and

coworkers by this reaction (Figure 4.1) was described as light

greenish-white in color and was obtained in moderate yields with no

clear melting point. Instead it decomposed at temperatures > 100°C

with the liberation of $(CH_3)_2S$. The monomer, obtained in the present

study, approached 95% yields by a slight modification of the synthesis

and purification procedures, and by extensive drying in vacuo. It was

a white crystalline powder with a clearly defined melting point of

149-151°C. Elemental analysis confirmed the purity:

	% C	% H	% S	% Cl
calculated	48.16	6.72	21.44	23.67
found	48.16	6.92	20.91	23.71

[1]H-nmr spectroscopy, using a Varian T-60 nmr instrument, was also

used to characterize the purity of the bis(sulfonium) monomer. Figure

4.2 shows the spectrum of the p-xylene-bis(dimethylsulfonium chloride)

recorded in d_6-DMSO using an external TMS standard contained within a

sealed capillary tube. XSC was only slightly soluble in the DMSO, but

was soluble enough to obtain a high quality spectrum which showed a
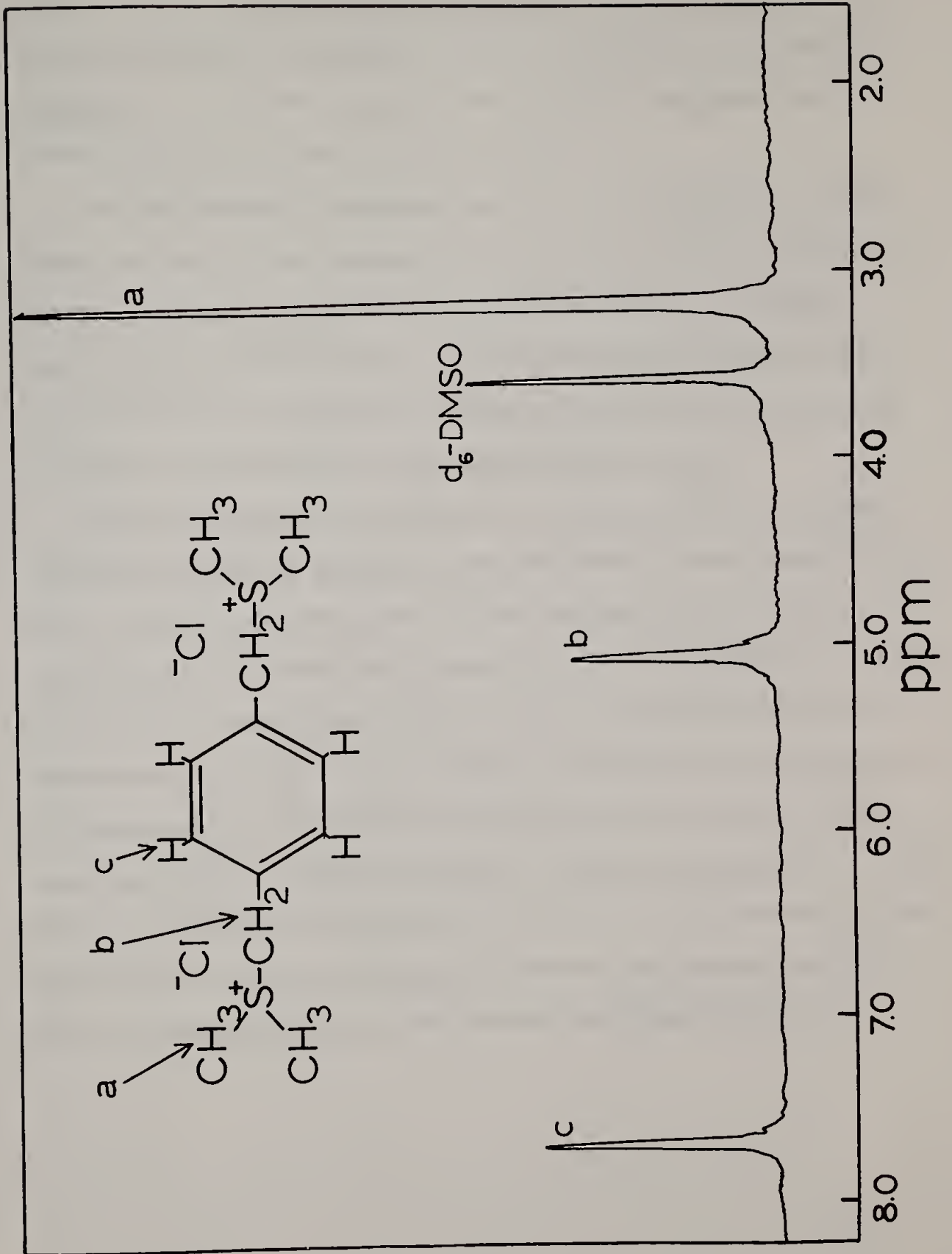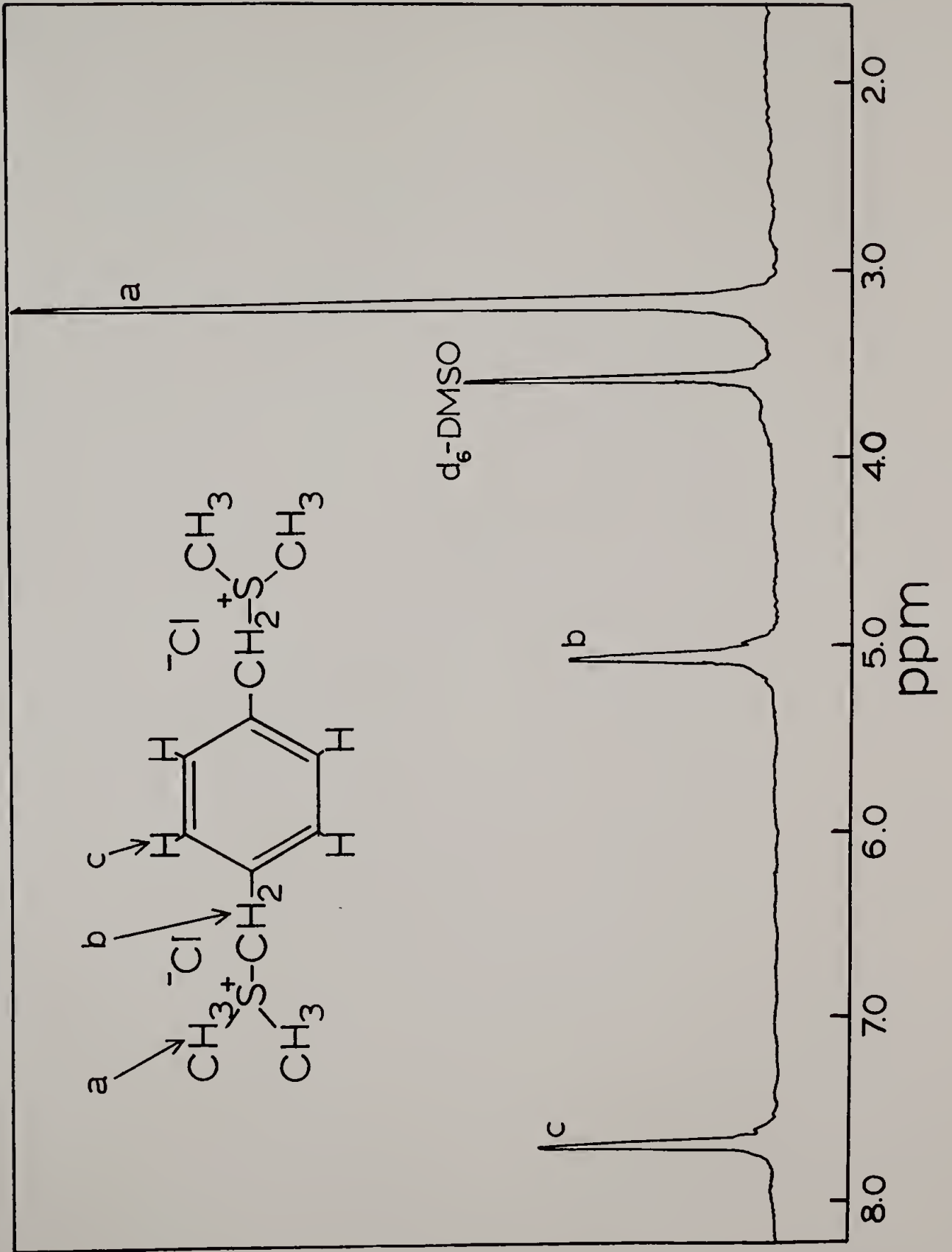
methyl peak at 5.2 ppm, and an aryl peak at 7.8 ppm, with respective relative integrated intensities of 12:4:4. There was no evidence of residual α,α'-dichloro-p-xylene which displays a methylene peak at about 4.6 ppm and an aryl peak at ∿ 7.4 ppm.

The modification of Wessling's method was the addition of a small amount of water to the methanolic reaction mixture, which retarded the reverse dealkylation reaction of the sulfonium salt to the benzyl halide and the dialkylsulfide. The increased ionic strength of the solution seemed to stablize the sulfonium salt and the result was an increased yield and purity of the bis(sulfonium) monomer.

The dry XSC monomer was found to be quite hydroscopic, and would increase in weight by absorbing water detectably within minutes if left open, especially on humid days. If not thoroughly dried after the precipitation in acetone (see Chapter III), it was obtained as a lumpy solid with a reduced broad melting range. XSC was stable at room temperature for up to 2 days, but after more than 3 days a strong odor of dimethylsulfide developed, indicating a slow reversal back to the starting reagents. Longer term storage required refrigeration at ∿ 0°C which was sufficient to maintain its purity for up to 4 weeks. It was found, however, that if sulfonium degradation had occurred, the XSC could be regenerated by a second reaction with dimethylsulfide.

Poly(p-Xylylene-α-Dimethylsulfonium Chloride)

Synthesis

As previously mentioned, the PPV products obtained by Kanbe and Okawara were oligomeric powders with a degree of polymerization of about 10. The formation of these low molecular weight products may be attributed to the elevated reaction temperature ($80^{\circ}C$), the use of the tetrafluoroborate counterion, and the excess base concentration used (molar ratio of base to monomer 3:1). Since elimination of the precursor polymer sulfonium groups is induced by both heat and base, premature elimination occurred under these conditions, which limited the solubility, and consequently the molecular weight. The success of Wessling and coworkers was primarly due to their choice of sulfonium chloride monomers, low reaction temperatures ($0^{\circ}C$), reduced base to monomer ratios (typically equinormal), and also to the rigorous exclusion of oxygen from the polymerization reaction. The monomers studied were of the following general type where

$$R = CH_3, C_2H_5, C_3H_7, C_4H_9, \text{and } X = Cl, Br, OH:$$

(4.4)

$$X^- \ \underset{R}{\overset{R}{>}}\overset{+}{S}-CH-\bigcirc-CH-\overset{+}{S}\underset{R}{\overset{R}{<}} \ X^-$$
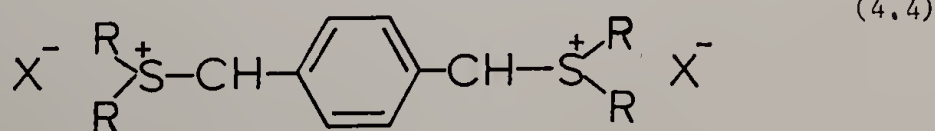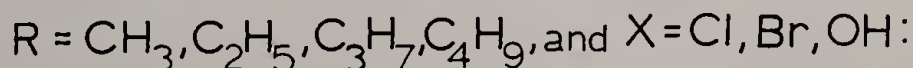
The molecular weights of THF soluble derivatives of the precursor polymer, prepared by substituting the sulfonium group with a thio-phenyl group, were measured using gel permeation chromatography and were reported to be in the range of 15,000 to 2,000,000 daltons,

but more typically polymers in the range of 50,000 to 600,000 daltons were obtained.[53]   These could be cast into films or coatings, which could be further thermally treated to yield fibers or foams of PPV.

Attempts to repeat the procedure outlined in Wessling's patent[53] were met with only limited success and resulted only in a partially soluble yellow polymer which could not be cast into coherent films. In the patent, he reported the use of equinormal monomer to base ratios. In the present work, the precursor polymer could only be prepared in a mostly uneliminated, soluble form by reducing the base stoichiometry to be equimolar to the monomer. With an equinormal ratio, the excess base induced the premature elimination of the precursor polymer to the insoluble PPV.

Even with the use of an equimolar base to sulfonium group ratio, the conversion of a small fraction of sulfonium repeat units to PPV units was unavoidable. The presence of the phenylene vinylene units was evidenced by the emission of blue fluorescence when the precursor polymer was illuminated with a hand-held broad band ultraviolet source. Thus, the intermediate polyelectrolyte which resulted from the equimolar reaction of (II) with sodium hydroxide is in fact a copolymer of structures (III) and (IV) with a relative composition defined by the m:n ratio shown below:

$$
\left(\underset{\substack{}}{}\text{—}\right)\quad (4.5)
$$
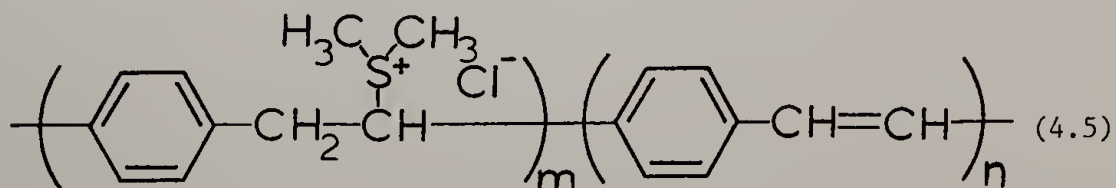
The control of reaction temperature and reagent concentration was found to be critical in limiting the amount of IV. The standardized polymerization conditions used for this study were a monomer concentration of 0.2M and a reaction temperature of 0°C which yielded a clear polyelectrolyte solution having an intrinsic viscosity of 2.5 dl/g (using 0.05 M Na_2SO_4 in an H_2O:CH_3OH (80:20) solvent). Polymerization reactions at higher concentrations, for example at > 0.3 M, resulted in the formation of yellow gels which could not readily be redissolved. And, if the reactions were carried out at or above ambient temperatures, a bright yellow, highly viscous solution was obtained with an increase in the unsaturation of the polymer backbone. Wet casting of films from these highly colored solutions resulted only in the formation of brittle films, with some precipitation occurring before a coherent film was formed. It was found that precipitation of the polyelectrolyte from the aqueous solution occurred at an m:n ratio of approximately 1:4. The standard reaction conditions previously stated (0°C for 1 hour) yielded a copolymer having an m:n ratio of about 10:1, which could easily be wet cast by solvent removal at 25°C _in vacuo_ to yield coherent clear films of controllable thickness. Dissolution of the films in polar solvents other than water resulted in yellow solutions with an increase in unsaturation, indicating that the sulfonium ion units, III, were stabilized by water.

Polymerization Mechanism

The overall mechanism for this polymerization is as yet not completely resolved. However, the results of this dissertation work are not inconsistent with the reaction scheme proposed by Wessling[89] and shown in Figure 4.3 involving sulfonium ylid formation and 1,6-elimination of dimethylsulfide to form either a diradical, or a p-xylylene intermediate which polymerizes to yield III. Kanbe and Okawara also proposed a diradical polymerization reaction.[61] It was found that addition of an aqueous radical initiator (Fenton's reagent) accelerated the reaction. That is, upon addition of trace amounts of this solution the viscosity of the reaction solution increased markedly. Also, when the polymerization reaction was carried out in the presence of oxygen a solution of III of low viscosity was obtained, and the product could not be cast into a coherent film.

The other possible polymerization mechanism is a condensation reaction of benzyl sulfonium groups. In 1961, Swain and Thorton reported the synthesis of p,p'-dinitro-p-stilbene in quantitative yields by the reaction of p-nitrobenzyldimethylsulfonium p-toluenesulfonate with equinormal aqueous sodium hydroxide at 100°C.[90] Nmr evidence of 97% deuterium exchange of the α-methylene hydrogens, and experiments which showed a second order kinetic dependence on [sulfonium salt][OH^-], led them to postulate the formation of a p-nitrobenzyl carbene intermediate which abstracts the

Figure 4.3. Proposed mechanism of p-xylene-<u>bis</u>(sulfonium) monomer

polymerization to the PPV precursor.

Sulfonium Ylid Formation

$$X^- \; {}^+_RS-CH_2-\langle\bigcirc\rangle-CH_2-S^+X^- \underset{\longleftarrow}{\overset{NaOH}{\longrightarrow}} X^- \; {}^+_RS-CH_2-\langle\bigcirc\rangle-CH-S^+X^-$$

1,6-Elimination

$$CH_2=\langle\bigcirc\rangle=CH-S^+ \; X^- \quad \Longleftrightarrow \quad {}^\bullet CH_2-\langle\bigcirc\rangle-C^\bullet$$
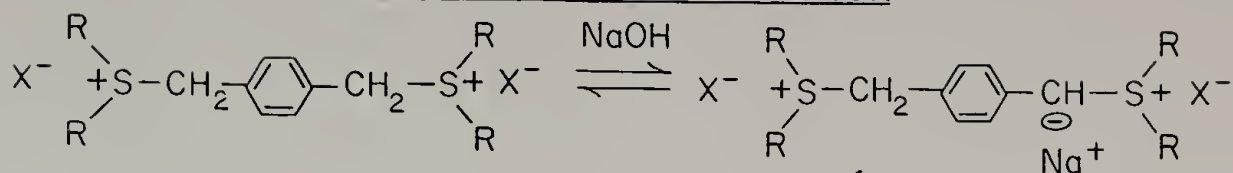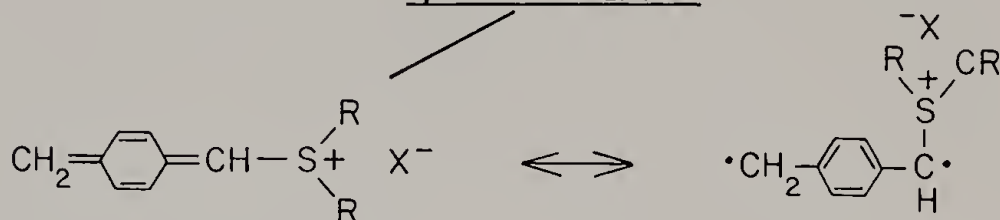
Diradical Initiator Formation

$$^\bullet CH-\langle\bigcirc\rangle-CH_2-CH_2-\langle\bigcirc\rangle-\overset{\bullet}{C}H$$

Addition

$$\left(\langle\bigcirc\rangle-CH_2-\overset{X^-}{\underset{}{\overset{R_S^+R}{CH}}}\right)_m\left(\langle\bigcirc\rangle-CH=CH\right)_n$$
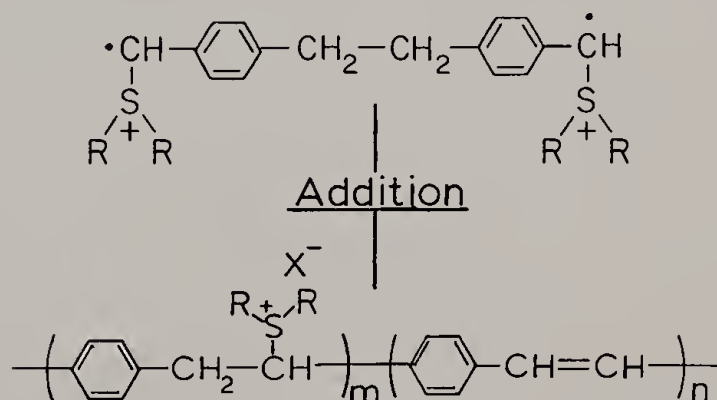
α-hydrogen of another sulfonium followed by attack on the methylene

carbon to form

$$O_2N-\underset{}{\bigcirc}-CH_2-CH-\overset{\overset{\displaystyle H_3C\diagdown\diagup CH_3}{\underset{|}{\overset{+}{S}}}X^-}{\underset{}{\bigcirc}}-NO_2 \qquad (4.6)$$
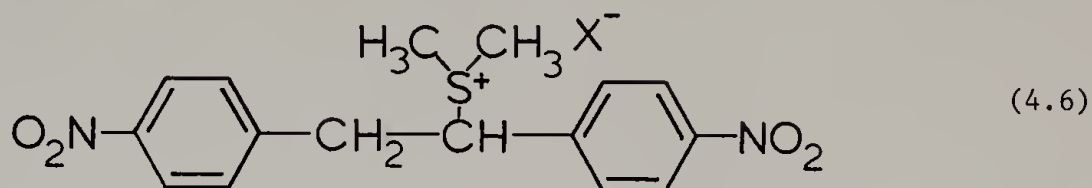
which then undergoes β-elimination to give the p,p'-dinitrostilbene. A

study of the phenyl substituent effect showed that a strongly electron

withdrawing group in the para-position was necessary for the reaction

to occur. Non-electron withdrawing substituents gave the corresponding

benzyl alcohol, and meta-substituents gave the corresponding stilbene

oxide. [91] Other evidence cited for the carbene formation, was that if

the reaction was performed in the presence of oxygen, a significant

amount of the p,p'-dinitrostilbene oxide was formed, due to carbene

oxidation to p-nitrobenzaldahyde which is known to react with sulfonium

ylides to form the epoxide. [92,93]

XSC has all of the characteristics required by this second

mechanism. The para-sulfonium group is highly electron withdrawing.

In the presence of oxygen, which has been shown to limit the precursor

polymer molecular weight, epoxide formation would then place a

non-electron withdrawing benzyl oxide para to the benzyl sulfonium,

which would be expected to effectively terminate the condensation

polymerization.

However, the condensation mechanism is in direct contradiction to

the observation that very high molecular weight precursor is formed

within minutes of base addition, even at yields less than 25%.

Therefore, it seems that only the radical addition mechanism depicted in Figure 4.3 can explain all the observations of the XSC polymerization.

Two mechanistic details still elude conformation. The first is whether the monomer diradical initially coupled to form the dimer diradical, or whether the reactive species is the monomer diradical; or of course, whether the reaction proceeds by both routes. In any case, as soon as two dihydrogen methylene radicals couple, the polymerization would proceed by head-to-tail addition to the quinoid sulfonium monomer. The second unanswered question is the mechanism of chain reaction termination. Other than an unsubstantiated speculation that some unflushed oxygen is responsible for termination, there is no data to provide a termination mechanism. These questions should be studied in the future, because they would be important to the preparation of copolymers.

Precursor Molecular Weight

Molecular weight studies of the polyelectrolyte precursor proved difficult because of the unique nature of the polymer. Intrinsic viscosity measurements were found to be highly dependent upon the added salt concentration, the type of salt and the solvent used, with some irreproducibility. Aqueous phase GPC was attempted using both Waters E-Linear Bondagel and Polymer Labs Aquagel columns for water soluble polymers. The polyelectrolyte in all cases was found to interact with the columns, and retention volumes were highly dependent upon the solvent and salts used. However, reproducible results were obtained by

membrane osmometry. The molecular weight of the polyelectrolytes, as determined in an aqueous 0.025 N Na_2SO_4 solvent, was found to be $\overline{Mn} \simeq$ 130,000 daltons.

Another method of determining molecular weight which has been developed specifically for high molecular weight polyelectrolytes at the Exxon Research and Engineering Company, combines centrifugation with low angle laser light scattering.⁹⁴   A sample analyzed by this technique yields an $\overline{Mn}$ of 496,500 daltons, $\overline{Mw}$ of 993,000 daltons and a $\overline{Mw}$:$\overline{Mn}$ ratio of 2.0.

An explanation for the discrepancy between these two results is probably that the elimination of low molecular weight products from the precursor polymer occurs to some extent even in solution at room temperature, and these byproducts would significantly lower the number average molecular weight (i.e., averaged over all solute molecules) which is measured by membrane osmometry. Because the light scattering method is relatively insensitive to this problem, the $\overline{Mn}$ from the light scattering method is probably more accurate.

Characterization of Precursor Elimination

Ultraviolet Visible Spectroscopy

As noted previously, exposure of these polymers to broad wavelength UV light irradiation causes visible fluorescence, which presumably results from the $\pi - \pi^*$ transition in the double bonds. Figure 4.4 shows the uv-visible spectra obtained for a clear polyelectrolyte film, (a), for a partially eliminated film, (b), and for a fully eliminated

Figure 4.4. Ultraviolet/visible spectra of (a) an uneliminated, (b)
a partially eliminated, and (c) a fully eliminated film
of the PPV precursor polymer, poly(p-xylylene-α-
dimethylsulfonium chloride).
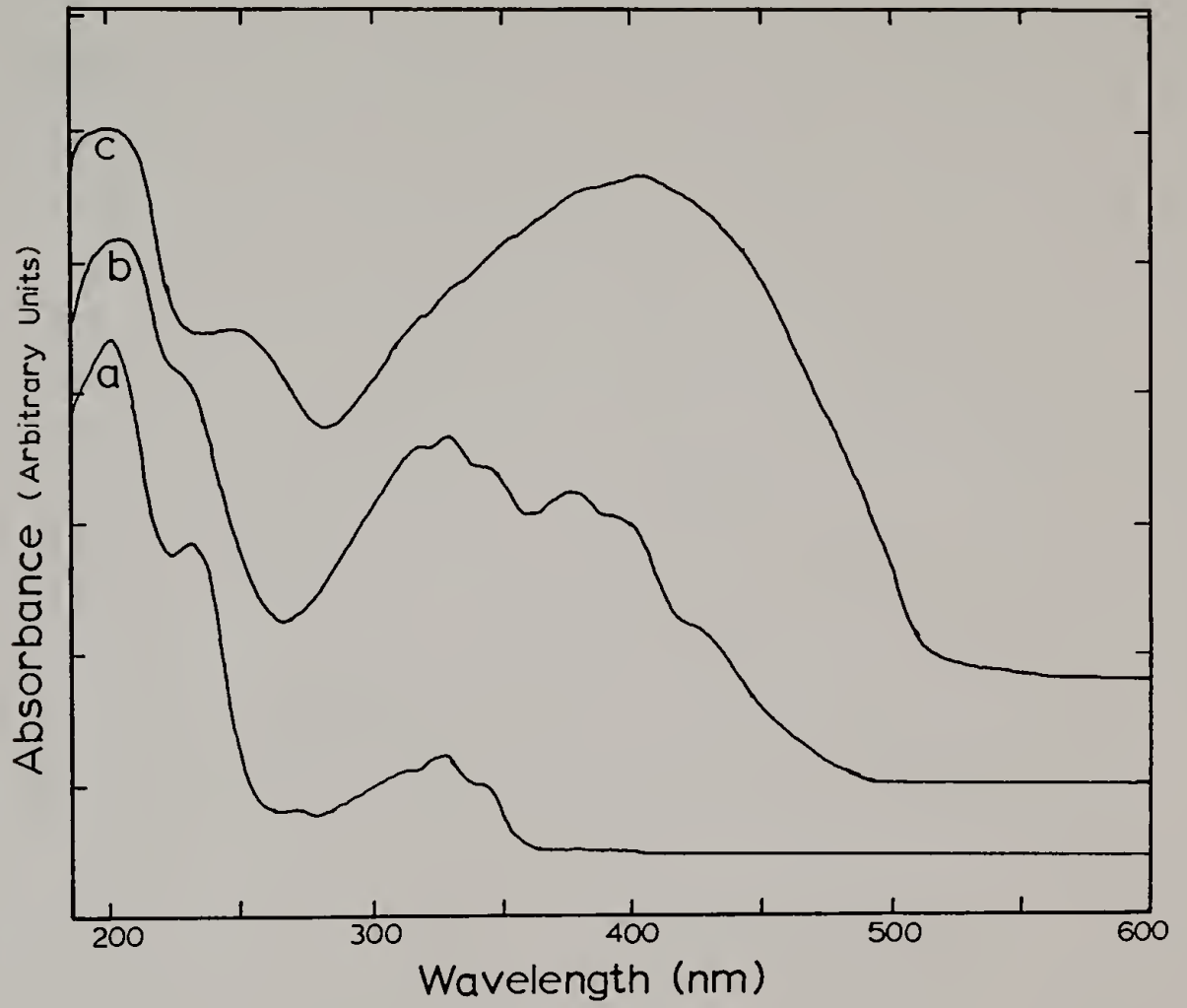
PPV film, (c). The uv/vis spectra for the clear, saturated films (a) contained three separate absorption bands associated with the phenyl group (λ = 198,229 nm), the sulfonium group (λ = 265,270,276 nm), and a small concentration of bathochromically shifted stilbene groups (λ = 305,318,332 nm). As the sample was thermally eliminated (b), the absorption bands broadened and new bands appeared at longer wavelengths until elimination was complete, at which point the uv/vis spectrum (c) showed a broad, continuous absorption with an edge centered at 512 nm (2.42eV) indicative of a highly conjugated system. Thus, the degree of unsaturation in the polymer can be controlled by varying the elimination temperature. It should be noted, however, that uv/vis light spectrophotometry becomes insenstive to increasing conjugation above a conjugation length of about 6 repeat units,[65] thus this method cannot be used as a quantitative technique for assessing the extent of elimination PPV films with high degrees of elimination.

Thermogravimetry

Thermogravimetric scans of the poly(p-xylylene-α-dimethylsulfonium chloride) precursor to PPV were made in order to reveal at which temperature elimination occurs and how much time was required at a series of temperatures to reach constant weight. Figure 4.5 shows that the elimination does not occur in one transition, but that 5 transitions occur. The top curve (b) of Figure 4.5 is the first derivative (dW/dT) of the lower curve (a) of the weight loss as a function of termperature at a scan rate of 10°/min. The minima of the dW/dT vs. T curve showed that the transition temperatures where the

Figure 4.5.   Thermogravimetric analysis of (a) percent weight loss,

and (b) rate of weight loss as a function of temperature

for a film sample of poly(p-xylylene-α-dimethylsulfonium

chloride).
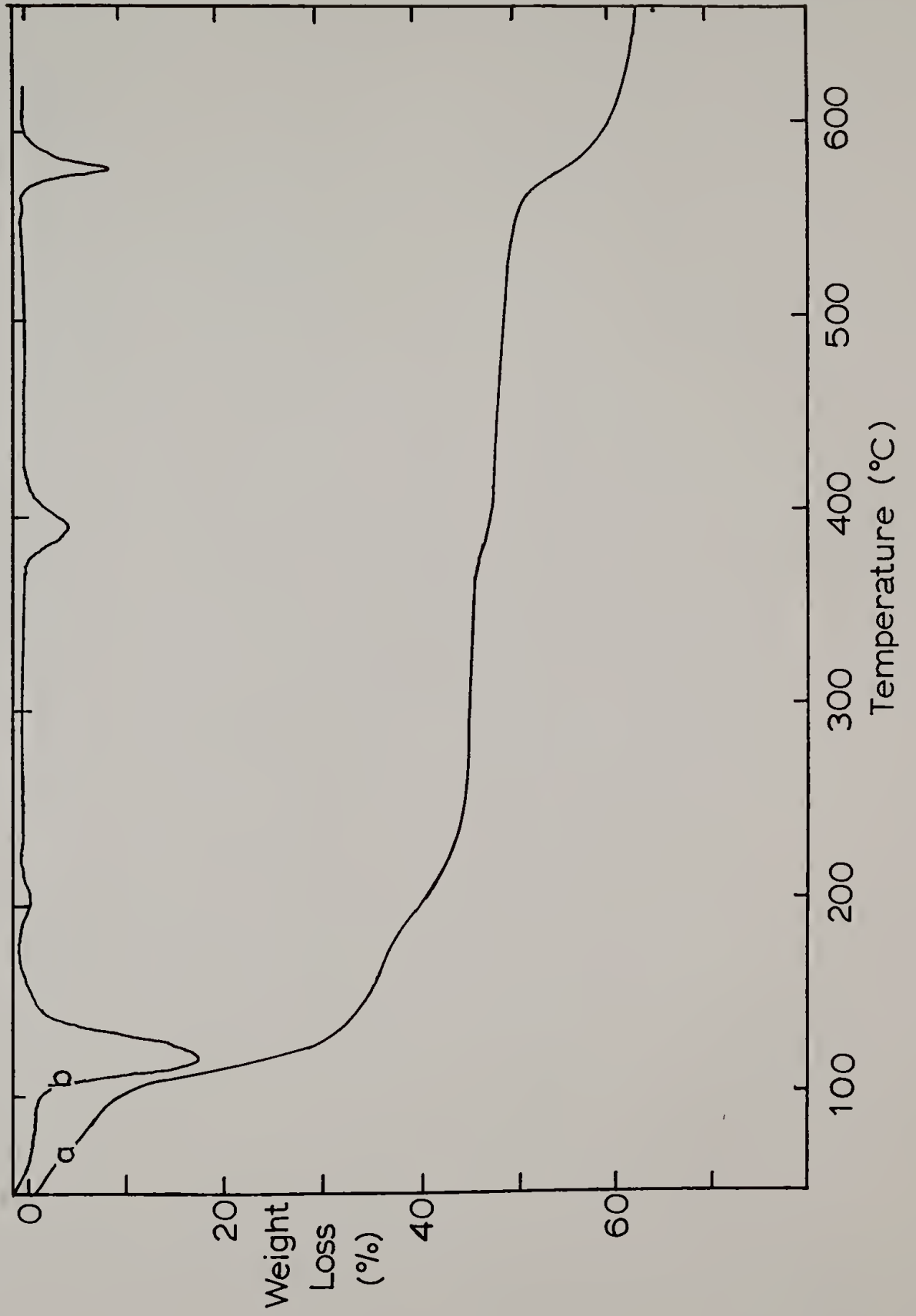
maximum rate of weight loss occur are at approximately $120^{\circ}C$, $150^{\circ}C$, $200^{\circ}C$, $395^{\circ}C$ and $580^{\circ}C$. This last transition is the degradation of PPV to a black graphitic film. Scans at higher scan rates, show a shift of these transitions to slightly higher temperatures, thus the data in Figure 4.5 should not be considered at equilibrium, and the true transition temperatures are probably shifted to lower temperatures by about $10^{\circ}C$. A scan rate of $40^{\circ}/min$ shifts the transition temperatures up by about $30^{\circ}C$ relative to the scan at $10^{\circ}/min$.

Figure 4.6 shows isothermal scans of weight loss as a function of time. It can be seen that the time to attain a stable weight decreases with a higher temperature; from about 30 minutes at $100^{\circ}C$ to about 5 minutes at $220^{\circ}C$. Thus, when preparing partially eliminated samples for analysis, elimination times of more than 30 minutes were required to ensure the relation of the elimination temperature to the composition without the uncertainty due to kinetic effects.

Elemental Analysis

Elemental analysis of the precursor polymer which had been eliminated for 24 hours at temperatures from 30° to $250^{\circ}C$ showed that the m:n ratio varies from 2:1 to 1:11 over that temperature range (Table 4.1). At $250^{\circ}C$ there was still a residual sulfur content of about 2.5 wt %, but residual chlorine was less than 0.1 wt %. Clearly, because of the lack of chlorine above $150^{\circ}C$, the simple elimination reaction involving only $(CH_3)_2S$ and HCl loss is not sufficient to characterize the thermal conversion mechanism of the precursor polymer.

Figure 4.6.   Isothermal weight loss versus time scans of

poly(p-xylylene-α-dimethylsulfonium chloride).
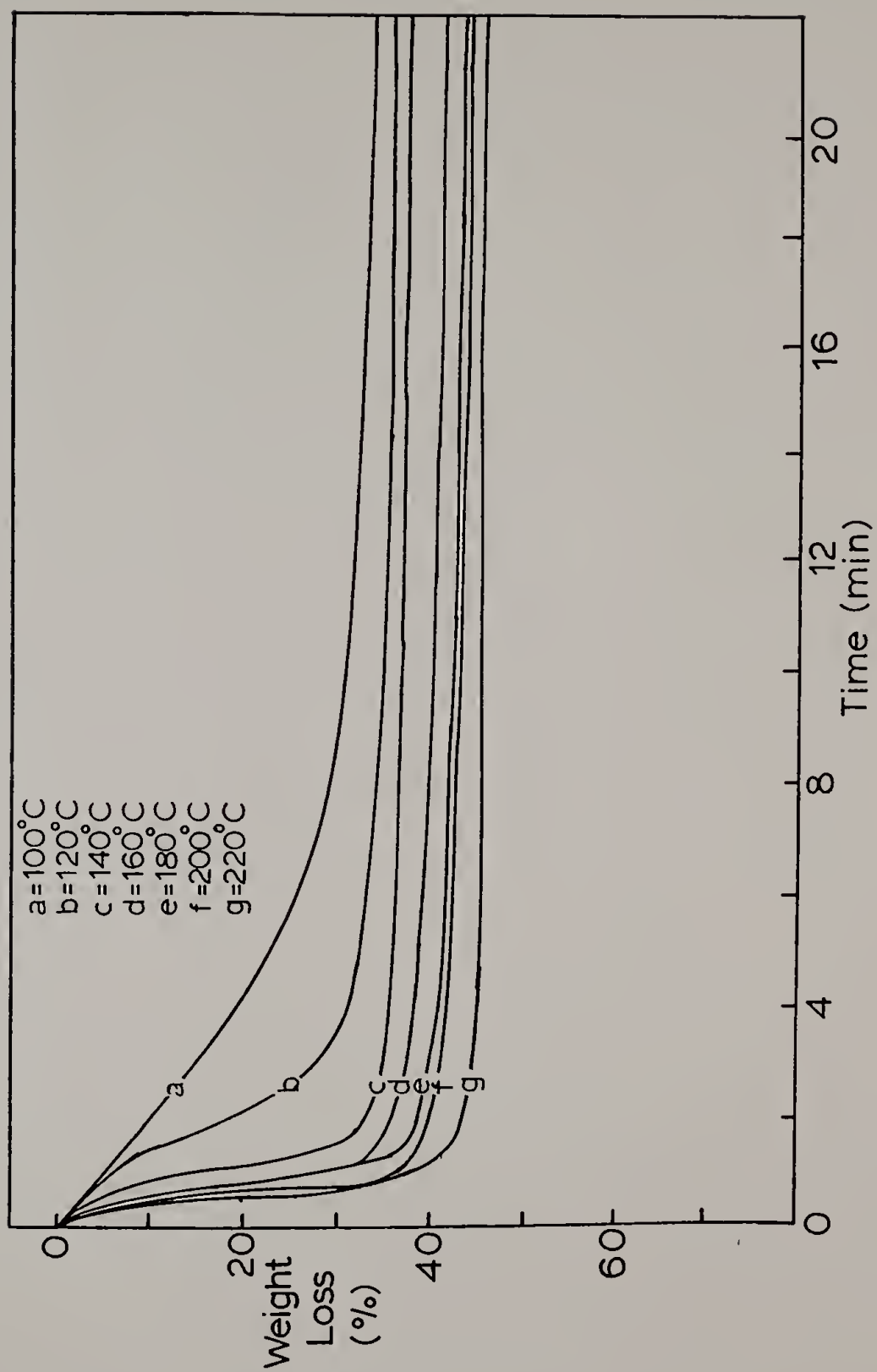
Table 4.1. Elemental analysis results for poly(p-xylylene-α-
dimethylsulfonium chloride) films eliminated at various
temperatures. The m:n ratios were calculated based upon
equation 4.5 in text.

Elimination Temp. (°C)	Weight %					m:n ratio
	%C	%H	%S	%Cl	%O	
25	50.8	7.1	9.6	--	--	1:2
30	52.9	6.9	8.9	--	6.0	3:4
85	74.9	6.1	7.9	6.7	4.4	2:1
130	84.4	5.8	4.5	1.4	4.0	5:1
148	84.9	6.0	4.3	<0.1	4.8	6:1
190	88.3	5.7	3.1	<0.1	2.6	8:1
240	88.2	5.6	3.3	<0.1	2.0	8:1
250	87.8	5.8	2.5	<0.1	3.8	11:1

As was discussed earlier in this chapter, and is depicted in Figure 4.7, sulfonium degradation can also occur by SN_2 attack of the halide counterion which yields an aklyl halide and a dialkylsulfide. Since no chlorine was detectable above 150°C, the formation of α-chloro-p-xylylene moieties (Equation 4.7 of Figure 4.7) does not occur to any great extent. This indirect evidence suggests that the other possibility, the loss of methyl chloride to leave p-xylylene-α-methylsulfide moieties (Equation 4.8 of Figure 4.7), is the probable elimination route. Thus at elimination temperatures between 150° and 250°C the partially eliminated copolymer can best be described as having the following structure:

$$\left(\underset{}{\bigcirc}-CH_2-\underset{\overset{|}{S-CH_3}}{CH}\right)_m\left(\underset{}{\bigcirc}-CH=CH\right)_n \qquad (4.9)$$
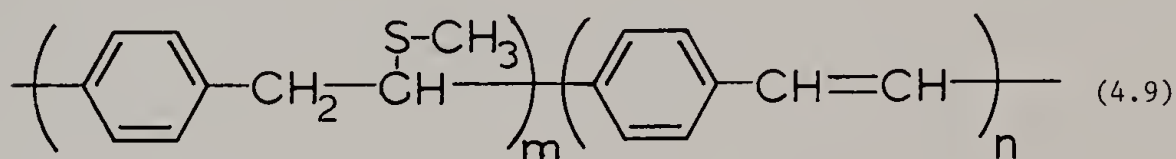
Thermogravimetry/Mass Spectroscopy

Further evidence supporting this elimination scheme has been obtained using thermogravimetric analysis coupled with mass spectrometry, MS, (Figures 4.8 and 4.9–4.11). The upper curve (a) of Figure 4.8 shows the rate of weight loss and the lower curve (b) shows total ion intensity data, obtained with the mass spectrometer, as a function of temperature. Three major thermal transition maxima occurred at 106°C (with a shoulder at 134°C), 360°C and 536°C corresponding, respectively, to two distinct elimination reactions and a degradation reaction.

Figure 4.7. Possible dealkylation side reactions of poly(p-xylylene-
α-dimethylsulfonium chloride): (Equation 4.7) chloride

attack at benzyl carbon, and (Equation 4.8) chloride

attack at methyl carbon.

$$\left(\!\!\!-\!\!\!\left\langle\!\!\!\!\!\bigcirc\!\!\!\!\!\right\rangle\!\!\!-\!\!CH_2\!-\!\!\underset{\underset{CH_3\overset{+}{S}CH_3}{|}}{\overset{^-Cl}{}}\!CH\!-\!\!\!\right)_n$$

$$\longrightarrow \left(\!\!\!-\!\!\!\left\langle\!\!\!\!\!\bigcirc\!\!\!\!\!\right\rangle\!\!\!-\!\!CH_2\!-\!\!\underset{}{\overset{\overset{Cl}{|}}{CH}}\!\!-\!\!\!\right)_n + (CH_3)_2S \qquad (4.7)$$

$$\longrightarrow \left(\!\!\!-\!\!\!\left\langle\!\!\!\!\!\bigcirc\!\!\!\!\!\right\rangle\!\!\!-\!\!CH_2\!-\!\!\underset{}{\overset{\overset{SCH_3}{|}}{CH}}\!\!-\!\!\!\right)_n + CH_3Cl \qquad (4.8)$$
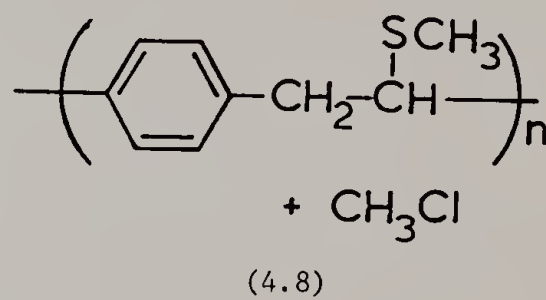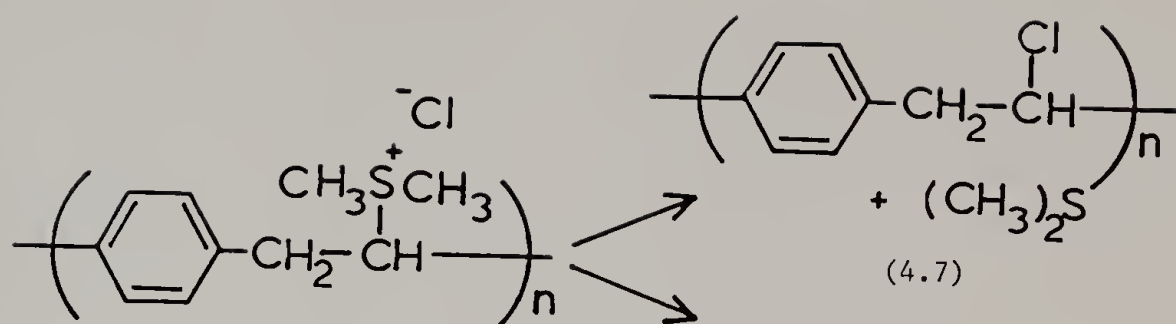
Figure 4.8.   (a) Rate of weight loss, dW/dT, and (b) total ion

intensity as a function of temperature. Curves obtained

from thermogravimetry/mass spectroscopy analysis on a

film of poly(p-xylylene-α-dimethylsulfonium chloride).
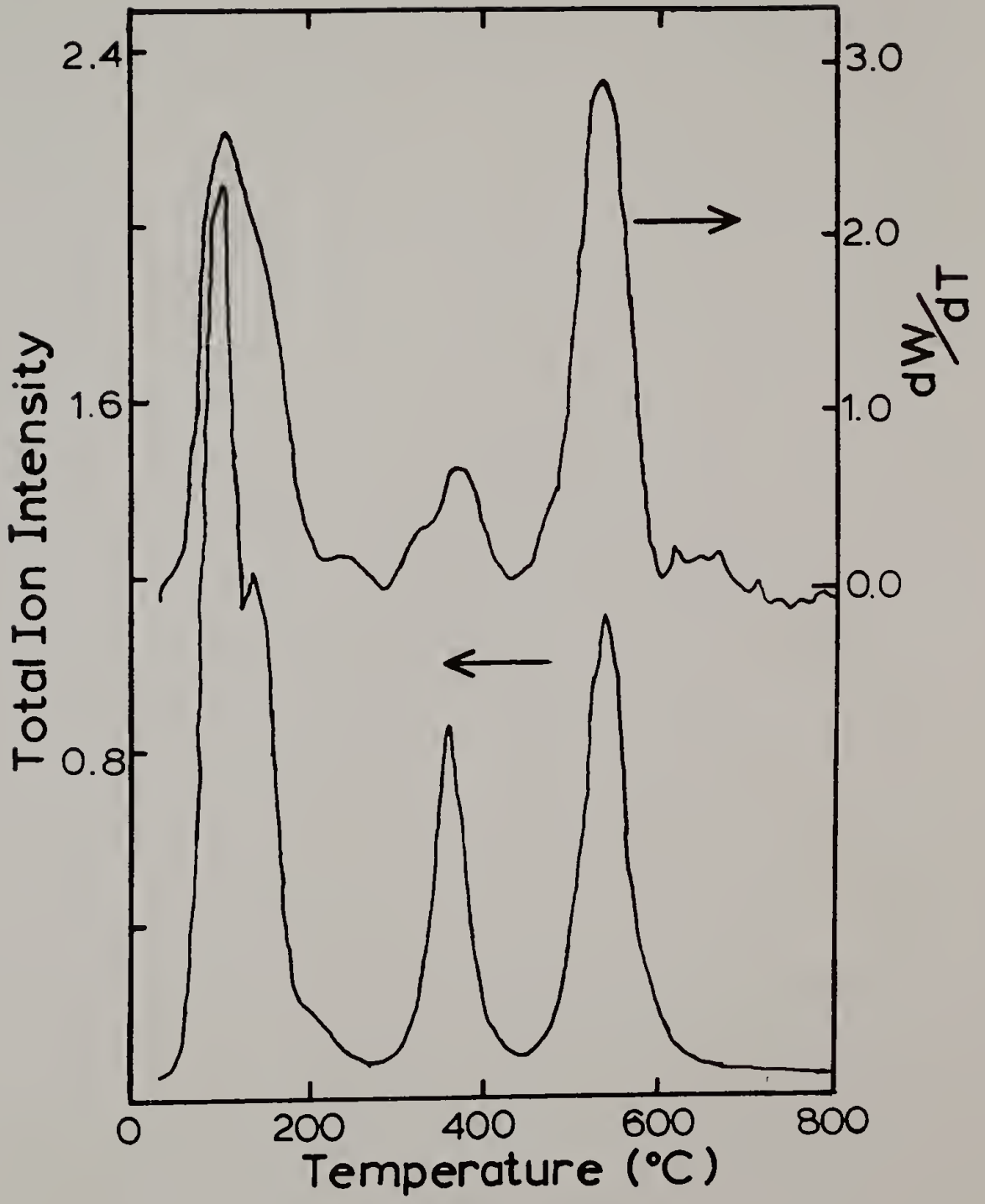
Figures 4.9, 4.10, and 4.11 show the MS composition analyses. The intensities of the peaks are roughly proportional to the amount of gas evolved but are not quantitative because of a dependence upon the electronic cross sectional area of the molecules, the fragmentation of the ion and the sensitivity of the mass spectrometer. The major components in the first peak were the water of hydration and the expected $(CH_3)_2S$ and HCl products formed from the ElcB elimination reaction. There was also a significant contribution from CH_3Cl formation by the dealkylation decomposition of the sulfonium salt as shown above. The second peak centered at $360^o C$ was associated with the radical thermal elimination of CH_3SH, and its radical combination products CH_3SSCH_3 and the presence of a small amount of CH_3SSSCH_3. Thus TGA/MS data, combined with information on the absence of any detectable sulfur (< 0.1 wt %) by elemental analysis in the samples eliminated at $370^o C$ for two hours, demonstrated that nearly quantitative conversion to PPV was only achieved above $360^o C$. The third peak, centered at about $550^o C$, corresponds to the degradation of the PPV backbone and is characterized by the loss of H_2, CH_4 and substituted benzenes.

PPV Film Characterization

Infrared Spectroscopy

Analysis by infrared spectroscopy of the fully eliminated PPV showed a strong absorbance at 963 cm^{-1} for the _trans_-vinyl CH out of plane bending mode, while no absorbance was observed at about 630 cm^{-1}

Figure 4.9. Ion intensity of H_2O, CH_3SCH_3, and CH_3SH as a function

of temperature. Data obtained as in Figure 4.8.
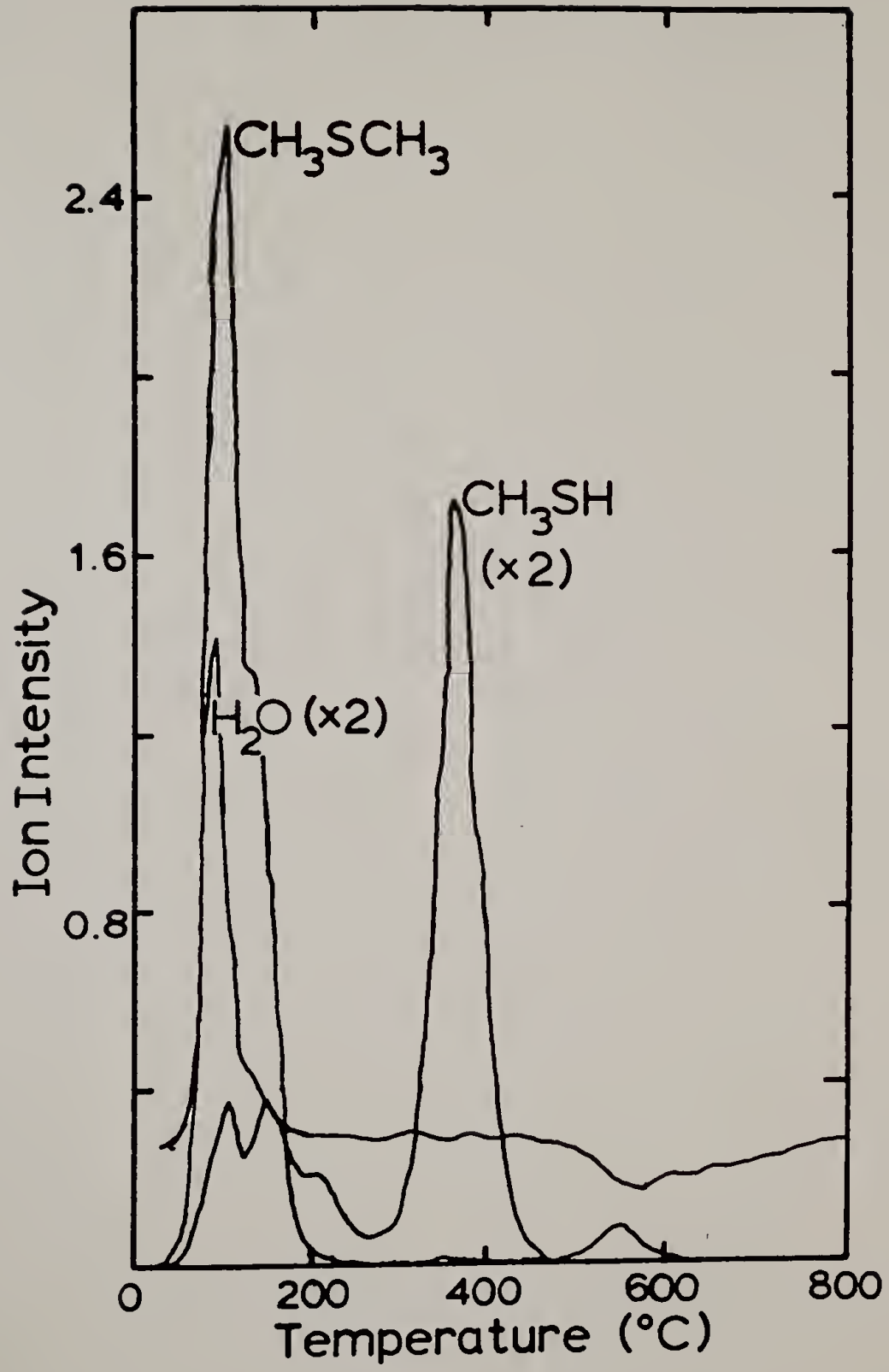
Figure 4.10. Ion intensity of CH_3Cl, CH_3SSCH_3, CH_4, and H_2 as a function of temperature. Data obtained as in Figure 4.8.
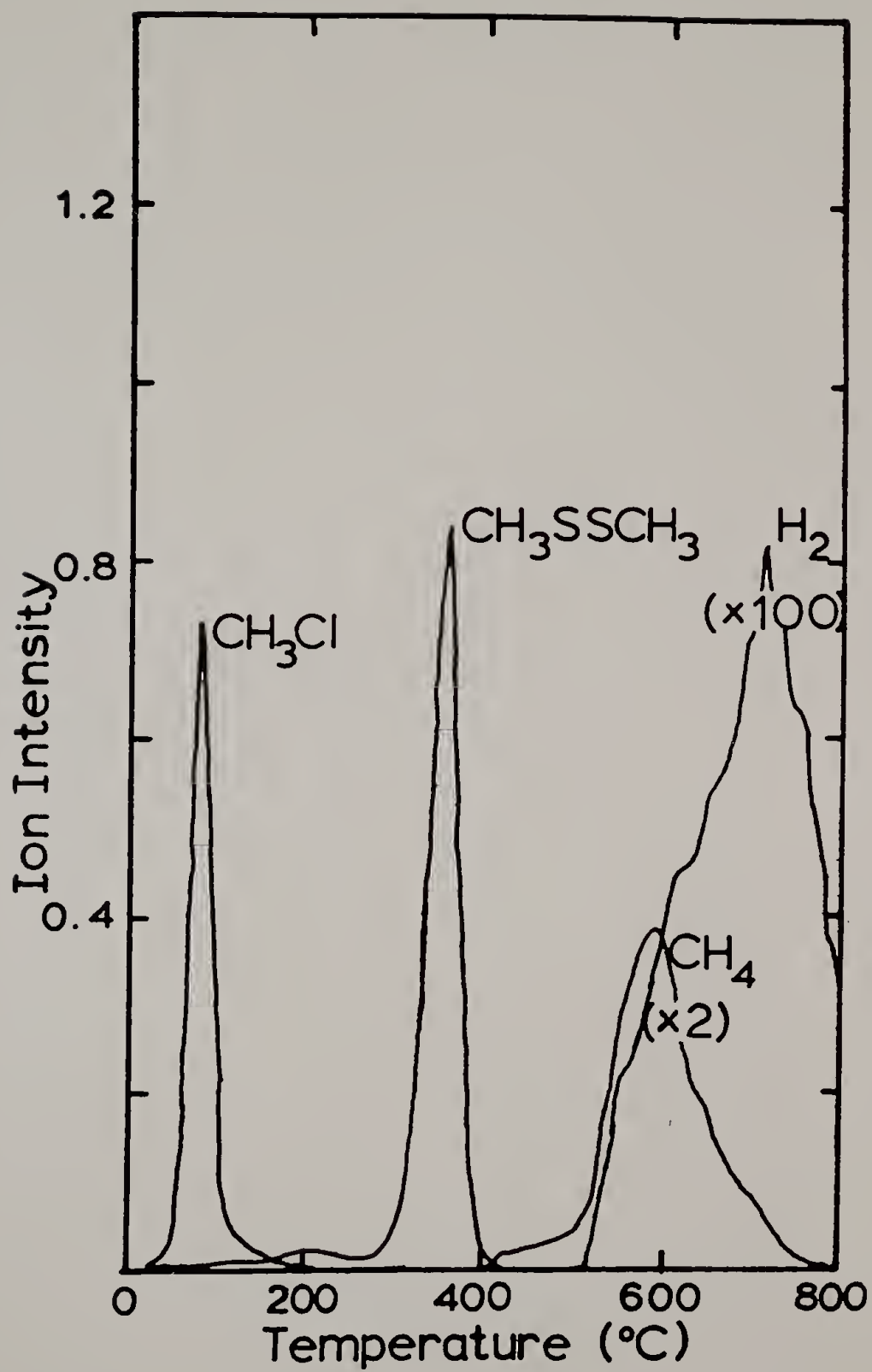
Figure 4.11. Ion intensity of HCl, CH_3SSSCH_3, and substituted

benzenes as a function of temperature. Data obtained

as in Figure 4.8.
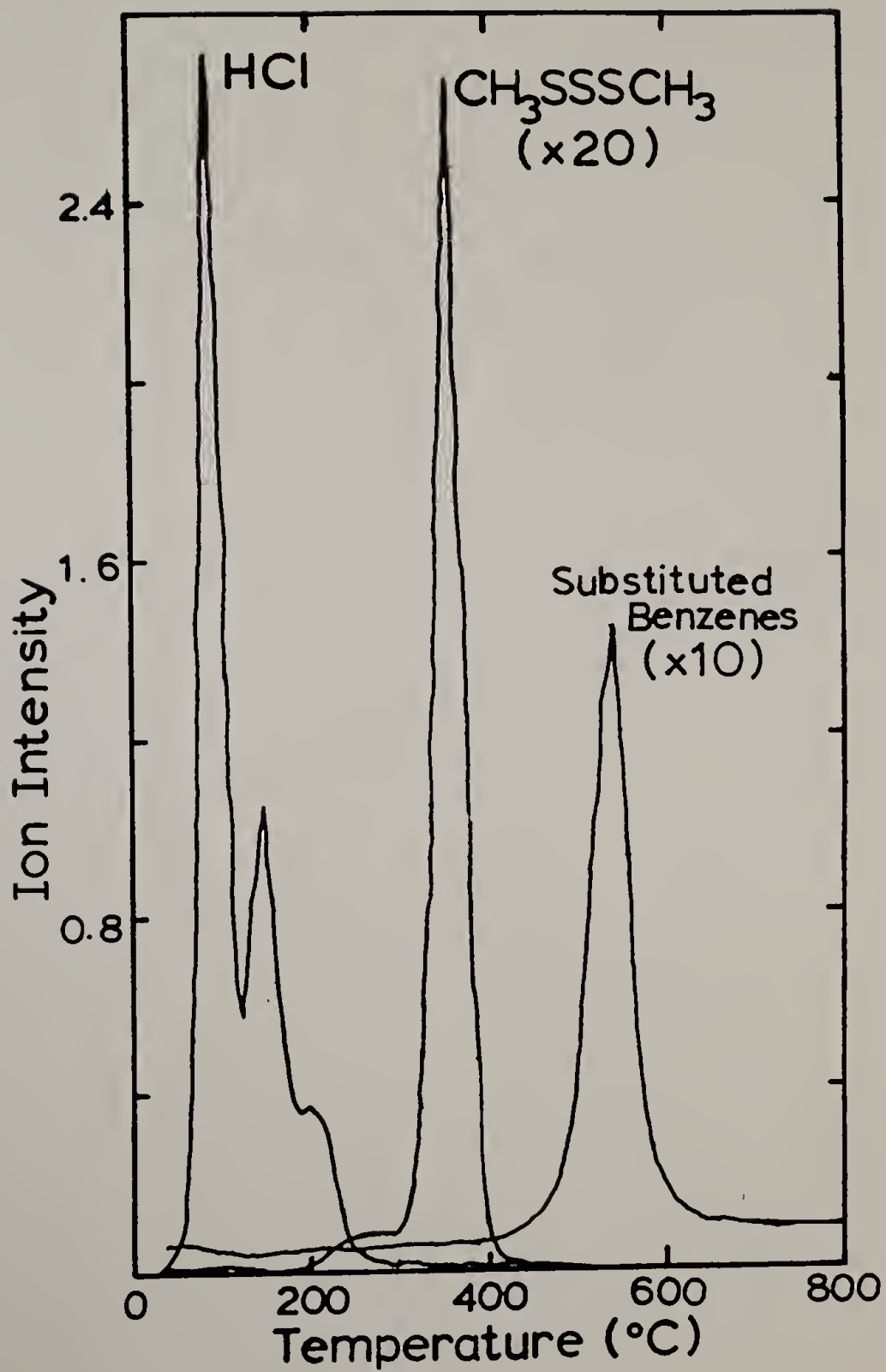
where the _cis_-vinyl CH bending mode would be expected (Figure 4.12).
Thus the elimination reaction yielded _trans_-PPV exclusively. The
presence of a small peak in the 2900 cm^{-1} sp^3 C—H stretch region
indicated, however, that there was a small fraction of uneliminated
units. Although these units have not been positively identified, their
concentration was so low that they were not expected to significantly
alter the doped electrical properties of the PPV films.

Differential Scanning Calorimetry

Analysis by DSC over a -196°C to 600°C temperature range of fully
eliminated PPV films showed that no glass or melt transitions occurred.
This confirms the highly rigid nature of the PPV chains and also
reconfirms the high temperature stability of PPV in an inert
atmosphere.

X-Ray Diffraction

Wide angle diffraction patterns of fully eliminated, unstretched
PPV films were recorded using the flat film Statton configuration.
These patterns (Figure 4.13) showed diffuse rings at d-spacings of
4.5Å, 3.2Å and 2.1Å. The diffuseness of these reflections indicates
that they correspond more to most probable close packing distances of
an amorphous system than to well defined crystalline reflections from a
semi-crystalline morphology. An analysis of the reflection breadth in
the 2θ direction will be presented in Chapter V to quantify this
conclusion.

Figure 4.12. Infrared spectrum of a fully eliminated PPV film.

119
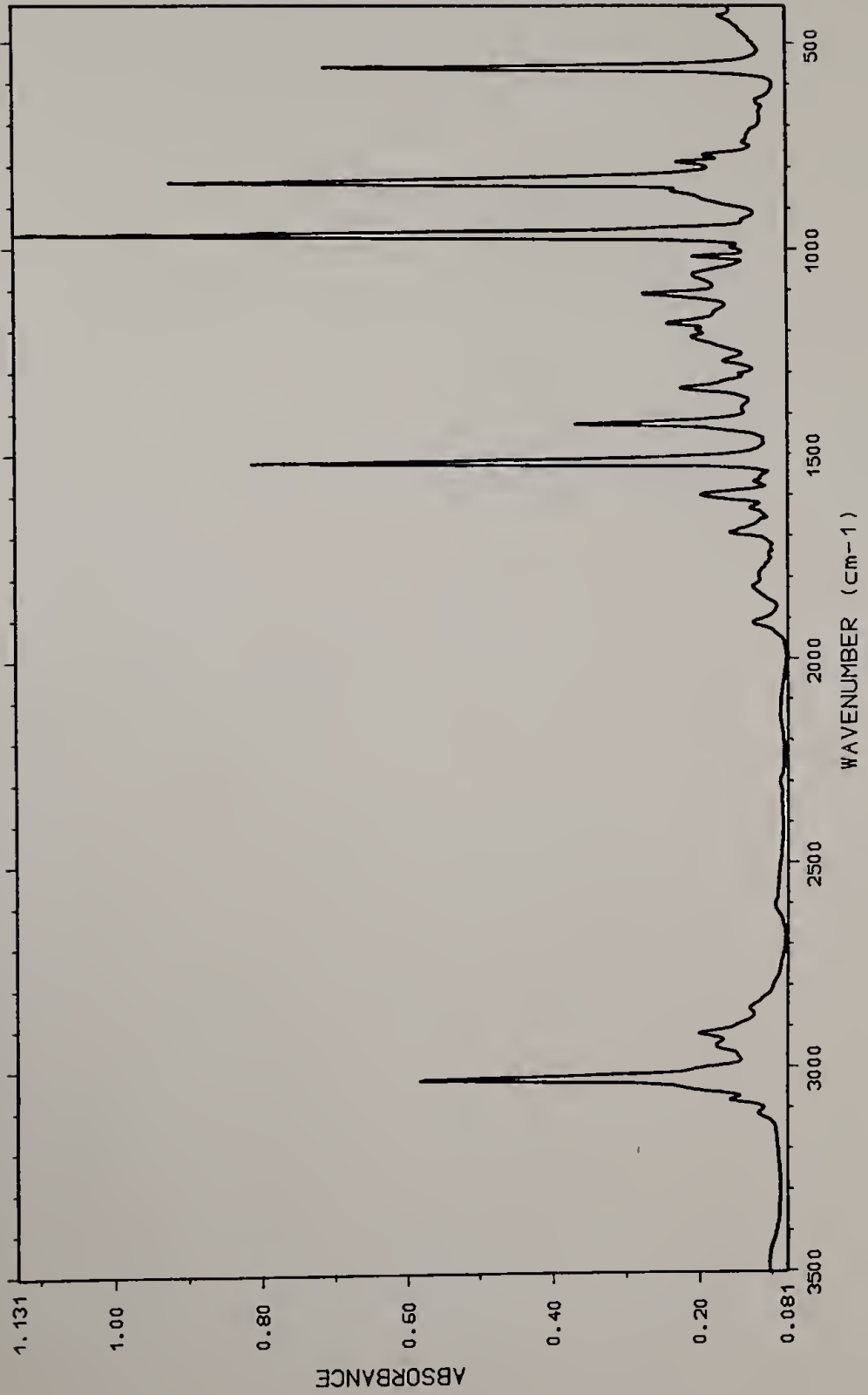
Figure 4.13. Wide angle x-ray diffraction pattern from a fully

eliminated PPV film.
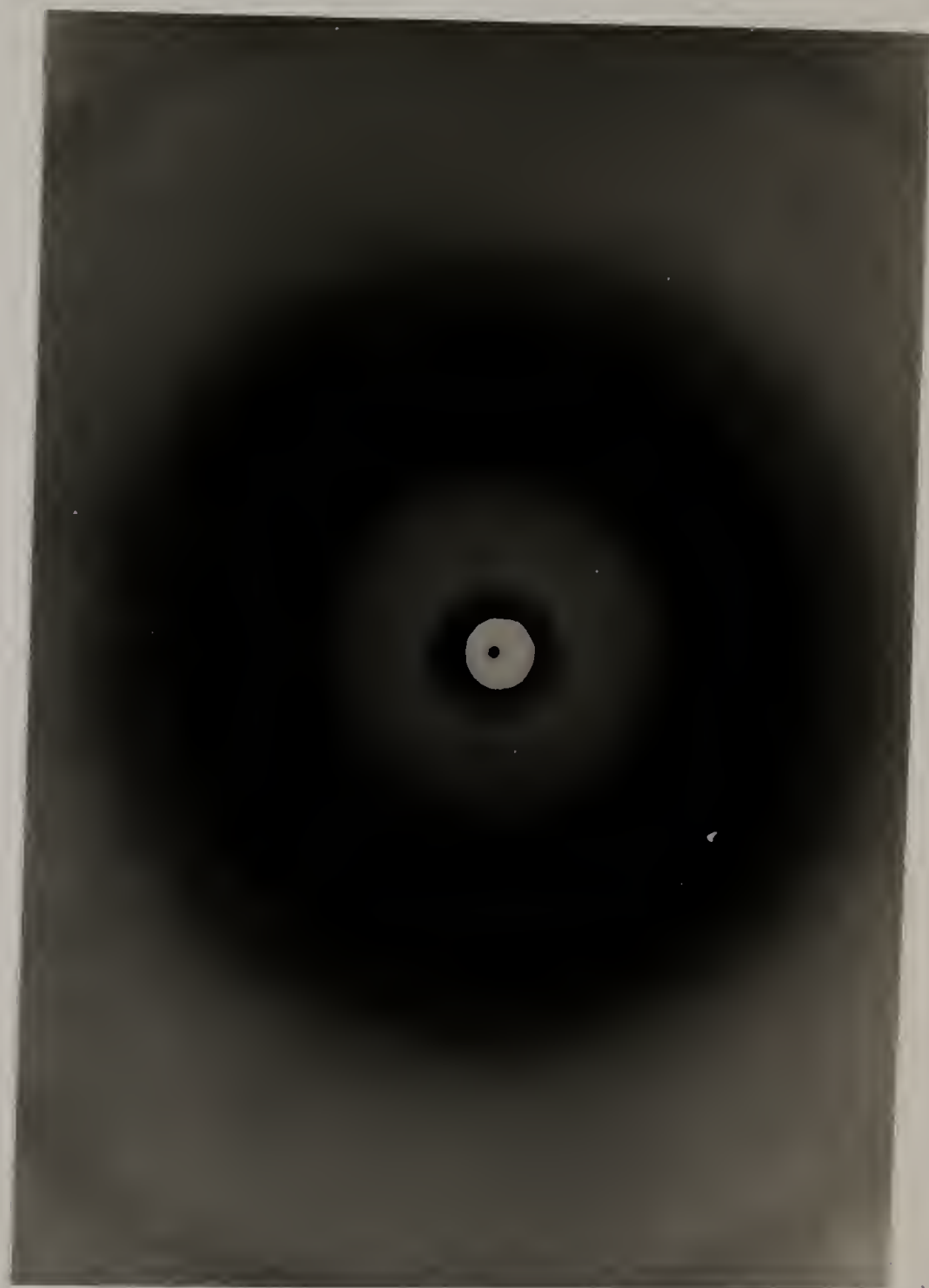
Optical Microscopy

Another indication that unoriented PPV unoriented films are amorphous is that viewing a PPV film between crossed polarizers with an optical microscope only showed optical extinction characteristic of an isotropic, amorphous material. Thus, if there are crystallites, they are not spherulitic in nature, nor are they larger than about 0.2 times the wavelength of light.

CHAPTER V

ORIENTED PPV

The ability to orient precursor films of PPV was due to the plasticization of the film by the volatile products produced from the thermal elimination conversion of the precursor PPV. In the previous chapter this reaction has been described in detail, and these results will be utilized in the first part of this chapter to understand the parameters which are important for the optimization of the stretching process.

The second part of this chapter details the results of experiments aimed at characterizing the microstructure of stretched PPV films. Highly oriented PPV films provided excellent specimens for electron diffraction studies which allowed the characterization of the crystallographic unit cell and of the rather unique paracrystalline type order of the system. The effect of the draw ratio upon the average molecular orientation in the stretch direction and upon the average transverse dimension of the crystallites are also presented in order to provide a structural foundation from which to understand the electrical conductivity results to be presented in Chapter VI.

Precursor Film Stretch Processing

Wessling and Zimmerman, in their 1972 patent[52b], first reported the stretching of PPV precursor polymer films which are intractable at

room temperature. The process they employed consisted of holding a strip of the film at the ends with tweezers and stretching it in a hot air stream at about 200°C. They reported draw ratios of up to 10 times the initial length, but did not report any details of the stretching mechanism involved, the physical characteristics of the process, or the molecular structure of final material.

Attempts to reproduce Wessling's work for the present study, proved quite successful. However, it was noticed that only the portion of the film which was placed in the hottest part of the hot air stream (from a heat gun) would stretch, and that the stretching occurred with necking similar to that observed in the stretching of semicrystalline thermo-plastics such as polyethylene. This observation, combined with the problem of film twisting induced by the high air flow velocity and the difficulty of controlling the temperature of the heat gun, gave impetus for the idea of the zone drawing process which has been used in this work as described in Chapter III.

The advantage of having the temperature control afforded by the zone drawing apparatus became apparent especially when studies of the elimination chemistry showed that the thermal elimination reactions occur at well defined temperatures. The observation that stretching could only be performed when the zone temperature exceeded 110°C was explained by the fact that the first elimination transition, consisting of the loss of the water of hydration and of methylsulfide and HCl, also occurred at $\sim 110^{\circ}$C. Thus, it was inferred that the volatile elimination products were acting as a plasticizer for the precursor polymer; or more precisely, for the partially eliminated precursor

co-polymer consisting of both uneliminated sulfonium repeat units and
of eliminated phenylene vinylene units.

Effect of Precursor Elimination Degree

The ease with which stretching could be performed depended upon the
initial amount of partial elimination which had occurred during the
casting of the films and during the storage of the cast films at room
temperature. Although the rate of elimination was a maximum at
$\sim$ $110^{\circ}C$, the sulfonium group was quite labile even at room
temperature. The presence of water was found to stabilize the
sulfonium moiety of the precursor polymer, but upon removal of the
water during casting a small amount of slow elimination took place.
Freshly cast films were generally a light green color and could be
described as a copolymer represented by

$$\left(\underset{\displaystyle}{\text{---}}\!\!\left\langle\bigcirc\right\rangle\!\!-CH_2-\underset{\overset{\displaystyle Cl^- \;\; H_3C\diagdown\overset{+}{S}\diagup CH_3}{\displaystyle}}{CH}-\right)_m\!\!\left(\left\langle\bigcirc\right\rangle\!\!-CH=CH\text{---}\right)_n$$
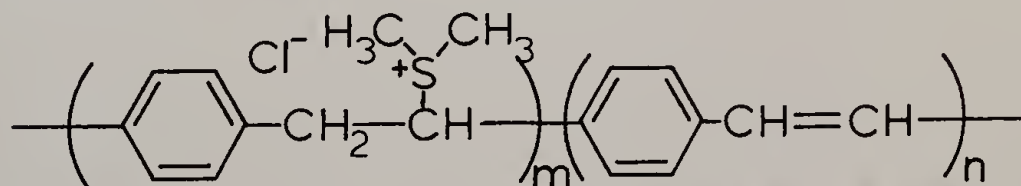
with an m:n ratio of about 4:1. After 3 weeks at room temperature this
ratio stabilized to an m:n ratio of about 1:2, and the film was bright
yellow in color. Therefore, the fact that the stretchability of the
films depended upon the age and color of the film was interpreted to
mean that stretching depended upon the total amount of plasticizer
available (i.e., the m:n ratio).

Effect of Stretch Temperature

The ability to stretch to high draw ratios also depended upon the

amount by which the zone temperature exceeded the 110° temperature at which stretching began. The loss of the volatile elimination products from the film was diffusion controlled, and the rate of elimination depended upon the temperature. Thus, the ability to stretch the precursor film was also a function of the instantaneous concentration of plasticizer within the film determined by the temperature. At temperatures above 180°C, however, elimination product formation occurred much too quickly and voids (bubbles) formed in the film. During stretching these voids elongated, resulting in highly fibrillated films with poor mechanical integrity especially in the transverse direction.

Based upon these considerations, the optimum conditions for obtaining coherent, uniformly stretched PPV films with high draw ratios were to begin with a precursor film having an m:n ratio of about 2:1 and to stretch at a temperature between 110°C and 180°C. It was difficult to obtain evenly drawn samples with low draw ratios by the admittedly crude hand stretching technique used in this study, especially when beginning with precursor films having an m:n ratio greater than 1:1. This was because once the zone temperature exceeded 110°C, the film stretched too easily to control well. Therefore, films of low to moderate draw ratios were obtained by beginning with a more highly eliminated precursor film and by using a lower zone temperature. Both of these two conditions limited the attainable draw ratio.

Prior to the final elimination of the unconstrained oriented films at 365°C in vacuum, the stretching procedure resulted in partially eliminated precursor films having an m:n ratio of about 1:5 by

elemental analysis. This high degree of elimination meant that as the stretching was being performed, the oriented structure was being locked in by the high rigidity of the conjugated sequences being formed. So even though the initial precursor film was basically amorphous (as will be shown below by x-ray diffraction), the orientation process occurred without any subsequent relaxation of the chains. Relaxation was further impaired by the zone drawing technique because the stretched portion of the film was continually being removed from the heat zone during the process which effectively quenched the polymer back to room temperature. Since the films were quite thin ($\sim$ 10 μm), the film cooled rapidly when removed from the heat zone. These factors provided a reasonable explanation of the extremely high efficiency of the drawing process for imparting the molecular orientation to be demonstrated in the following sections of this chapter.

Crystal Structure of Highly Drawn PPV

Wide Angle X-ray Diffraction

Flat film wide angle x-ray diffraction, WAXD, patterns of highly oriented PPV films consisted of sharp equatorial reflections perpendicular to the stretch direction and up to 3 orders of layer lines at regularly spaced intervals along the stretch axis (the fiber axis). Figure 5.1 shows a typical diffraction pattern of a sample stretched to a draw ratio of 14. The ring of intensity which is present is due to sodium chloride dusted on the sample to enable calibration of the camera length (see Chapter III). Unfortunately,

Figure 5.1. Wide angle x-ray diffraction pattern obtained from PPV

film stretched to a draw ratio of 14.

flat film WAXS experiments were plagued with the problem of Ewald
sphere distortion at high scattering angles,[67] thus the higher order
layer lines and equatorial reflections became diffuse and could not be
observed clearly, making measurements of the reflection Bragg angles
imprecise.

These patterns were, however, quite useful for initial character-
ization of the structural order imparted to the stretched PPV film
because they clearly demonstrated a high degree of uniaxial order. The
sharpness of the equatorial reflections in the equatorial and azimuthal
directions indicated respectively, both well defined lateral packing
order and nearly perfect molecular alignment along the draw direction.
The distinctive feature of the layer lines was that they were composed
of diffuse streaks of varying intensity perpendicular to the fiber
axis; that is, they did not show any evidence of hkl type reflections.
This continuous streaking of the layer lines is a clear indication that
the nearly perfectly aligned polymer chains have a considerable amount
of axial translational disorder,[95] a structure similar in concept to
a frozen nematic liquid crystal.[96] Another way to conceptualize this
structure is as a bundle of periodic rods where there is little or no
correlation to the equivalent axial positions of the adjacent periodic
units of the rods. Disorder such as this has been observed previously
in some biological materials including collagen,[97] α-keratin,[98]
muscle,[99] and in some synthetic polymers including isotactic
polystyrene,[100] poly(β-propiolactone),[101] aromatic
copolyesters,[102] and aromatic heterocyclic polymers including
poly(p-phenylene benzobisthiazole).[103,104] This translationally

disordered structure will be discussed in greater detail below in light of the information obtained from electron diffraction experiments.

A quantitative measure of the reflection Bragg angles was obtained using a Siemens D-500 wide angle x-ray diffractometer. D-500 scans in the meridional direction (i.e., along the fiber axis) enabled precise calculation of a polymer repeat unit spacing of 6.58 Å which corresponded exactly to that calculated based upon the bond lengths and bond angles reported for <u>trans</u>-stilbene by Finder et al.[105] Figure 5.2 shows a D-500 scan in the equatorial direction from a PPV sample with a draw ratio of 13.5. Three well defined reflections and a broad, weak reflection could be resolved at d-spacings of 4.31 Å, 3.98 Å, 2.41 Å, and 1.87 Å. There was also a poorly resolved shoulder on the first reflection at about 3.98 Å. With only three clearly resolved reflections, indexing of the PPV unit cell would be ambiguous at best, and the weakness of the reflection at the highest scattering angle made the measurement of its Bragg angle suspect. One of the primary difficulties in obtaining scans with higher reflection intensity was that the oriented films were generally only less than 10 μm thick. The usual procedure for thin films is to stack them to increase the scattering volume. But in this case, where the film is so highly oriented, stacking could not be done without introducing artificial orientational disorder. Thus, x-ray diffraction did not provide enough information to index the crystallographic unit cell. However, x-ray diffraction analysis of the first two strong reflections was useful for studying the degree of molecular orientation and the transverse crystallite size as a function of the draw ratio.

Figure 5.2.   Wide angle x-ray D–500 diffractometer scan of equator

for a PPV film stretched to a draw ratio of 13.5.
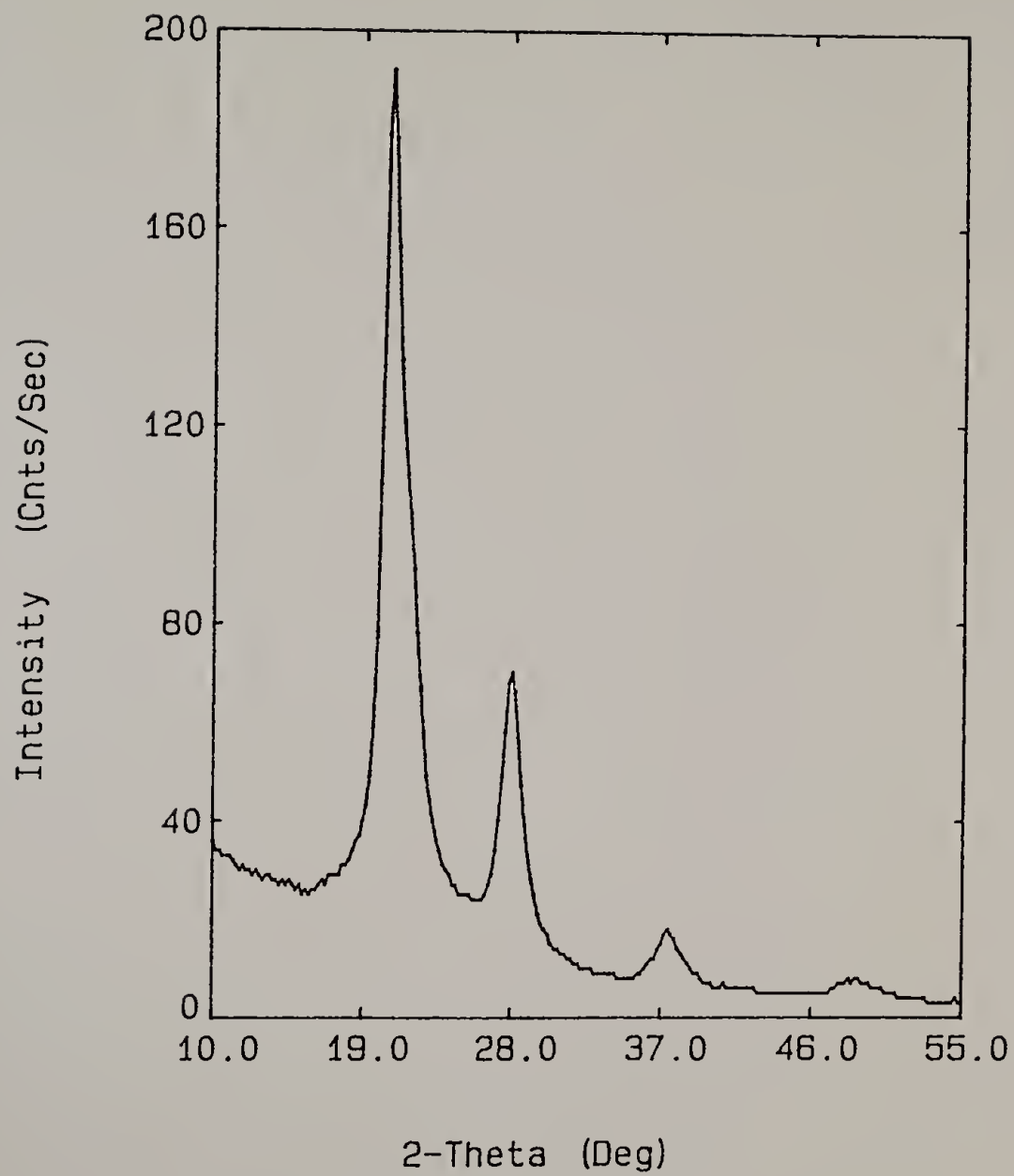
Unit Cell Analysis by Electron Diffraction

Electron diffraction was the method of choice for obtaining the
necessary information to analyze the crystal structure of PPV primarily
because it requires only very thin samples (< 1000 Å) which could be
easily prepared by mechanical fibrillation of oriented films, and
because Ewald sphere distortions are minimized by the small wavelength
of the electron radiation. The electron diffraction pattern obtained
from a PPV film sample, stretched to a draw ratio of 14.5, is shown in
Figure 5.3. The pattern exhibited 7 observable sharp equatorial
reflections and 7 layer lines. Again, as with the WAXD patterns, the
layer lines showed an absence of any sharp hkℓ type reflections. The
first layer line did, however, show reflections located off of the
meridian with a broad intensity profile symmetric about and
perpendicular to the meridian. The d-spacing, measured between the
reflections on the first layer line, was 5.09 Å.

The indexing of the equatorial and first layer line reflections by
Dr. Thierry Granier gave a monoclinic unit cell with the following
dimensions: a = 7.90 Å, b = 6.05 Å, c = 6.58 Å (chain axis), α = 123°,
and a setting angle, ϕ, (the angle between the plane of the molecule
and the b axis) of $\sim$ 56°.[106] The unit cell contained 2 repeat units
and yielded a calculated density of 1.28 g/cm^3 which agreed well with
the density of oriented PPV films, obtained by the floatation method,
of 1.24 g/cm^3. Figures 5.4 and 5.5 show the a-axis and c-axis
projections of the PPV unit cell. Table 5.1 lists the indices of the
equatorial reflections along with their observed and calculated values
for the d-spacings and intensities. The intensities were calculated

Figure 5.3. Electron diffraction pattern from a PPV film stretched

to a draw ratio of 14.5.

Figure 5.4. a-Axis projection of unit cell for oriented PPV.
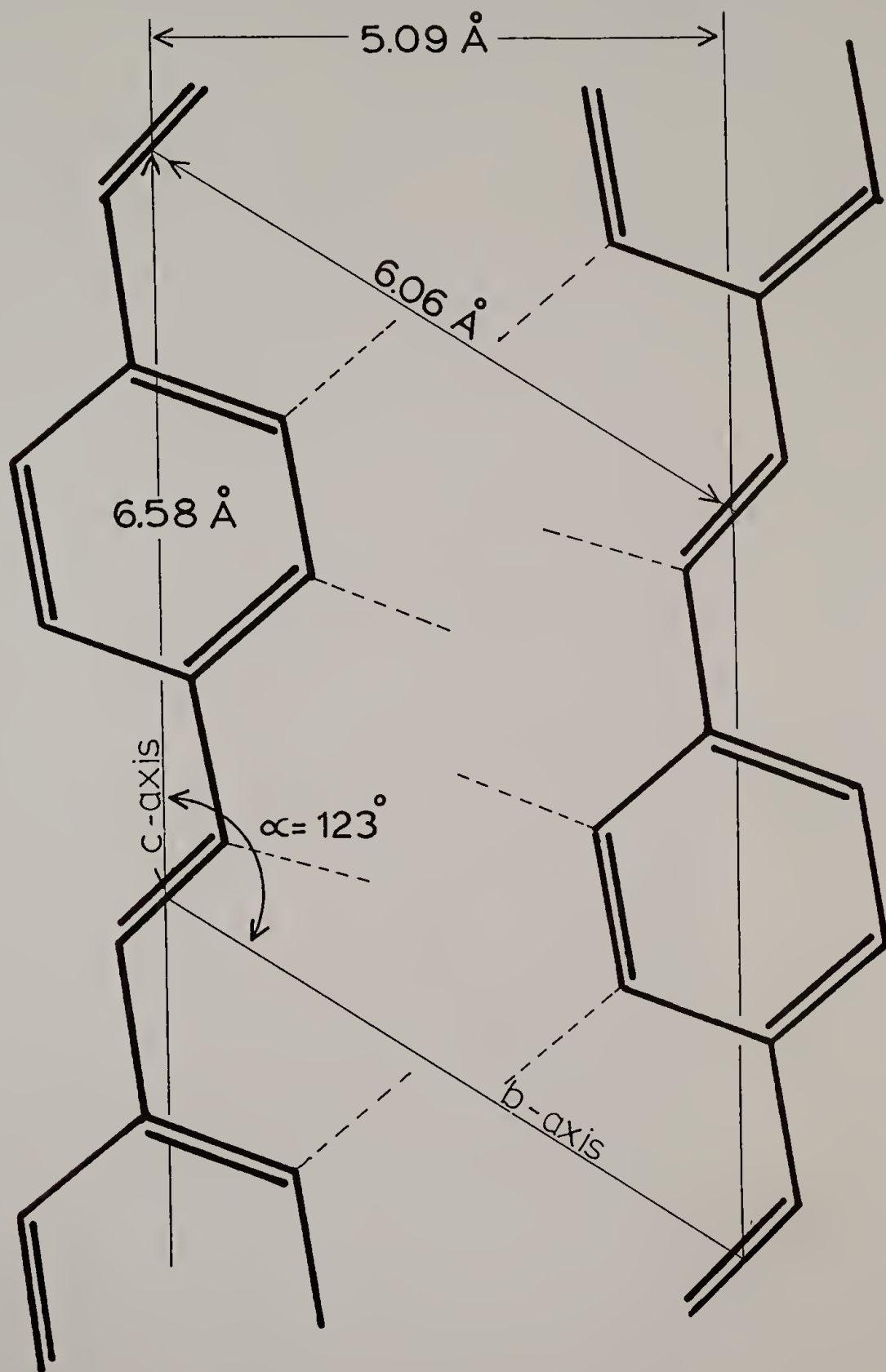
Figure 5.5. c-Axis projection of unit cell for oriented PPV.
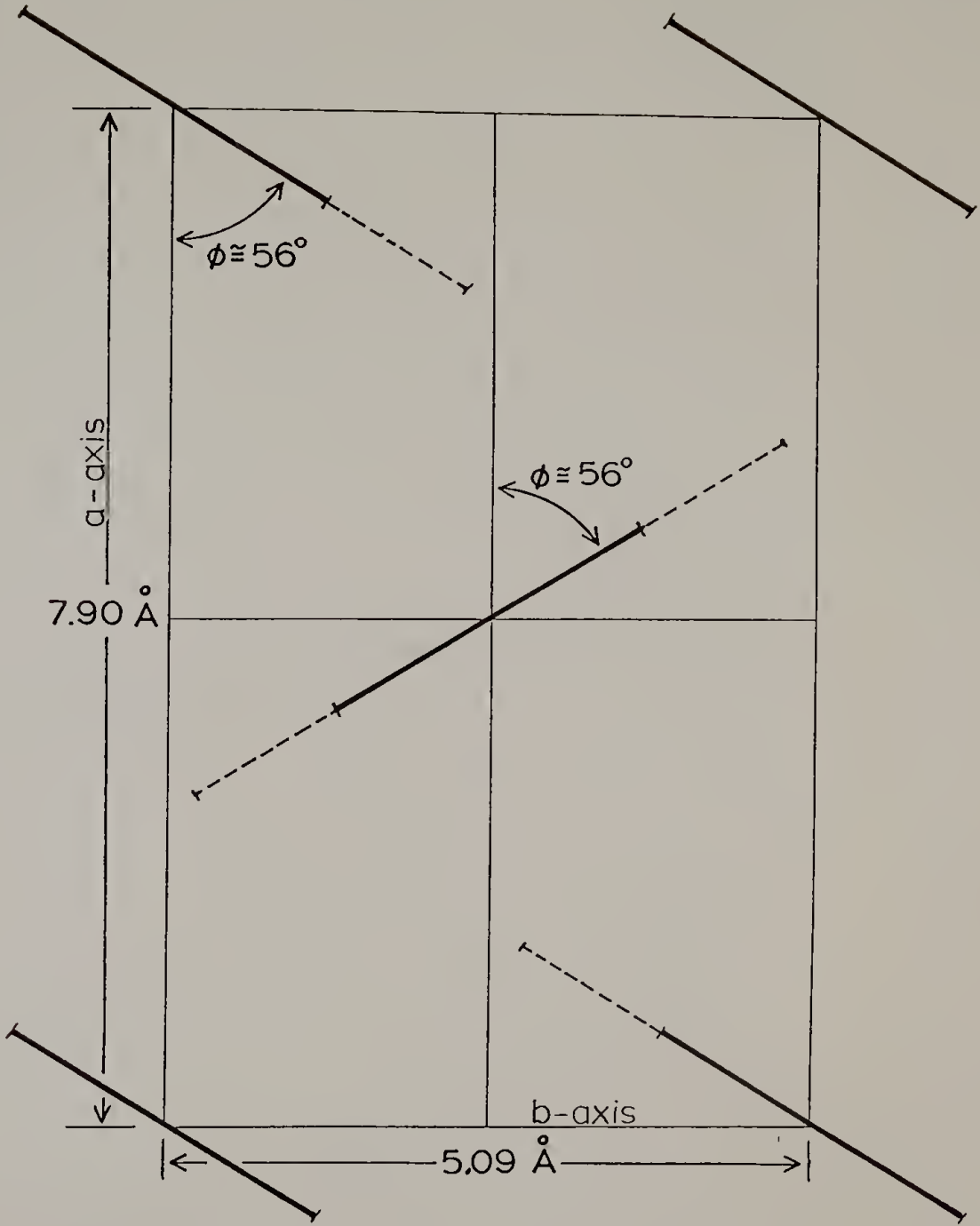
Table 5.1. Indices, d-spacings, and intensities of the equatorial
reflections obtained from the electron diffraction
pattern of Figure 5.3 and calculated from the unit cell
parameters.

hkl	d calc.	d obsd.	I calc.	I obsd.
110 200	4.28 3.95	4.28 3.95	166	241
210	3.12	3.10	51.6	26.6
020	2.54	---	0.2	---
120	2.42	---	0.5	---
310	2.34	2.32	5.8	5.9
220	2.14	2.14	0.4	0.3
400	1.98	1.98	0.0	0.1
320 410	1.84 1.82	1.84	1.1	2.7
130	1.66	---	0.0	---
420 510 230	1.51 1.56 1.55	1.55	0.1	0.4

based upon a planar stilbene model shown in Figure 5.6; and since they correlated well with the observed intensities, the planar model seemed to be quite plausible. In Finder's study,[105] stilbene was shown to have a small dihedral angle (3° – 5°) between the vinyl segment and the phenyl ring. However, variation of 0° to 10° did not affect the intensity calculations for PPV. Thus, due to the long range conjugation shown by the uv/vis spectrum, there was no reason to suspect PPV was not itself planar.

The streaking of the intensity on the higher order layer lines and the appearance of partially streaked reflections on the first layer line could be understood using the concept of paracrystallinity.[106] The intensity profiles along the layer lines for a system of oriented chains where there is no interchain correlation of the repeat unit positions at all, can be calculated just from the knowledge of the atomic structure of the repeat units in a single chain using molecular transform calculations.[101] In a paracrystalline system, there is only a small degree of interchain positional correlation of nearest neighbors, thus the probability of positional correlation drops off rapidly when considering smaller scale dimensions; that is, the relative disorder becomes larger. Higher order layer lines probe shorter range positional correlations in real space. Thus, if there is poor positional registration, the higher order layer line intensity profiles would correspond to those calculated by the molecular transform method for complete axial randomness, but the lower order layer line profiles would deviate significantly from the random model.

143

Figure 5.6. Planar model of PPV showing bond lengths and
105
bond angles.

-------	1.44 Å
———	1.39 Å
═══	1.33 Å
———	1.09 Å
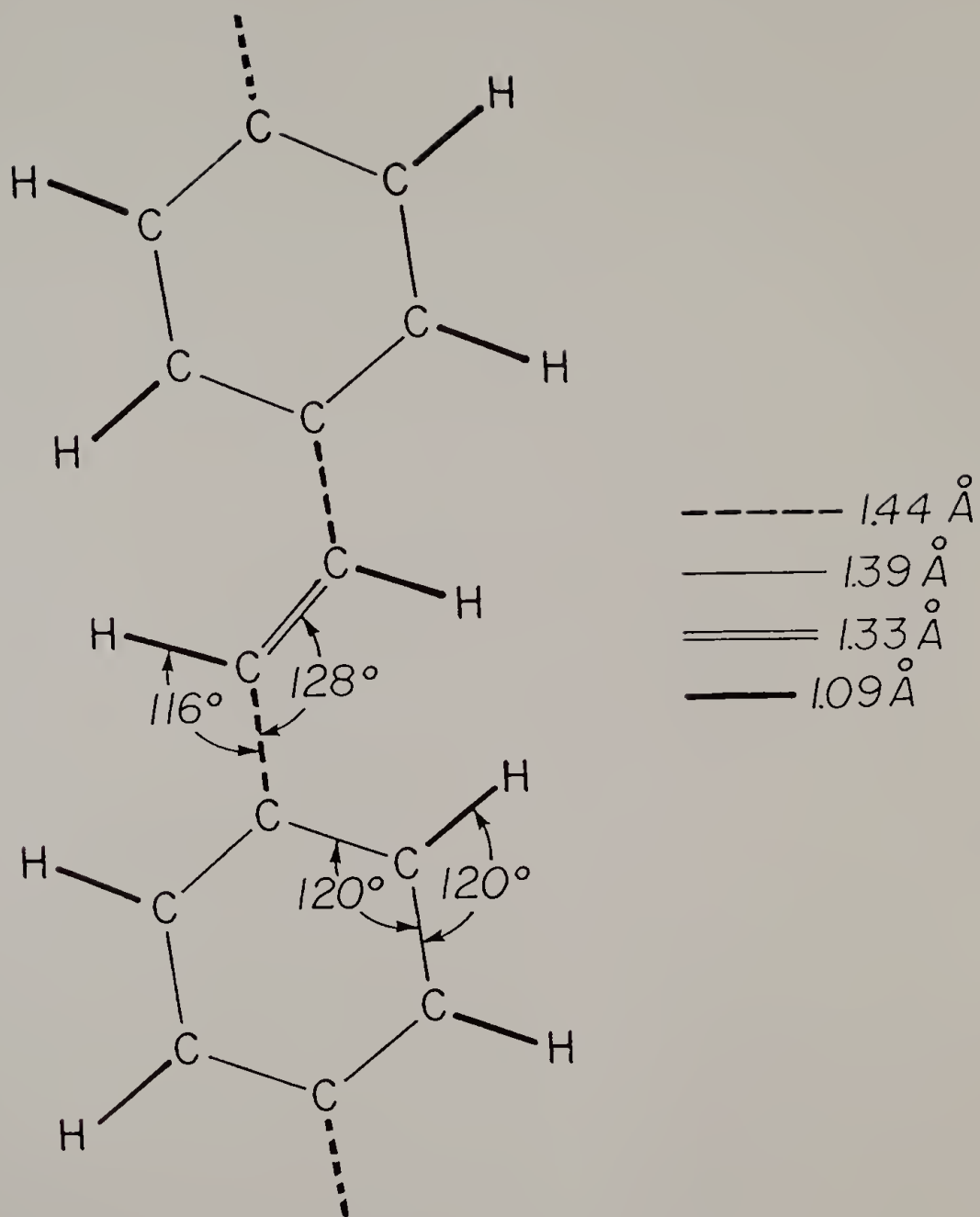
Figure 5.7a shows a schematic of the experimentally obtained ED pattern of PPV (λ = 14.5), and Figure 5.7b shows the layer line intensity profiles obtained by the molecular transform calculation using atomic positions based upon those reported for trans-stilbene by Finder.[105]   Also included in the lower half of these figures is the indexed reciprocal lattice and the reciprocal axis vectors of the PPV unit cell. The layer line intensity profiles, ℓ = 4, 5, and 6, of Figure 5.7a agreed quite well with the intensity profiles from the molecular transform calculations in Figure 5.7b. The deviation from Figure 5.7b became greater, however, with decreasing layer line index. The ℓ = 3 line shows that the calculated single central maximum was experimentally split into two maximum. The ℓ = 2 line had an extra maximum on the meridian. And the ℓ = 1 line deviated completely from what would be expected from a system with totally random axial translational disorder. The most interesting piece of structural information gained from this analysis, though, was that the first layer line only showed reflections due to positional correlations in the bc plane of the unit cell. What this means, is that the structure of highly oriented PPV films consisted of chain extended crystallites which were quasi-sheet-like in nature. That is to say that, there was virtually no registration in the a axis direction between parallel bc planes, while the degree of paracrystalline disorder within the bc planes, had an axial shift magnitude of about $0.5\overset{\circ}{A}$. This structure has important implications on the understanding of the electrical anisotropy displayed by oriented PPV and the possible charge transport mechanism responsible for conduction, because a high degree of axial

Figure 5.7. (a) Schematic of the experimentally obtained electron

diffraction pattern of Figure 5.3 including Miller

indices, (b) calculated layer line intensity profiles

based upon random translational disorder model.
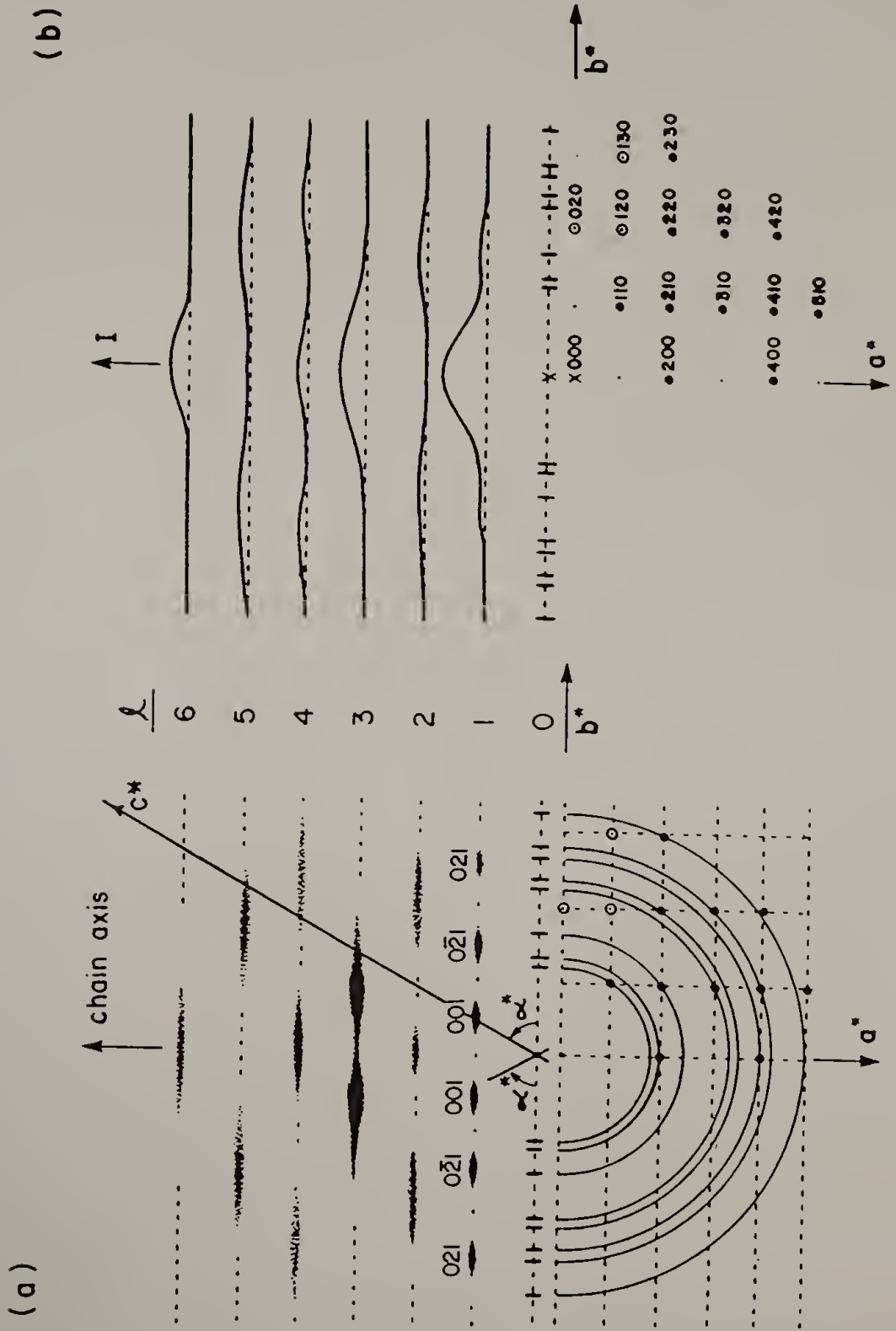
fluctuation would reduce the probability of interchain π-orbital overlap. Future structural and conductitivy studies should be done on the effect of tensile stress during the final thermal elimination registration and hence higher interchain π-orbital overlap.

Molecular Orientation

X-ray Diffraction Results

Figure 5.8 shows a series of flat film x-ray diffraction patterns obtained from PPV films stretched to draw ratios ranging from 1.0 (unoriented) to 14.8. Focusing attention on the equatorial reflections, there was a remarkable decrease in the azimuthal spread of these reflections with increasing draw ratios which indicated that the molecular orientation of the PPV chains was strongly dependent upon the draw ratio. In order to quantify this dependence, the intensity of the first equatorial peak, the (110) reflection, was measured as a function of the azimuthal angle away from the equator using the D-500 x-ray diffractometer. Ideally, a meridional reflection would be used to obtain a direct measure of the average chain orientation with respect to the fiber axis. However, with PPV, there were no useful meridional reflections available due to the axial translational disorder of chains. By choosing to use an equatorial reflection and an equatorial frame of reference, the average orientation of the perpendicular of the chain axis was actually measured with respect to a direction perpendicular to the fiber axis. Since PPV is highly conjugated and thus rigid, this convention should be a good approximation to the

Figure 5.8. Wide angle x-ray diffraction patterns obtained from films of PPV stretched to draw ratios, λ, in the range of 1 (unoriented) to 11.

λ=1.2

λ=1.1

λ=5.7

λ=2.7
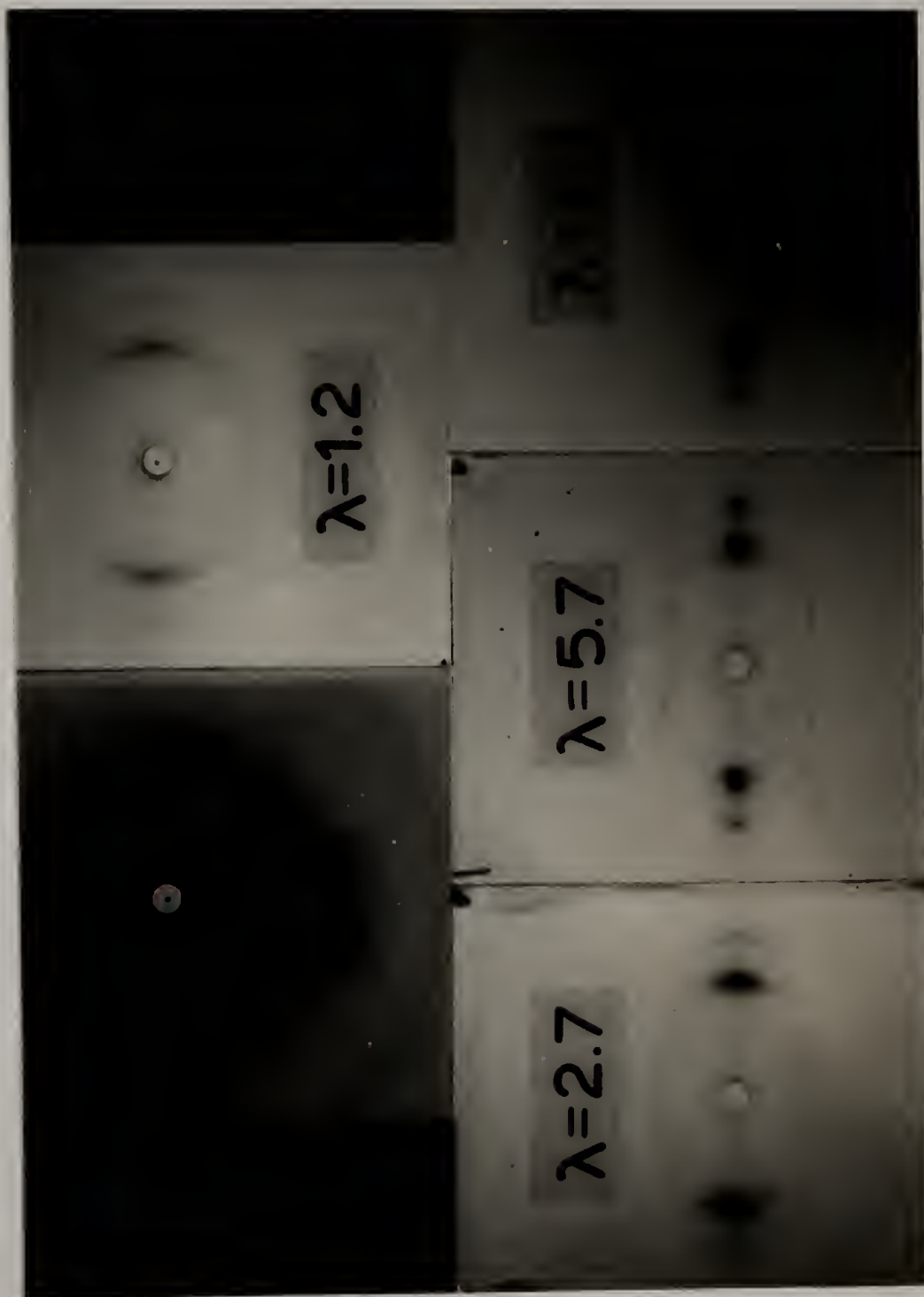
average chain orientation. It was certainly sufficient to analyze the dependence of the orientation upon the draw ratio.

Figure 5.9 shows the azimuthal scans of samples stretched to draw ratios of 2.2 and 5.7 as an example of the data obtained from the D-500. As was mentioned in Chapter III, the diffracted intensity was rather weak, so that long collection times were necessary to obtain reasonable x-ray photon counting statistics. In order to keep the total scan time down to a reasonable length (18 hours), the diffracted intensity was measured at angular intervals too large to determine the precise line shape at high angles. This was a problem especially for the lower draw ratios, where the intensity was very weak, and where there was also overlap interference due to diffraction from the first layer line at high azimuthal angles. This interference can be seen as a weak shoulder on the trace for λ = 2.2 in Figure 5.9. For these reasons, the full angular width at half the maximum (FWHM) intensity was used to estimate <∅> to be used in the Hermans orientation function (see Chapter III).

$$f = \frac{3 \cos^2 <∅> -1}{2}$$

Figure 5.10 shows the Hermans orientation function, f, plotted as a function of the draw ratio which is tabulated in Table 5.2. The error bars are based upon an approximation of the error in the graphical measurement of the intensity half maximum and the peak width. There is a sharp increase in f up to a draw ratio of about 5, where it begins to level off to a value of f = 0.96. As was suspected from the flat film x-ray and electron diffraction patterns, the magnitude of f is

Figure 5.9. X-ray diffractometer scans of the (110) equatorial

reflection intensity as a function of the azimuthal

angle, ϕ, obtained from PPV films stretched to draw

ratios of 2.2 and 5.7. 0° is on the equator and 90°

is on the meridian.
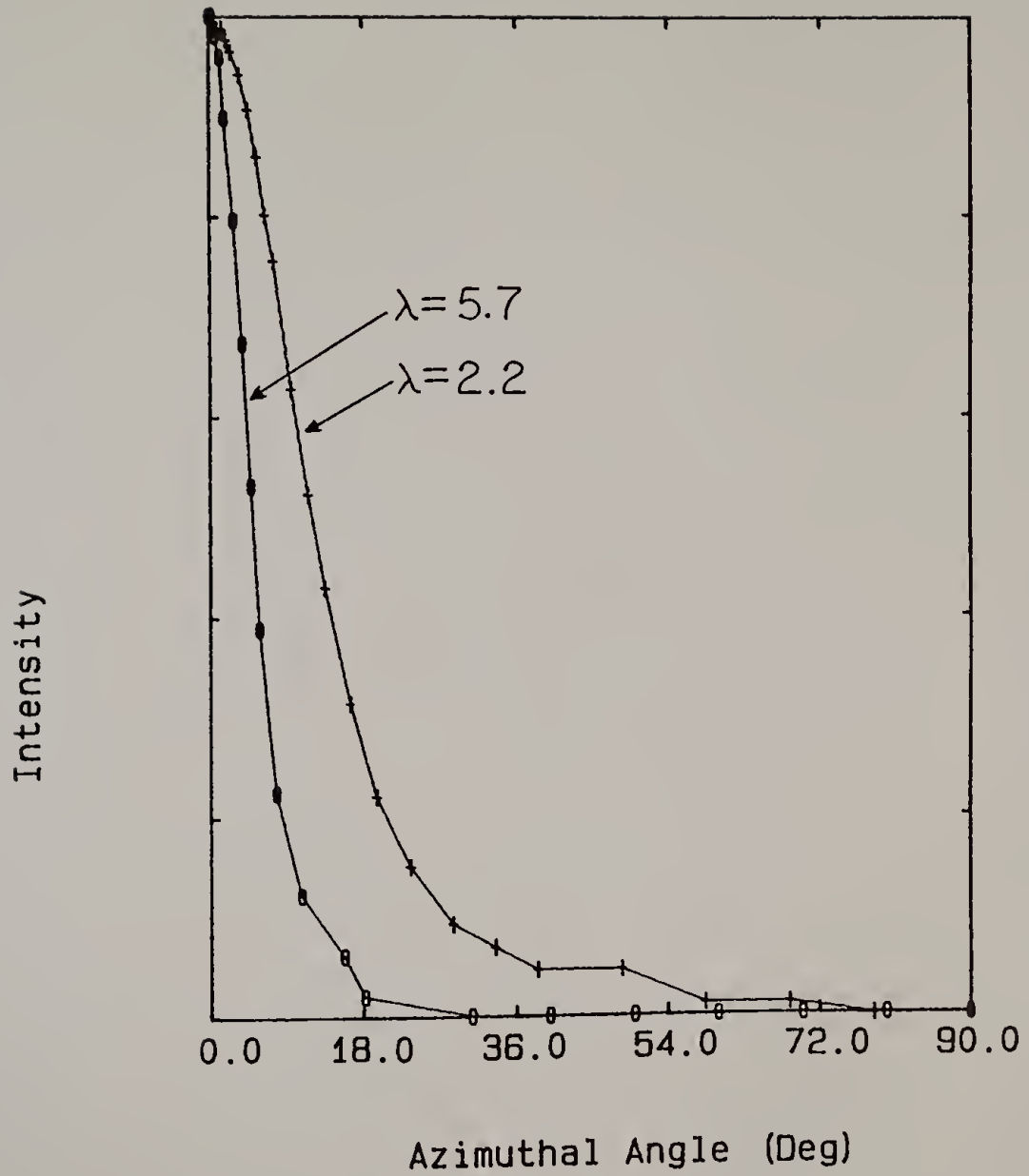
Figure 5.10. The Hermans molecular orientation function, f, of stretched PPV films plotted against the draw ratio, λ.
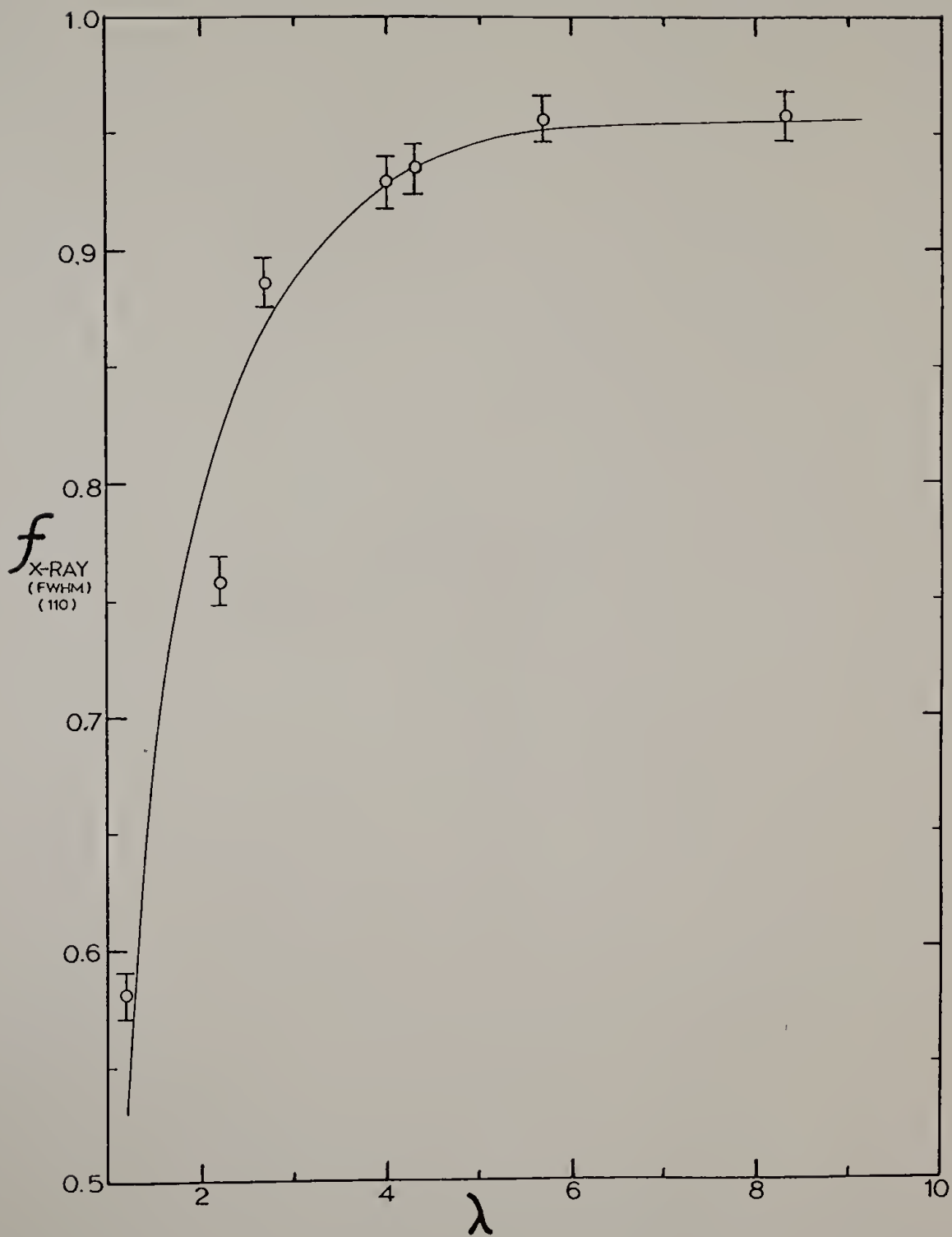
Table 5.2.   FWHM average azimuthal angle, $\langle\emptyset\rangle$, $\cos^2\langle\emptyset\rangle$, and Hermans orientation function, f, measured from WAXD azimuthal scans of PPV films of draw ratio, λ.

λ	$\langle\phi\rangle$	$\cos^2\langle\phi\rangle$	$f_{\text{x-ray}}$
1.2	32.00	0.719	0.579
2.2	23.66	0.839	0.758
2.7	16.17	0.923	0.884
4.0	12.57	0.953	0.929
4.3	12.05	0.956	0.935
5.7	9.93	0.970	0.955
8.3	10.26	0.968	0.953

extremely high, especially when considering that the initial precursor film was basically amorphous. In contrast, amorphous poly(dimethyl-siloxane), drawn by a factor of 6.15 only has an orientation function of 0.56.[107] But in the case of PPV, f is 0.58 at a draw ratio of only 1.2 (i.e., 20% elongation).

There are at least two possible reasons to account for the high PPV molecular orientation. The first is that as the stretching of these thin films was being performed, the conversion of the precursor polymer units to highly rigid PPV units and the fact decrease in temperature as the film was removed from the heat zone effectively quenched any chain relaxation in a phenomenon similar to strain induced crystallization. The second reason is that as the volatile elimination products were lost, the sample volume decreased by a factor of about 2. This volume decrease means that the actual draw ratio was slightly higher than that measured, by a factor of about equal to the cube root of 2 (assuming an isotropic volume decrease).

Infrared Dichroism Results

Infrared dichroism was also used to characterize the degree of molecular orientation. The major drawback of this technique, is that the direction of the transition moment of the absorption band used must be known accurately with respect to the chain axis direction. If the atomic structure of the molecule is known, then it is usually safe to use an absorption from a bond stretching vibrational transition, where the transition moment is directed along the bond direction. In the case of PPV, however, the various C–H stretching absorptions were

overlapped with each other, and quantitative absorption measurememts were nearly impossible. Therefore, as was discussed in Chapter III, the strong absorption due to the out-of-plane vinyl C–H bending transition at 963 cm^{-1} was chosen, and an initial assumption that the transition moment was directed perpendicular to the chain axis was made. Again, as in the x-ray case, a frame of reference perpendicular to the fiber axis was chosen, so that the f being calculated was actually that of the average orientation of the bending transition moment with respect to the perpendicular of the stretch direction. And, again it was argued that this was a good approximation of the molecular orientation to the fiber axis because of PPV's rigidity. With this convention, the dichroic ratio, D, was calculated from the ratio of the absorbance perpendicular to the draw direction, $A_{\perp}$, to the absorbance measured parallel to the draw direction, $A_{/\!/}$.

The results of the infrared measured orientation function with the draw ratio are plotted in Figure 5.11, superimposed upon the x-ray results of Figure 5.10, and are also tabulated in Table 5.3. The orientation function measured by infrared dichroism was consistently lower than that obtained by x-ray measurements, but it showed exactly the same trend of a very high orientation with a strong dependence upon λ. The obvious explanation for f_{IR} being lower than f_{x-ray} is that the initial assumption that the transition moment direction with respect to the chain axis perpendicular, $\alpha = 0^{o}$, is not valid.

Figure 5.11. The Hermans orientation function, f, of stretched PPV
films obtained from infrared dichroism, superimposed
upon the x-ray data of Figure 5.10, plotted as a
function of the draw ratio, λ.
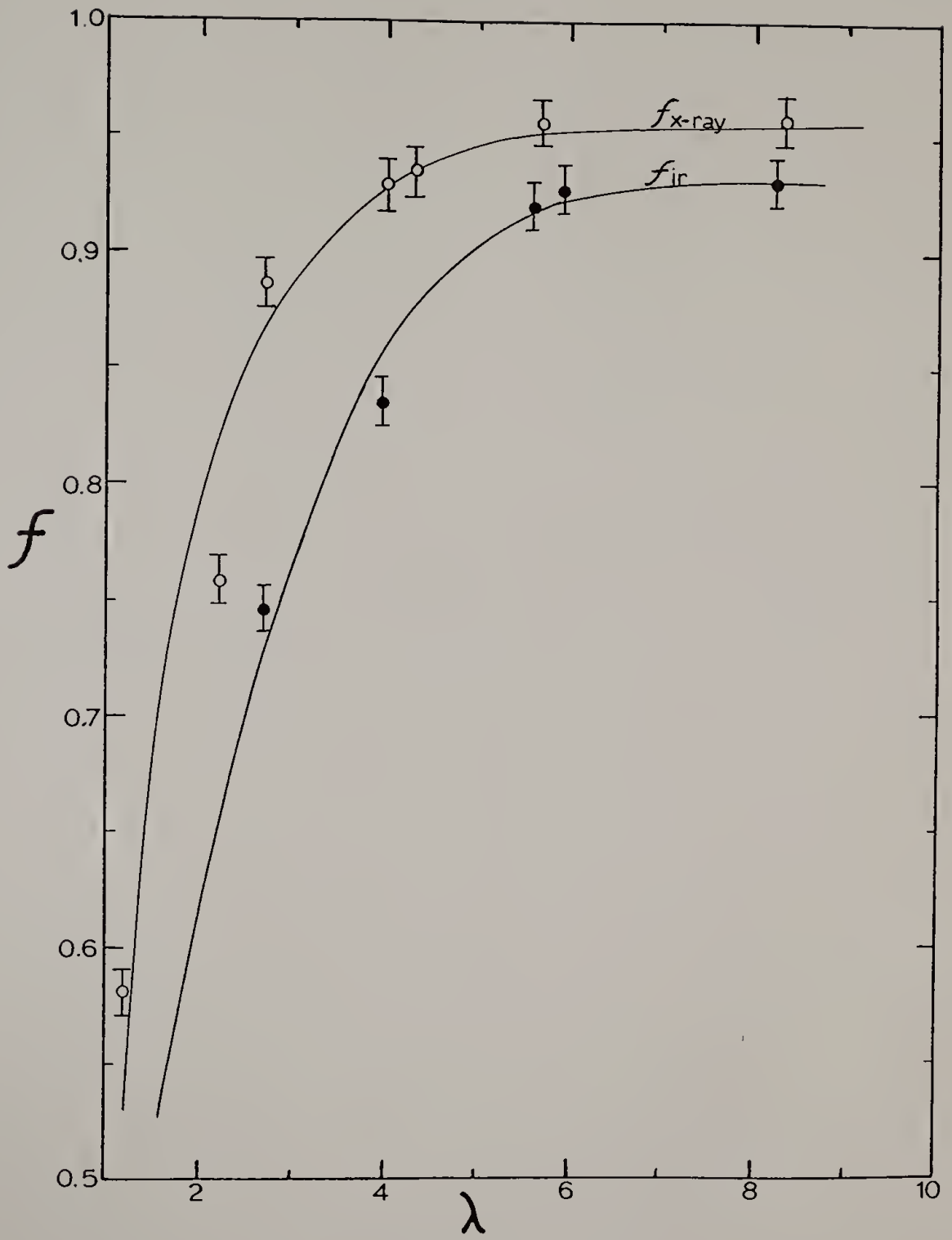
Table 5.3. Infrared dichroism, D, and the calculated orientation function, f_{IR}, for stretched PPV films of draw ratio, λ.

λ	$D=A_{//}/A_{\perp}$	f_{ir}
2.7	9.66	0.743
4.0	15.91	0.833
5.7	35.00	0.919
6.0	37.84	0.925
8.3	40.00	0.929

If $\alpha \neq 0^{\circ}$, and if the f_{x-ray} is regarded as the true orientation function, then can be back calculated from

$$f_{x-ray} = \frac{D-1}{D+2} \left(\frac{D_o+2}{D_o-1}\right) = f_{IR} \left(\frac{D_o+2}{D_o-1}\right)$$

and $D_o = 2 \cot^2 \alpha$.

Using the values of f_{IR} and f_{x-ray} for PPV having a draw ratio ranging from 2.7 to 8.3, α ranged from 19° to 8° from the chain axis perpendicular. The reason why α should not equal 0° or should change with the draw ratio, however, is unclear since the vinyl group is located symetrically between identical molecular units which should each have an equal effect upon the transition moment. Only a full normal mode analysis of the infrared transitions of PPV will be able to give an answer to this question.

The second possibility for f_{IR} being less than f_{x-ray} is that the x-ray diffraction intensity weights larger, well ordered crystallites more than small, imperfect crystallites, and that alignment of the PPV chains would be expected to be better within the larger crystallites. Infrared measurements, on the other hand, probe molecular units independently and equally weigh those molecules within well aligned crystals, those located in less perfect crystals, and those located at crystallite interfaces. Using this argument, f_{IR} can be considered a better measurement of the average orientation function of all the chains, and f_{x-ray} would then be an upper bound for f. The only problem with this explanation is that polymers which are composed of crystalline and amorphous regions, such as polyethylene,[108] generally show a splitting of absorption bands due to components in the

crystalline and amorphous phases. In the case of PPV, there was no apparent splitting of the 963 cm^{-1} band. This might be accounted for by assuming a morphology which has no large scale amorphous phases, but only has contributions from less perfect crystals which would not be expected to have a drastically different absorption energy.

Crystallite Size

Proponents of the theory that interchain charge transfer is the dominant or only mechanism for charge transport in conducting polymers predict that the conductivity should be a strong function of the size of the crystallites of the polymer.[18] In order to explore this dependence, the average crystallite dimension perpendicular to the fiber axis was investigated with x-ray diffraction as a function of the draw ratio.

The lateral crystallite diameter has been approximated by a Scherrer analysis of the 2θ breadth of the (210) equatorial reflection. The (210) reflection was chosen because it was the lowest order reflection which was not overlapped as were the (110) and (200) reflections. The crystallite diameter, t, was calculated from

$$t = \frac{K\lambda}{\beta_{corr} \cos\theta}$$

where K was the Scherrer constant taken to be 0.94 (see Chapter III), λ was the wavelength of the x-rays, θ was the Bragg angle of the (210) reflection, and β_{corr} was the corrected reflection breadth obtained from an equatorial D-500 scan as detailed in Chapter III. It must be

emphasized that this equation only provided an approximation of the average crystallite diameter because it does not take into account the presence of paracrystalline disorder or imperfection of the crystallites. It is based upon the assumption that the only source of reflection broadening is due to small crystallite size. Within these interpretational limitations the calculation still had value in discerning the effect of the draw ratio upon t.

The results of the calculations of t are plotted in Figure 5.12 as a function of the draw ratio. There was an increase in t from a value of about 87 $\overset{\circ}{A}$ for unoriented PPV to about 121 $\overset{\circ}{A}$ for a draw ratio of 6. Above $\lambda = 6$, there was no significant change in the crystallite size. Thus, the trend was similar to that observed for the orientation function with draw, however the crystallite size increased by a factor of less than 1.4, whereas the chain axis orientation changed more drastically. The fact that the crystallite diameter was nearly the same order of magnitude for all draw ratios means that the number of crystallite-crystallite interfaces was not changed much by orientation. Thus, little effect on the conductivity would be expected by this amount of increase in the crystallite diameter.

Figure 5.12. Crystallite diameter, t, perpendicular to the fiber

axis for stretched PPV films, plotted as a function

of the draw ratio, λ.
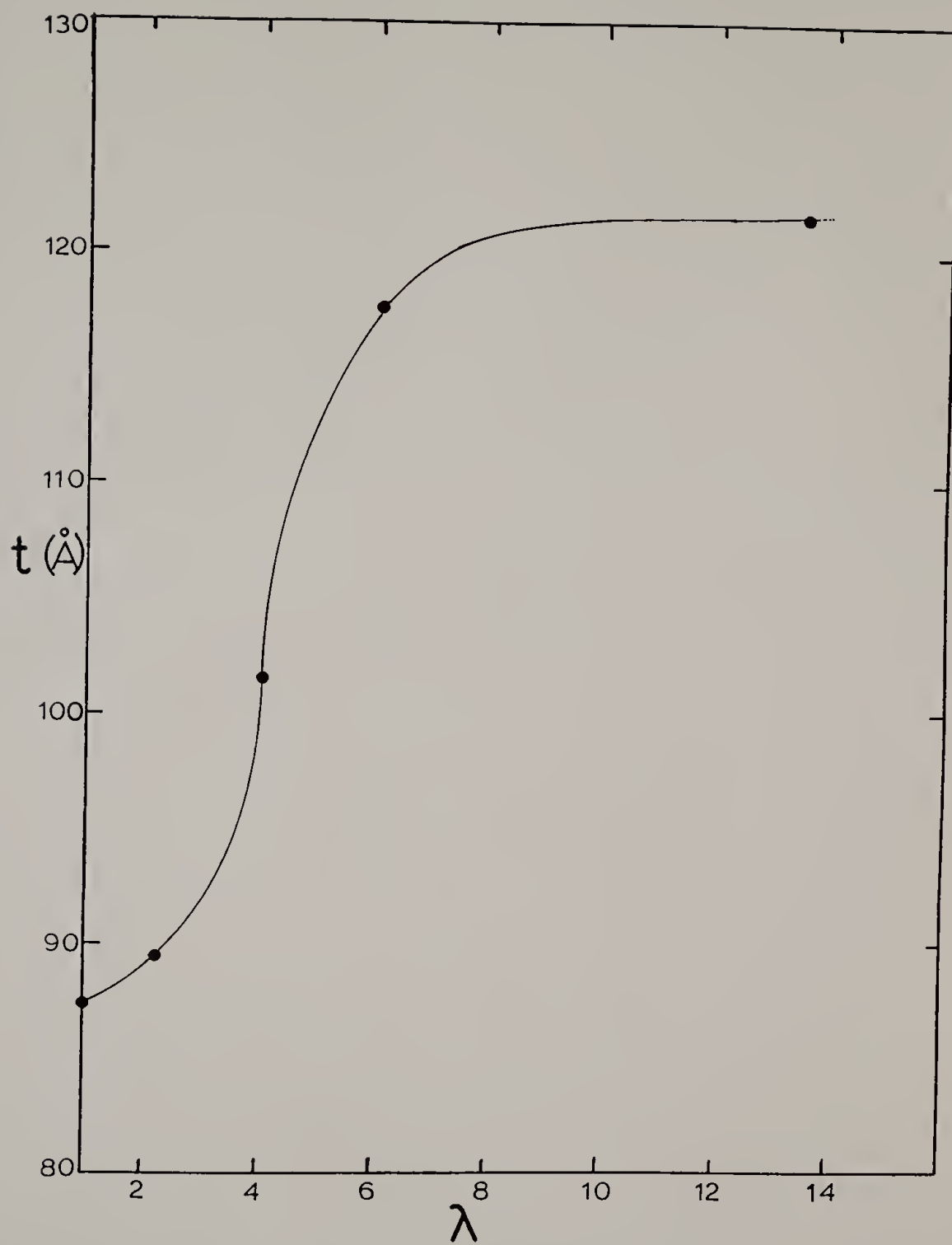
CHAPTER VI

ELECTRICAL PROPERTIES OF PPV

In the undoped state, fully eliminated PPV is an excellent
insulator and has a conductivity of 10^{-13} S/cm. For any material to
conduct electricity, there must be free charges with which to carry the
current, and there must be some mechanism by which the charge can move
through the material when the electrical potential is applied across
the sample. As was discussed in Chapter II, charges are created in
conducting polymers by either oxidation or reduction with a dopant; and
because of the highly conjugated electronic structure of the polymer,
the charges are not bound tightly to any one particular lattice site.
The fact that these charges are not tightly bound is revealed by the
high conductivities observed in these systems. The question though is
whether the mobility of the charged species is greater within the
individual polymer chains, or whether the mobility is greater between
chains.

This chapter begins with a presentation of the conductivity results
obtained by reacting PPV with various dopants commonly used for
conducting polymers including iodine, sulfuric and perchloric acids,
and sodium naphthalide. The rest of the chapter concentrates on the
electrical characterization of arsenic pentafluoride doped PPV.

The conductivity of arsenic pentafluoride doped, unoriented PPV was
studied as a function of the degree of conversion of the precursor
polymer to PPV. With fully eliminated films, the conductivity was

measured as a function of time of doping and of dopant weight uptake in order to qualitatively study the kinetics of the doping process.

By measurements of the conductivity of arsenic pentafluoride doped, oriented PPV samples in directions parallel and perpendicular to the orientation direction, the question of the anisotropy of charge transport is addressed. The chapter concludes with the measurement of the Arrhenius temperature dependence of conductivity in both oriented and unoriented doped PPV samples.

Conductivity of PPV Doped with Various Dopants

Iodine

Iodine has been known to be a useful dopant for polyacetylene, PA, since the pioneering work of Shirakawa et al. in 1977.[109,110] Iodine in either vapor or solution form imparted a conductivity of about 360 S/cm by oxidation of the polyacetylene backbone to yield a composition having a mole ratio of iodine to PA of roughly 25 mole percent.[110] The reactivity of iodine towards PA was attributed to its low oxidation potential of 0.7 V.[111] The low oxidation potential of PA also resulted in the fact that it was highly unstable to the atmosphere, even in its undoped state.

PPV, on the other hand, apparently had a much higher oxidation potential as it could not be readily doped by iodine. Iodine doping of PPV either by introducing iodine vapor or a 0.2 M I_2 solution in pentane into the 4-probe did not change either the conductivity or the appearance of PPV, even with doping times of 5 days. This confirmed

the previous results of Wnek et al., for iodine doping of powders of
oligo-PPV synthesized by the Wittig method.[56]

Murase and coworkers have reported iodine doping of stretched PPV
(λ = 9), prepared via the Wessling precursor route, to a conductivity
of 1.2×10^{-2} S/cm,[112] however their results are suspect on the
grounds that they did not fully eliminate the precursor film to PPV
quantitatively. Since the maximum elimination temperature they
reported (300°C) was well below the onset of the final conversion
temperature, the iodine reactivity may be associated with the
uneliminated units in the chain. It was also revealed that their
measurements were made in the presence of free iodine vapor; that is,
they did not pump off the excess iodine before making their
conductivity measurements.[113] They also did not investigate the
possibility of whether there was any ionic contribution to the measured
conductivity.

Protonic Acids

In 1979, Gau demonstrated the effectiveness of doping with protonic
acid dopants such as sulfuric and perchloric acids.[114] PA was doped
with the vapor of these acids to a conductivity approaching 10^3 S/cm.
The exact nature of protonic acid doping is still unknown at this
time.[9] What is known, however, is that it does not involve
prontonation of the conjugated backbone which would interrupt the
-conjugation. Evidence for this is that reaction of $HClO_4$ doped PA
with triethylamine did not result in the formation of the quaternary
ammonium salt of polyacetylene, which would be expected if PA had been

protonated. Only the salt, not involving PA was formed, $(Et_3N^+H\ ClO_4^-)$, and this neutralization resulted in an 8 order of magnitude decrease in conductivity. More than 80% of this salt could be removed from the film demonstrating that it was not covalently bound to PA.

Sulfuric acid. Sulfuric acid vapor was used to p-dope PPV over a period of 4 days to a conductivity of 125 S/cm. This is the highest conductivity achieved with unoriented PPV films. The blackish purple PPV film absorbed 1.73 times its initial weight in H_2SO_4 which gave a calculated composition of 1.8 moles HSO_3^- for each mole of PPV repeat units. An extremely high molar ratio such as this led to the suspicion that there was a significant amount of excess acid or water absorbed which was not being removed by simple vacuum line pumping. If there was an excess, then there is a good chance that the measured conductivity was really the sum of contributions from both the electronic conductivity of doped PPV and the ionic conductivity of free acid.

The simplest method to test for ionic conductivity, is to apply a constant voltage across the doped polymer and observe the magnitude of the current with time. If mobile ionic species are contributing to the conductivity, they should migrate to one electrode with time; and since platinum electrodes block the further flow of ions, there would be a decrease in the number of charge carriers with time. A constant 1 volt potential was applied across the doped sample using an EG&G model #173 Potentiostat/Galvanostat and the total number of coulombs passed through the sample was measured with an EG&G model #179 Digital

Coulometer. When the voltage source was first turned on, the current
was 150 mA. Within 3 minutes the current had decreased to a value of
50 mA at which time 1.0 coulomb had been passed through the sample.
After 50 coulombs had been passed, the current was down to 34 mA.

In order to check for ion build-up at the cathode, the polarity of
the applied voltage was switched. If simple ion migration alone was
responsible for the observed decrease in current with the number of
coulombs passed, then with this polarity switch the magnitude of the
current should have been observed to be even higher than the 150 mA
observed at the beginning of the experiment. However, what was
observed upon polarity switch was an unexpected continued decrease in
current with the number of coulombs passed in the reverse direction.
By the time 1300 coulombs had been passed through the sample the
current had stabilized at 18 mA and the resistance had risen from the
initial 6.7 Ω to 55.6 Ω. Thus, it was shown that a significant portion
of the conductivity of H_2SO_4 doped PPV is ionic in nature. A possible
explanation for the anomalous polarity behavior is that the sulfonate
anions being swept by the current are also being electrochemically
neutralized. This idea might be tested by using an applied voltage
which is below the oxidation potential of H_2SO_4 of 0.43 V.

Perchloric acid. Doping of unoriented PPV films by perchloric acid
vapor gave a material with a conductivity of 0.28 S/cm after 1 day of
exposure and turned the color of the film black with a copper luster.
The ionic nature of these $HClO_4$ doped films was even more apparent then
it was with H_2SO_4 in that the resistance increased during the

resistance measurement with even the small 1 mA current produced by the multimeter when in the four-probe mode. The major problems associated with perchloric acid doping were that the $HClO_4$ vapor partially degraded the Electrodag contact, and that slight swelling of the PPV film tended to break the contact with the platinum wire electrodes. Because of these problems, no further $HClO_4$ doping experiments were performed.

Sodium Naphthalide

Many electronic device applications require both p-doped and n-doped polymers. Diodes, for instance, are made by directly mating a p-doped material with an n-doped material. Anticipating the possible application of PPV in such devices, n-doping was performed by reacting PPV with a 1.0 molar solution of sodium naphthalide in THF. The film was immersed in the solution for 2 hours, and after cryogenic distillation of THF back into the four-probe to wash out the excess sodium naphthalide, the film was a light metallic bluish color with some darker blue and greenish regions and with a golden hue to the reflectance. The conductivity of this material was found to be 2 x 10^{-4} S/cm.

It should be noted that the first attempts to dope samples which were mounted on the electrodes using the usual Electrodag adhesive were unsuccessful because the Electrodag contact degraded. Also, the control sample became brittle and broke apart during the cryogenic distillation of the THF into the four-probe for washing. This experiment had been performed by immersing the mounted sample and a

control sample in the dopant solution for 12 hours. Thus, successful n-doping with sodium naphthalide required a reduction of the doping time to 2 hours, and the casting of four platinum electrodes within the initial precursor film prior to elimination rather than using Electrodag. The cast-in electrodes were attached to the four-probe's electrodes by wrapping them tightly around the four-probe electrodes, followed by applying a small bead of solder to ensure electrical contact. The contact of the cast-in electrodes to the film was extremely tight, because the precursor film shrinks during the elimination to PPV.

The n-doped PPV was found to be much less stable to atmospheric impurities than was the p-doped PPV. Even in the glove box, where moisture and oxygen concentrations are below 5 ppm, there was a decrease in conductivity by one order of magnitude and the color changed to a darker bluish purple color within 30 minutes. When the sample was opened to the ambient atmosphere, the color returned to nearly the same yellow as the undoped film within only 5 minutes. P-doped PPV stays dark black for weeks prior to returning to a yellowish color. If the n-doped polymer is considered in terms of basic organic chemistry concepts, it makes sense that a polymer with a negative charge (which is really a secondary anion) would be less stable than its p-doped counterpart which is a secondary cation.

For device applications, not only must n-doping be possible, but it must also be reversible.[9] The reason for this is that electrical components such as diodes work because, at the junction of the p- and n-doped materials, there is a shallow neutralization reaction at the

film contact surfaces called a depletion layer which is responsible for the diode behavior. The fact that the sodium naphthalide doped PPV was neutralized so quickly in air proves the reversibility of the n-doping of PPV. Since device assembly was really beyond the scope of this dissertation work, and since the n-doped PPV was so unstable, no further n-doping studies were performed. The potential for important and novel research in this area is there however, and should be pursued in the future.

Arsenic Pentafluoride Doped PPV

Arsenic pentafluoride is a powerful electron withdrawing agent and has been used as a dopant for conducting polymers such as polyacetylene since 1977.[115] AsF_5 reacts with an electron source (i.e., a conjugated chain) by the following equation:

$$3 \; AsF_5 + 2 \; e^- \rightarrow 2 \; AsF_6^- + AsF_3$$
$$2PPV^o \rightarrow 2 \; PPV^{\cdot +} + 2 \; e^- \quad .$$
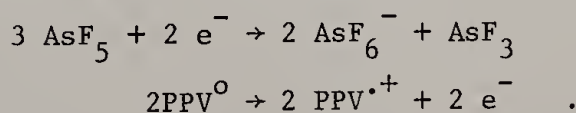
In the past, one of the difficulties with AsF_5 doping of conducting polymers was that the doping side product, AsF_3, remains in the material and inhibits further diffusion of the AsF_5 into the matrix, resulting in doping inhomogeneity. One technique which has been used to circumvent this problem by Warakomski[116] was to admit a very small concentration of AsF_5 (< 0.01 torr) into the four-probe vessel for about 15 minutes. The unreacted AsF_5 and the AsF_3 by-product was then pumped off for about 2 minutes. This process was repeated as many times as was necessary to attain the desired doping level.

An alternate, more elegant, technique has been devised for use in this dissertation research which takes advantage of the fact that AsF_3 has a much lower vapor pressure at $-90^{\circ}C$ than does AsF_5. Figure 6.1 shows the vapor pressure of AsF_5 and AsF_3 plotted as a function of temperature. Also included on Figure 6.1 is the data for HF, which is the primary impurity from reaction of AsF_5 with residual moisture adsorbed on to the apparatus glass surface. Thus, by maintaining the AsF_5 gas bulb resevoir cold finger at $-90^{\circ}C$, and by keeping it opened to the four-probe vessel, AsF_3 and HF were continuously cryogenically distilled out of the four-probe into the resevoir during the doping reaction. The long term temperature control was excellent using the Neslab Cryocool-100II, and this open system doping technique could easily be maintained for the 5 weeks necessary to dope PPV films to their maximum conductivity.

Doping Homogeneity

Unoriented films of PPV could be doped to a conductivity of 8 S/cm with AsF_5. Evidence that the doping was homogeneous was provided by the fact that within the experimental error of $\pm20\%$, the conductivity was the same for films ranging in thickness from 5 µm to 20 µm. Previous doping of pressed pellets of oligomeric PPV by Wnek et al.[57] gave a material which had a doped skin and an undoped core. However, if such an effect occurred with the cast films used in the present study, the skin thickness was greater than that of the film thickness. Thus, there was no doped skin in fully doped films.

Figure 6.1. Vapor pressure of AsF_5, AsF_3 and HF as a function of
temperature.

117
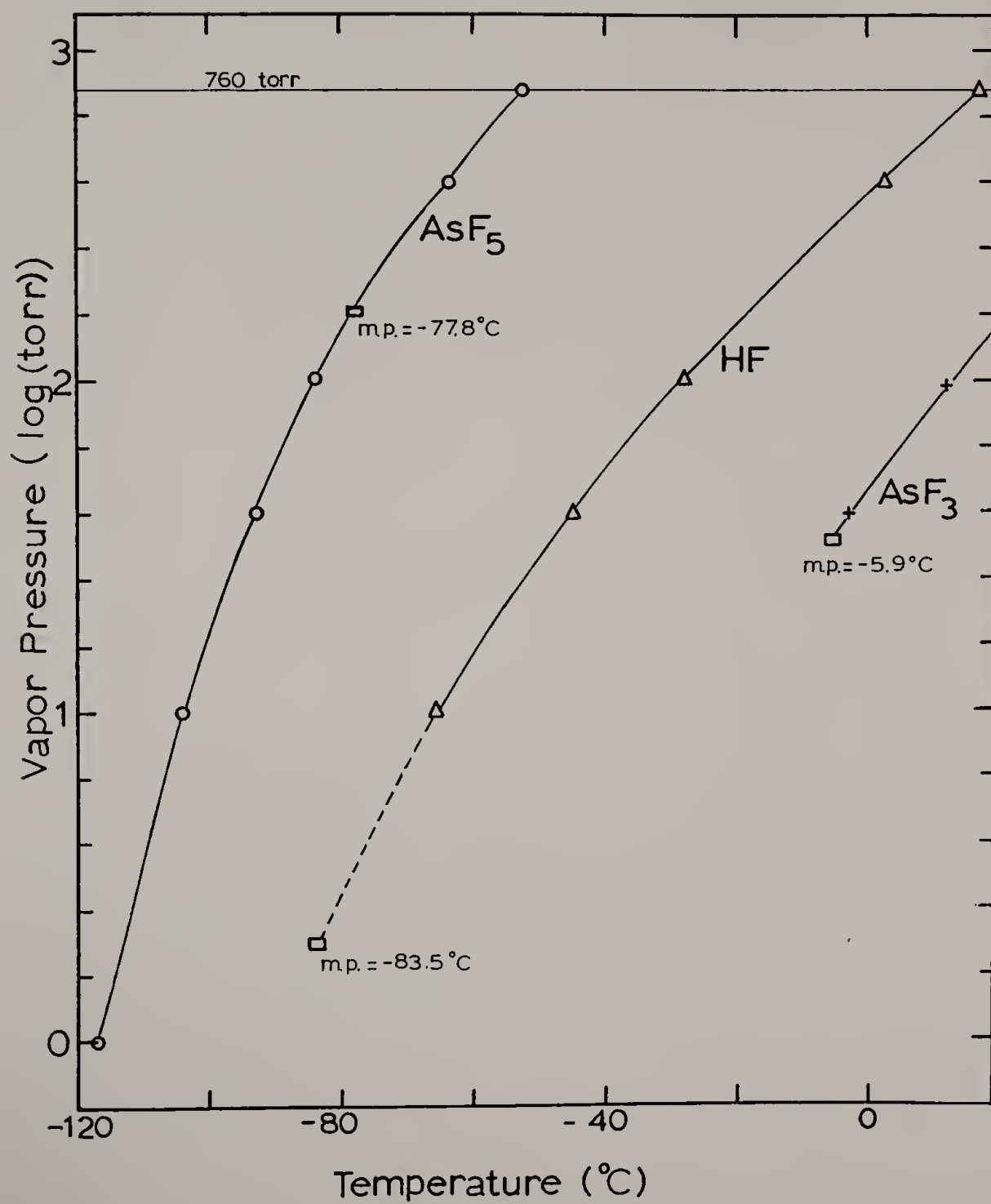
Conductivity as a Function of Dopant Concentration

The amount of dopant which is reacted with conducting polymers is generally measured by weighing the sample before and after doping. An experiment was designed to allow the measurement of weight uptake of AsF_5 in PPV during the doping reaction, while at the same time monitoring the conductivity. The apparatus consisted of a large four-probe vessel which was fitted with a sensitive fused quartz spring and a quartz sample pan (both obtained from Worden Quartz Products, Houston, Texas). The spring had a linear force constant, over the extension range used, and a sensitivity of 0.408 cm/mg, thus percent weight uptake could be measured directly from percent elongation of the spring during doping of the preweighed PPV sample placed on the sample pan. The elongation of the spring was easily measured to within ± 0.002 cm using a cathetometer.

Figure 6.2 shows a plot of the conductivity of AsF_5 doped PPV as a function of the mole fraction of AsF_6^-. The conductivity increased steeply with initial concentration of AsF_6^- until about 5% AsF_6^-. Above 5% the slope of the curve began to decrease and the conductivity leveled off by about 20% AsF_6^-, which was a ratio of one AsF_6^- counterion for each 4 PPV repeat units. This agreed quite well with other doping experiments used the usual weight uptake method which showed that PPV doped to maximum conductivity absorbed about 25 mole % AsF_6^-.

Figure 6.2. Log (conductivity) for AsF_5 doped PPV plotted as

a function of AsF_6^- mole fraction.

$$\left[PPV^{+y} (AsF_6^-)_y \right]_n$$
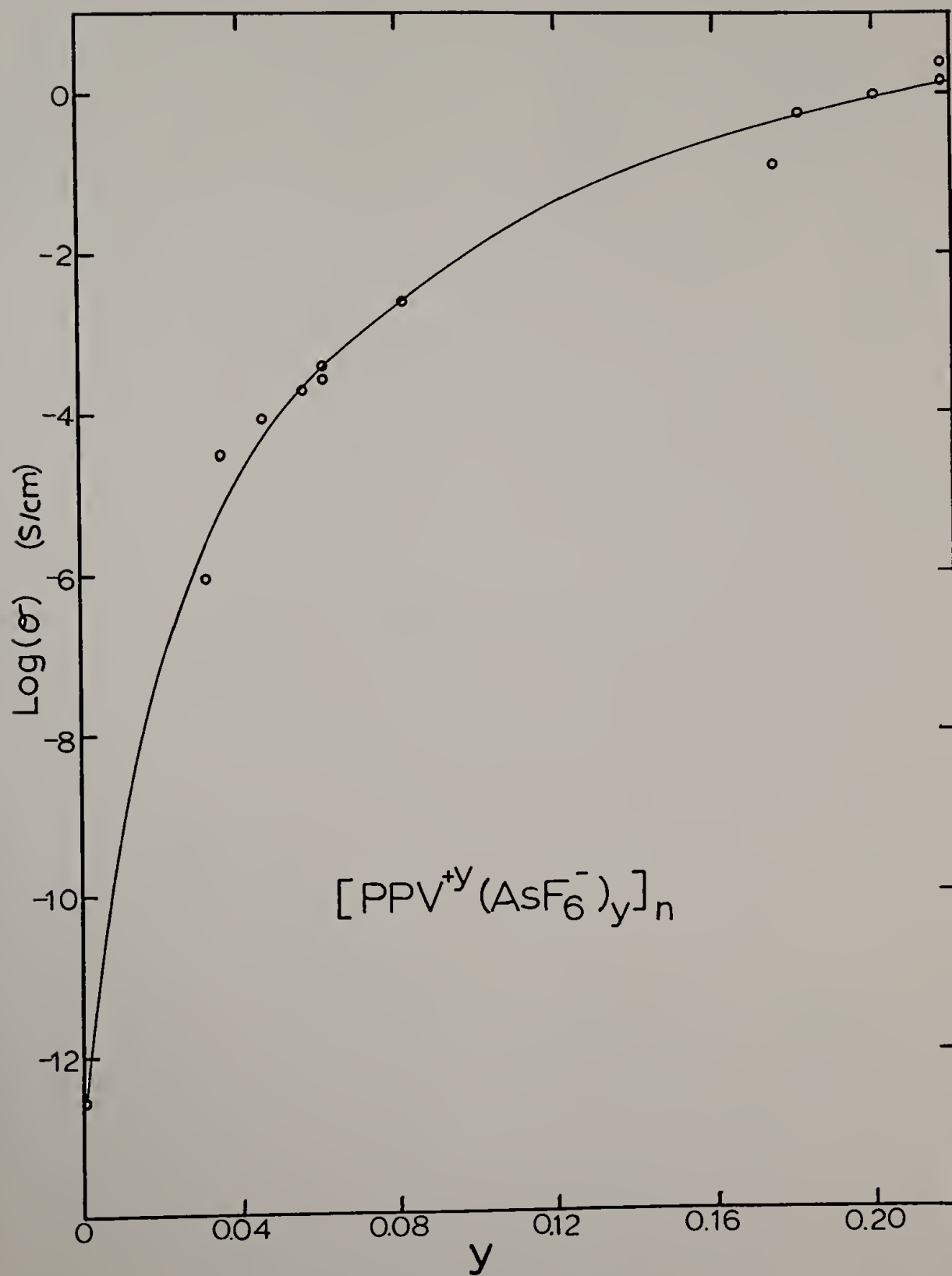
Although AsF_5 doped PPV is apparently homogeneous when fully doped, this is no assurance that there is not some initial inhomogeneity due to the diffusion controlled nature of the vapor phase doping process. If the polymer film is doped at the surface during the initial stages of the reaction, a model containing a low resistance surface, R_s, in parallel with a high resistance core, R_c, could explain the extremely fast rise in conductivity even at low doping levels since the overall resistance of the sample, R, would be $R = (1/R_s + 1/R_c)^{-1}$. With this model, the surface would contribute the most significantly to the decrease in R. Thus, if this model is valid, then any future experiments aimed at studying doped PPV as a function of the doping level must be designed with extremely thin films or must utilize extremely low dopant vapor pressures to reduce the inhomogeneity. Of course, the problem with extremely thin films is that analysis of the dopant weight uptake will be difficult.

Conductivity of Partially Eliminated PPV

The effect of the conjugation length upon the conductivity is one of the central questions involved in trying to understand the charge transport mechanism in conducting polymers. If charge transport via interchain hopping of charges is the only mechanism operative, then there should be little or no effect upon conductivity as long as the conjugation length is long enough to support a stable charged species. Charge transfer, C-T, complexes, such as cation radical salts of $(naphthalene)_2^+PF_6^-$,[118] attain conductivities as high as 1 S/cm even

though each naphthalene unit only contains 5 double bonds. The conductivity in these cases is due to the presence of well ordered columns of the aromatic units that are crystallized in the presence of the dopant in which every other unit possesses a formal charge. Since each unit is crystallographically identical, these charges are in reality distributed equally among the rings in the stack though intermolecular π–π orbital overlap of the stacked units. The counterion is only present to provide overall electrical neutrality, and does not play a role in the conduction process.

The analogy of charge transfer salts to conducting polymers suffers from the major deficiency that for the C–T salts to possess high conductivity, high quality crystals must be carefully grown from solution to impart the long range electronic delocalization necessary for conduction. This ideal is rarely realized in conducting polymers. Even though some evidence for the formation of a regular packing arrangement (intercalation) of iodine dopant in crystalline polyacetylene fibrils has been seen,[119-122] this is the exception rather than the rule in conducting polymers. Polypyrrole can be doped to high conductivity, but its structure is basically amorphous before and after doping.[123] Indeed, the PPV films prepared in the present study are amorphous, and doping of unoriented films only increases the disorder as seen by a broadening of the x–ray diffraction rings and an increase in the background scattering.

Polyacetylene had been prepared with various conjugation lengths in order to determine the effect upon conductivity. Soga and Nakamaro,[124] and Yaniger et al.,[125] neutralized Shirakawa type

polyacetylene, which had been n-doped by sodium or potassium naphthalide, with an alcohol in order to introduce sp^3 carbon sites which would interrupt the conjugation. By varying the concentration of the n-dopant they were able to control the number of these sites, and thus control the effective conjugation length. Particular care was taken in the Yaniger study to insure that the n-doping and subsequent alcohol neutralization was homogeneous throughout the PA fibrils. By subsequently p-doping the PA films obtained by this technique, the conductivity was measured as a function of the average conjugation length. It should be noted that this technique provided a much better comparison of the conjugation length dependence on conduction than would the use of oligomeric model compounds, because the molecular structure of Shirakawa materials is essentially the same as is used in the many other conductivity studies of polyacetylene. The result was that the conductivity had an approximate power law dependence upon the conjugation length, ℓ, which could be fit by $\ln\sigma/\ln\ell \sim 3.2$. This relationship was valid over a range of ℓ varying from 7 to about 200 $\{CH = CH\}$ units.

The precursor route to PPV provided an excellent alternative to the neutralization of an n-doped polymer. In Chapter IV, it was shown that the degree of conversion of the precursor to PPV could be controlled by limiting the temperature at which elimination was performed. The m:n ratio found by elemental analysis of the partially eliminated polymer was a direct measure of the average conjugation length without the problem of compositional inhomogeneity which had to be so carefully avoided with polyacetylene. The assumption which must be made with

PPV, however, is that the elimination of each repeat unit occurred randomly, such that the creation of one stilbene unit did not induce the elimination of the adjacent unit. In elimination reactions of polymers such as poly(vinyl chloride), the first HCl elimination causes the adjacent chlorine to be allylic and thus more easily eliminated, creating conjugated sequences in blocks. In PPV, however, each sulfonium group is already activated because it is benzylic, thus the added activation effect of a stilbene unit should be minimal. The uv/vis evidence in Figure 4.4 which shows a gradual increase in the maximum wavelength of absorbance tended to support this reasoning.

The results for the conductivity of AsF_5 doped PPV as a function of the elimination temperature, Te, and the conjugation length are shown in Figure 6.3. [126] Each sample was doped to approximately a 20 mole % doping level. At low conjugation lengths, there was a strong maximum conductivity dependence upon the conjugation length up to a length of about 6 repeat units, where it becomes insensitive to longer sequences. 6 repeat units can be considered analogous to a conjugation length of 18 $\{CH=CH\}$ units having a <u>cis</u>-configuration. Precursor polymers with m:n ratios of 1:1 could not be studied since elimination occurred when the sample vessel was evacuated prior to attempted doping. The reason for the observed insensitivity to conjugation lengths above 6 might be rationalized in the same way as is the uv/vis absorption shift insensitivity to PPV conjugation lengths greater than 6 units. That is, there is an electron localization effect due to the presence of aromatic rings which inhibits long range delocalization.

Figure 6.3. Log (conductivity) plotted as a function of the
precursor elimination temperature, Te. The numbers in
parenthesis correspond to the conjugation length
calculated by elemental analysis in terms of the m:n
ratio of the copolymer shown at the top of the Figure.
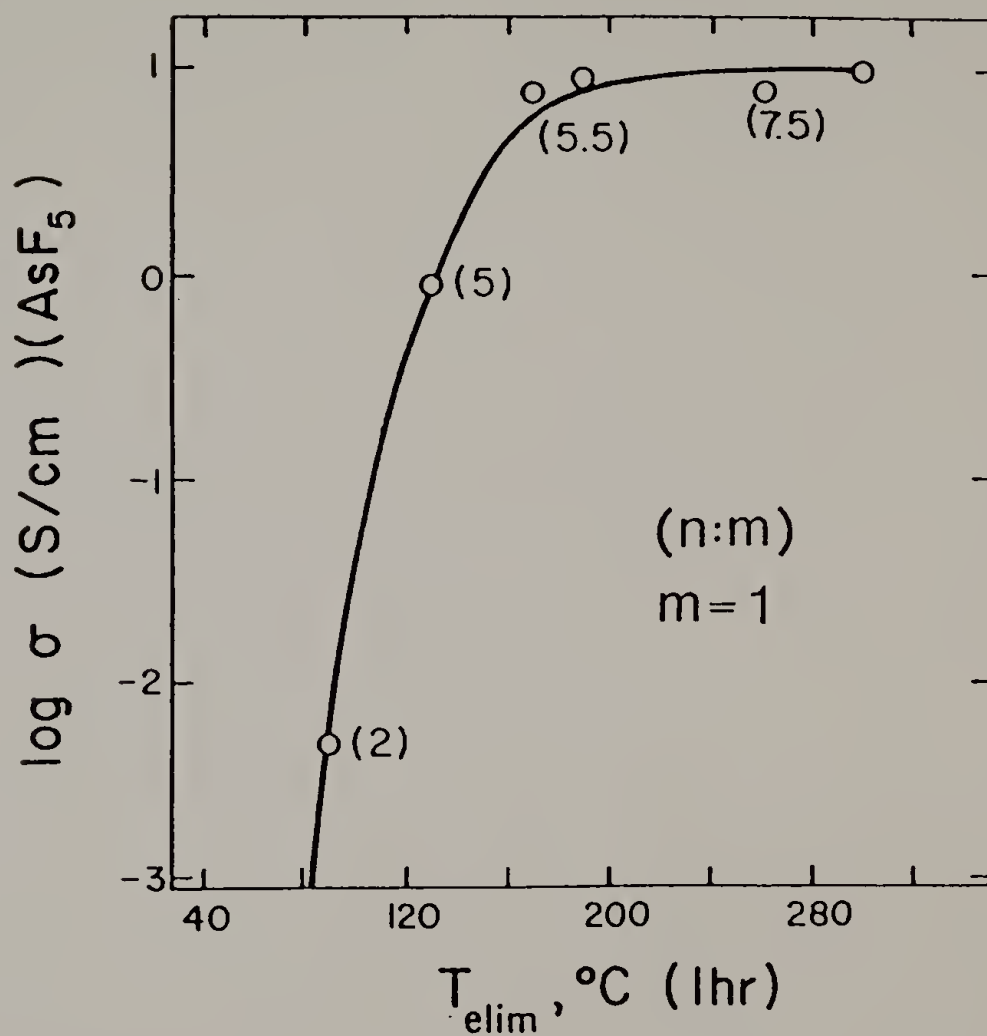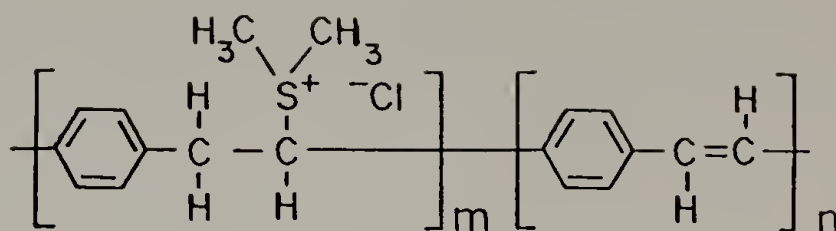
A previous study of the effect of the conjugation length dependence upon the conductivity of a series of PPV oligomers by Wnek et al.,[56] failed to find any effect. The reason for this absence of an effect was postulated to be that because AsF_5 is a potent Lewis acid, and as such can induce Friedel–Crafts type arylation reactions, doping caused an increase in the degree of polymerization. Thus, the use of PPV oligomers may not have been a valid test of the conjugation length effect. The precursor method of PPV preparation, on the other hand, should not be nearly as susceptible to this type of chemistry. Even if arylation reactions occur, they will cause cross–linking at sites which are meta-to one end of the chain, and thus would not be expected to have a significant effect upon the overall conjugation length.

Plotting $log(\sigma)$ as a function of $log(\ell)$ in Figure 6.4 showed that, as in the polyacetylene case, there was an approximate power law dependence but with a larger slope of 5.8. Thus, it appeared that the conjugation length dependence of this aromatic conducting polymer was greater than that of polyacetylene. The problem with this type of comparison is that there are many fundamental differences between PA and PPV. These include the fact that PPV has a non–degenerate ground state which cannot support neutral radical carriers as PA's degenerate ground state is proposed to support. The morphology of PPV was amorphous and continuous, whereas PA was composed of semicrystalline fibrils. Also, although care was taken during the preparation of the PA to insure conjugation length homogeneity, there was no direct confirming evidence.

Figure 6.4. Log (conductivity) plotted as a function of the log
(conjugation length).
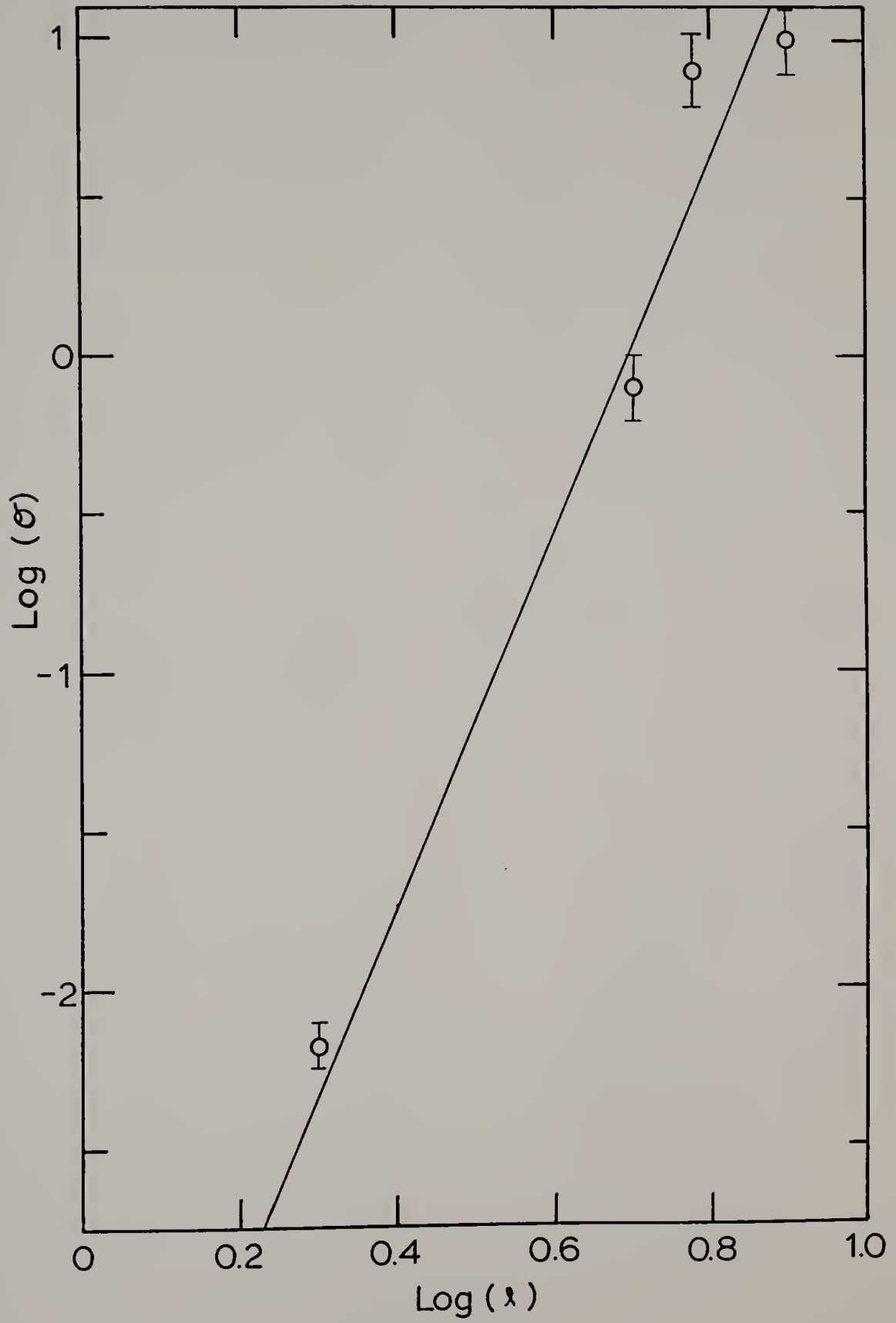
The above differences between PPV and PA either explain the observed difference in conjugation length dependence, or they make the comparison invalid. But, what is clear is that there was a strong dependence of conductivity upon conjugation length. As was discussed at the outset of Chapter I, it is obvious that some interchain charge transport mechanism must be operative, and in fact it may be via C-T complexes analagous to systems like $(naphthalene)_2 \ PF_6^-$. This data shows, though, that there was also a strong intrachain mechanism for charge transport superimposed upon the interchain mechanism. Since the PPV films did not possess the long range crystalline order of the C-T complexes, the charged species apparently propagated along the chain until it reached a site where the π-orbital overlap was sufficient to allow interchain propagation.

Conductivity of Oriented PPV

Another key to understanding the mechanism of charge transport in conducting polymers is the effect of long range alignment of the conjugated sequences. Chapter II provided a review of the difficulties associated with alignment of the chains of highly conjugated conducting polymers, and Chapter V showed how these problems have been circumvented by the precursor processing of PPV films having varying degrees of molecular orientation (i.e., from isotropic to nearly perfect uniaxial alignment).

By measuring the conductivity of AsF_5 doped oriented PPV films both perpendicular and parallel to the orientation direction a measure of the anisotropy of charge mobility through the bulk film can be obtained. If interchain charge transport is the only mechanism responsible for conduction, then the conductivity should improve greatly perpendicular to the draw direction because of the increased lateral molecular packing order, which would increase the probability of interchain π orbital overlap in this direction. However, if intrachain charge transport contributed significantly to the mobility of the charged species then alignment of the chains would increase the propagation efficiency of the charges parallel to the draw direction.

The initial measurements of the conductivity anisotropy of AsF_5 doped, oriented PPV films were limited to two-probe measurements, because of the narrowness of the films, only two electrodes could be mounted perpendicular to the draw direction. Figure 6.5 shows the data obtained by these measurements. There was a sharp increase of the parallel conductivity, $\sigma_{//}$, and a slight decrease of the perpendicular conductivity, $\sigma_\perp$ with increasing draw ratio. The conductivity anisotropy, $\sigma^* = \sigma_{//}/\sigma_\perp$, also increased with draw. The maximum shown in Figure 6.5 for σ^* is probably not real because at draw ratios higher than 10, the film was beginning to fibrillate along the draw direction. The use of the two-probe measurement technique also meant that the additional contact resistance of the Electrodag had been added to that of the sample, making the values reported on Figure 6.5 useful only for the qualitative observation of the trend.

Figure 6.5. Two-probe conductivity and conductivity anisotropy of

oriented PPV plotted against the draw ratio, λ. Refer

to left axis for (a) log (parallel conductivity) and (b)

log (perpendicular conductivity). Refer to right axis

for (c) conductivity anisotropy, σ^*.
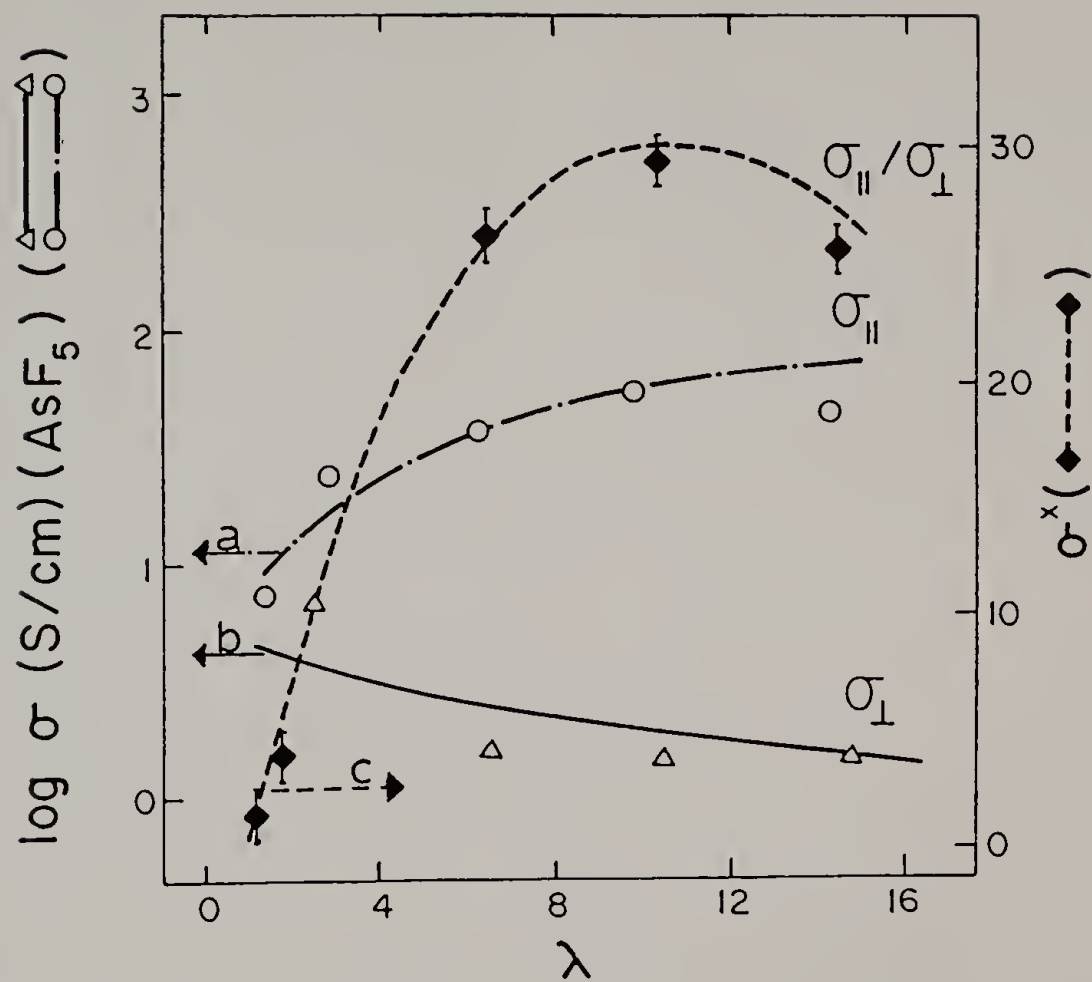
The data was, however, good enough to provide incentive to produce wider, less fibrillated films with which to perform four-probe conductivity studies. Improved samples of oriented PPV were made in draw ratios from 1.2 to 14. Samples wide enough to permit the mounting of four electrodes across the width of the film were produced in draw ratios up to 5. The parallel and perpendicular conductivity of these AsF_5 doped films is shown in Figure 6.6. The most remarkable observation was that the highly oriented samples of $\lambda > 11$ reached conductivities of over 10^3 S/cm; and in one case, $\lambda = 11.5$, a conductivity of 2500 S/cm was measured. These values were as high as the most highly conducting oriented films of polyacetylene. Thus, orientation of the molecules significantly enhanced the charge transport along the draw direction.

The perpendicular conductivity of the oriented samples decreased by almost an order of magnitude with a draw ratio of 5. The conductivity anisotropy, σ^*, at this draw ratio was approximately 300. Plotting $\log(\sigma_{/\!/})$ and $\log(\sigma_\perp)$ against the orientation function (Figure 6.7), obtained from the x-ray diffraction measurements (see Figure 5.10), it was seen that $\sigma_\perp$ decreased only by a factor of about 2 at the most above an orientation value of $f = 0.56$, whereas $\sigma_{/\!/}$ continued a dramatic increase even after the maximum f of 0.96 had been achieved. It is unfortunate that the more highly drawn samples could not be prepared wide enough to permit four-probe $\sigma_\perp$ measurements above $\lambda = 5$, although the data did seem to indicate that $\sigma_\perp$ became constant above $\lambda = 5$.

Figure 6.6.   (a) Log (parallel conductivity) and (b) log (perpendic-
ular conductivity) from four-probe measurements of
oriented PPV plotted as a function of the draw ratio,
λ.
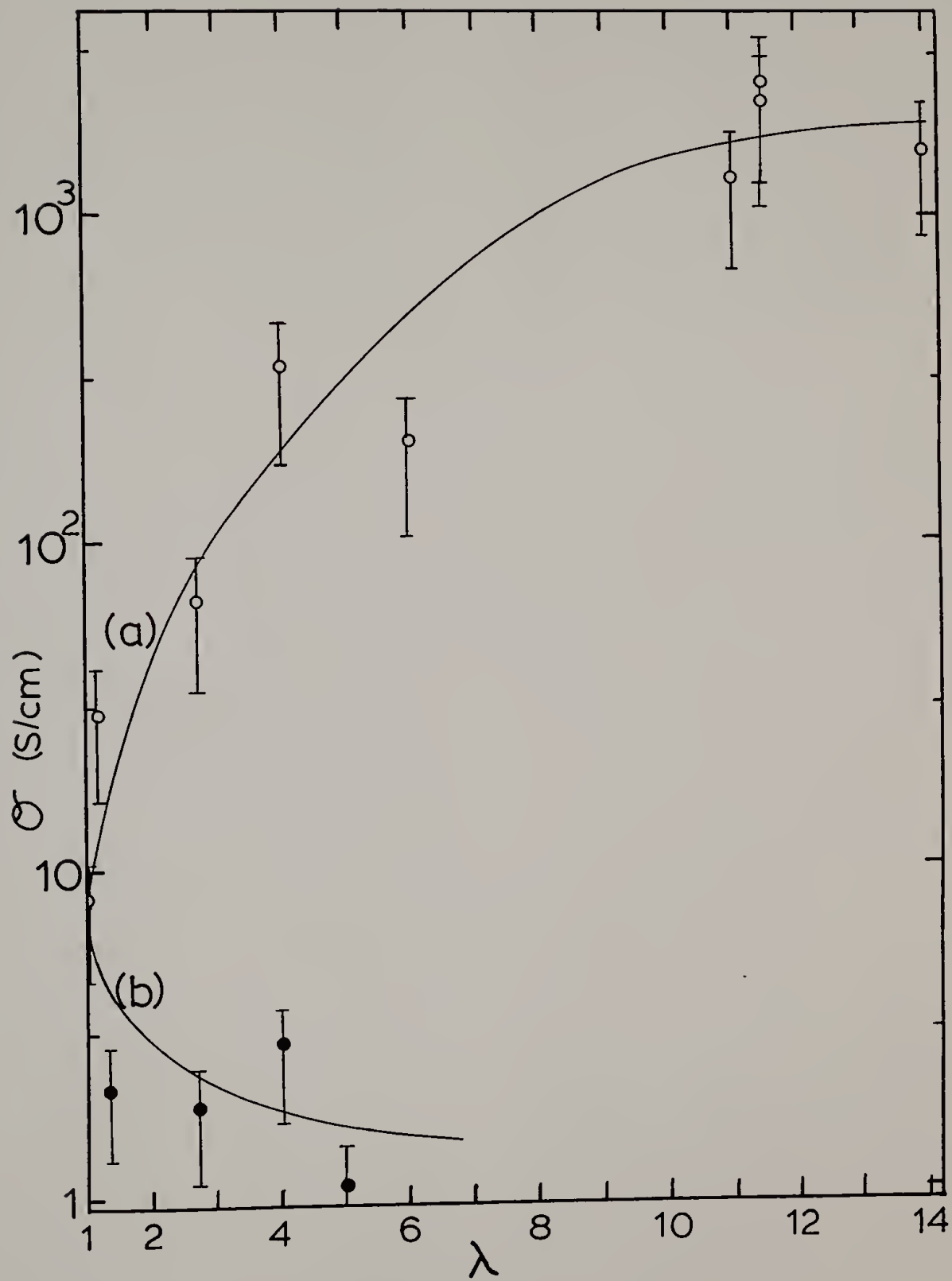
Figure 6.7. (a) Log (parallel conductivity) and (b) log (perpendic-
ular conductivity) of oriented PPV plotted against the
Hermans orientation function, f.
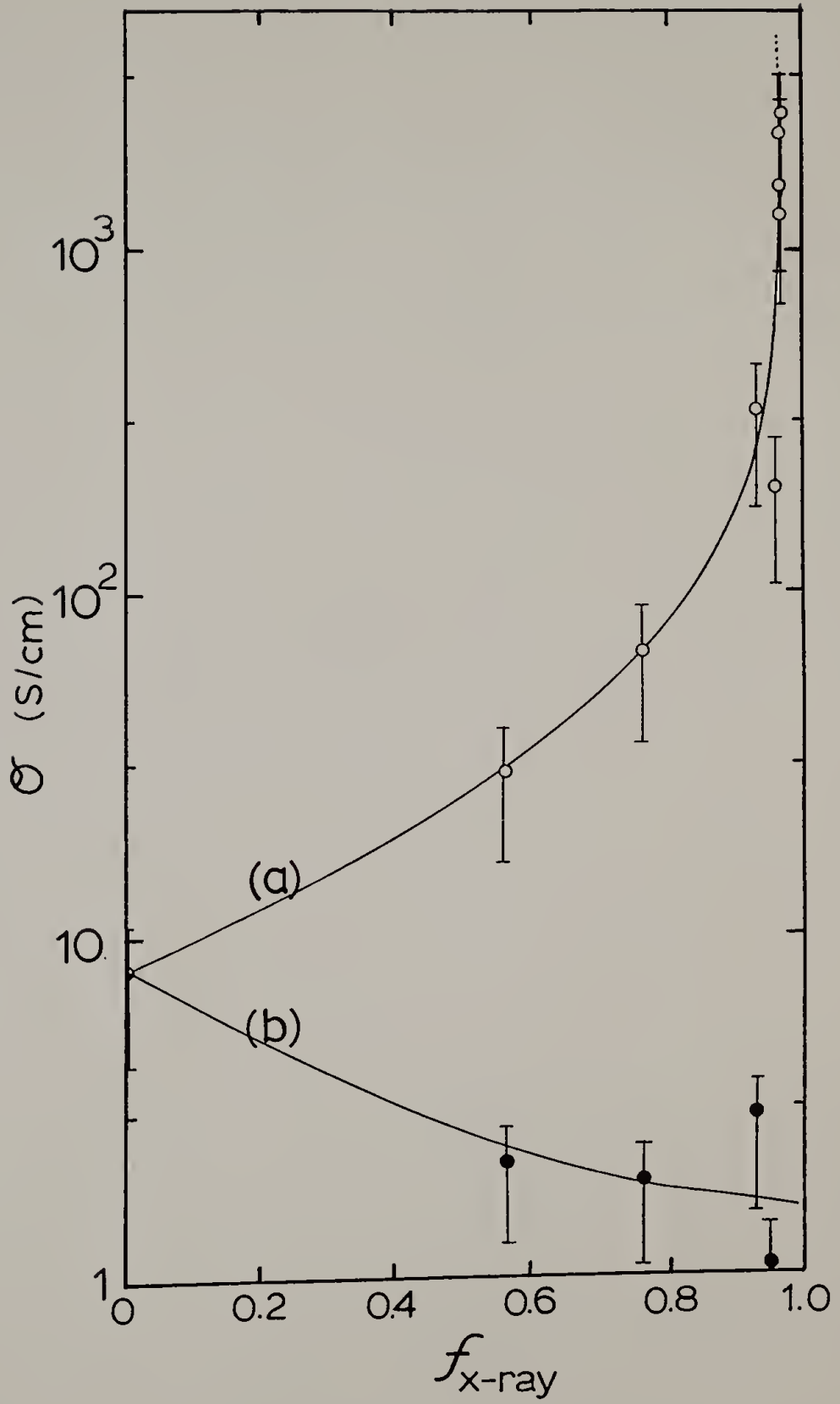
The reason for the continued increase in $\sigma_\parallel$ even after attaining
the maximum orientation function is not known. An explanation cannot
be based upon changes in the crystallite size, because this too had
become constant above a draw ratio of 6 (Figure 5.11). Also, the x-ray
and electron diffraction patterns did not show any obvious difference
in the intensity profile of the first layer line, which would indicate
a difference in the degree of paracrystallinity. This last point is
qualitative however, and with the ongoing progress towards improvements
in the calculations of the degree of paracrystallinity being worked on
by Dr. T. Granier, it should be possible to analyze this more
quantitatively in the future. The other factor which might play a role
in the conductivity, especially at high draw ratios is micro-
fibrillation along the stretch direction. Small angle x-ray scattering
as a function of draw ratio should be performed in the future to study
this phenomenon.

The result that is clear, though, was that given the fact that the
samples were all doped to about 20 mole % AsF_6^- (well above where
theconductivity is not sensitive to small variations in dopant
concentration), the mobility of the charges responsible for conduction
were greatly increased in the orientation direction, and were
significantly decreased in the perpendicular direction. In a well
oriented system, the charge only makes progress in the perpendicular
direction through interchain transport. That is, when the electric
field is applied perpendicular to the chains, the charge only moves
along the chain until it finds a place where the interchain π-oribtal
overlap has sufficiently low energy so that transport can occur. When

the electric field is applied parallel to the orientation direction, the charge can move down the conjugated chain until it reaches some defect which interrupts the conjugation. At that point it must move to an adjacent chain to continue moving in the field direction. The anisotropy of the charge mobility observed can be understood in terms of this model, because the conjugated sequences are longer than the interchain spacing distance. Thus the charge moving along the orientation direction is not forced to make as many high energy (i.e., slow) interchain hops to go the same distance as is the charge moving perpendicular. Thus, since the dopant concentration is essentially the same in all samples, the conductivity anisotropy is a direct measure of the mobility anisotropy, and with this model it is proposed that the interchain charge transport is the mobility limiting charge transport mechanism.

Temperature Dependence of Conductivity

By plotting the natural logarithm of the conductivity as a function of $1/T$ over a temperature range of $80^{\circ}K$ to $300^{\circ}K$ in an Arrhenius fashion, an apparent activation energy, Ea, for charge transport could be calculated from the slope. Figure 6.8 shows such a plot for an unoriented sample and a sample stretched to a draw ratio of 11.5. The measurements were made by slowly heating the sample from $80^{\circ}K$, but the temperature dependence was reversible. Although no claim is made to the linearity of these plots, an apparent activation energy could be extracted from a least squares fit, and for the oriented sample, Ea was

Figure 6.8. Natural log of the conductivity of (a) PPV with $\lambda = 11$, and (b) unoriented PPV plotted against inverse temperature in an Arrhenius fashion.
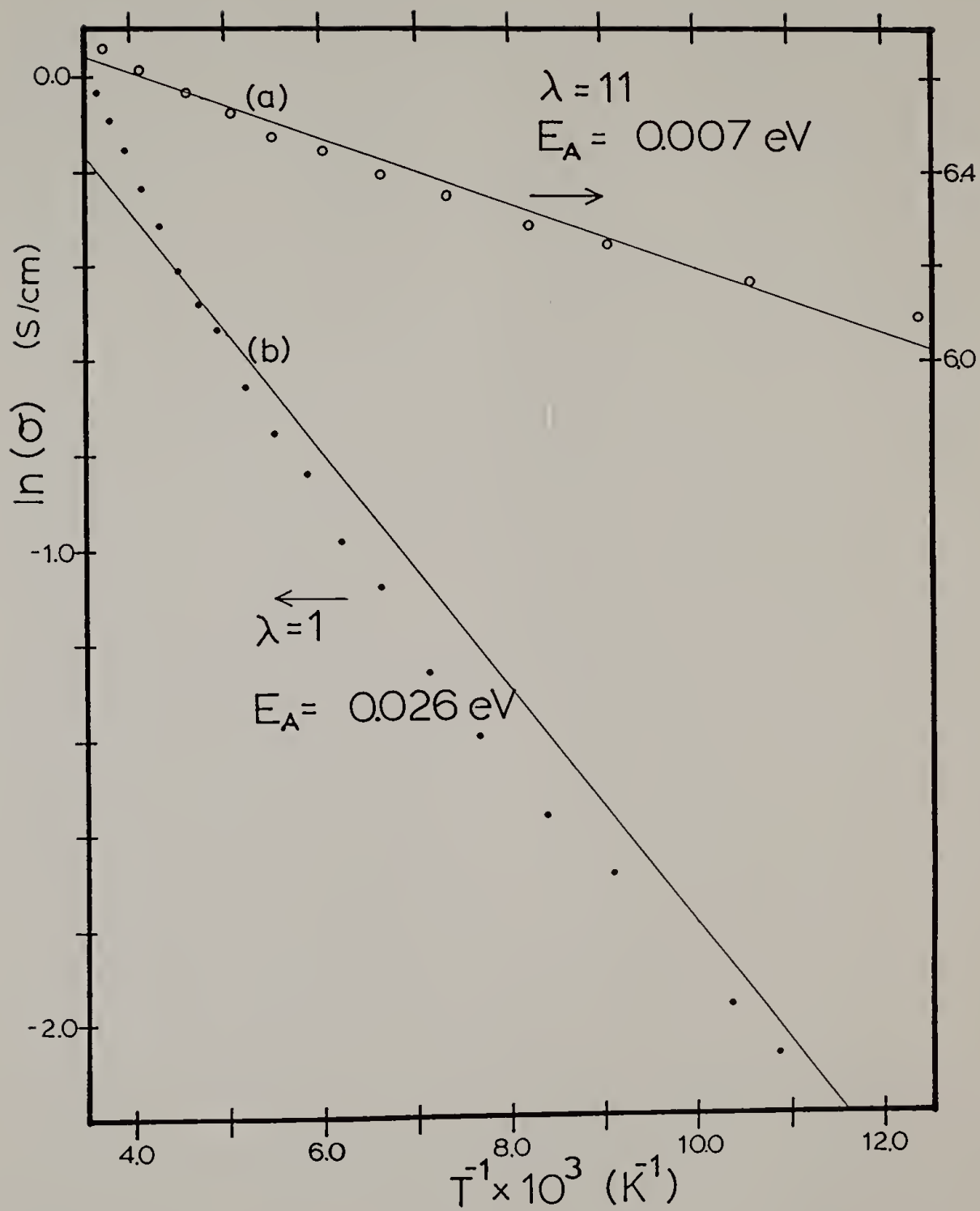
0.007 eV which was 3.7 times less than the unoriented PPV of activation

energy of 0.026 eV. The activation energy for AsF$_5$ doped oligomeric

PPV, measured by Gourley,[60] was 0.03 eV which agreed well with the

unoriented film of PPV in this study. The activation energy primarily

reflects that of the highest energy process of charge transport, which

according to the model described above is the interchain hopping

energy. Thus, Ea was decreased in the oriented sample probably due to

the improved lateral packing order which increased the probability of

interchain π-orbital overlap. It should be noted that these Ea values

are quite low, especially in the oriented sample, when considering that

the thermal energy available at room temperature is about 0.025 eV.

There are a number of theories for charge transport in conducting

polymers which predict the dependence of the log of conductivity in

isotropic, amorphous semiconductors as a function of some exponent of

temperature.[9] Since none of these theories is applicable to

oriented, highly crystalline polymers, a detailed analysis of the

temperature dependent conductivity data for oriented PPV in terms of

these theories would be meaningless. However, for completeness,

Figures 6.9 and 6.10 show the natural log of the conductivity for

unoriented and oriented (λ = 11.5) doped PPV plotted against $T^{-\frac{1}{2}}$ and

$T^{-\frac{1}{4}}$. These temperature dependencies correspond respectively to

theories of variable range hopping of charge carriers in one and three

dimensions.

In both the unoriented and oriented cases, the temperature

dependence was quite weak, thus there was little difference between the

quality of the fit to either theory. The unoriented sample appears to

Figure 6.9. Natural log of the conductivity of unoriented

PPV plotted against (a) Temperature$^{-\frac{1}{4}}$ and
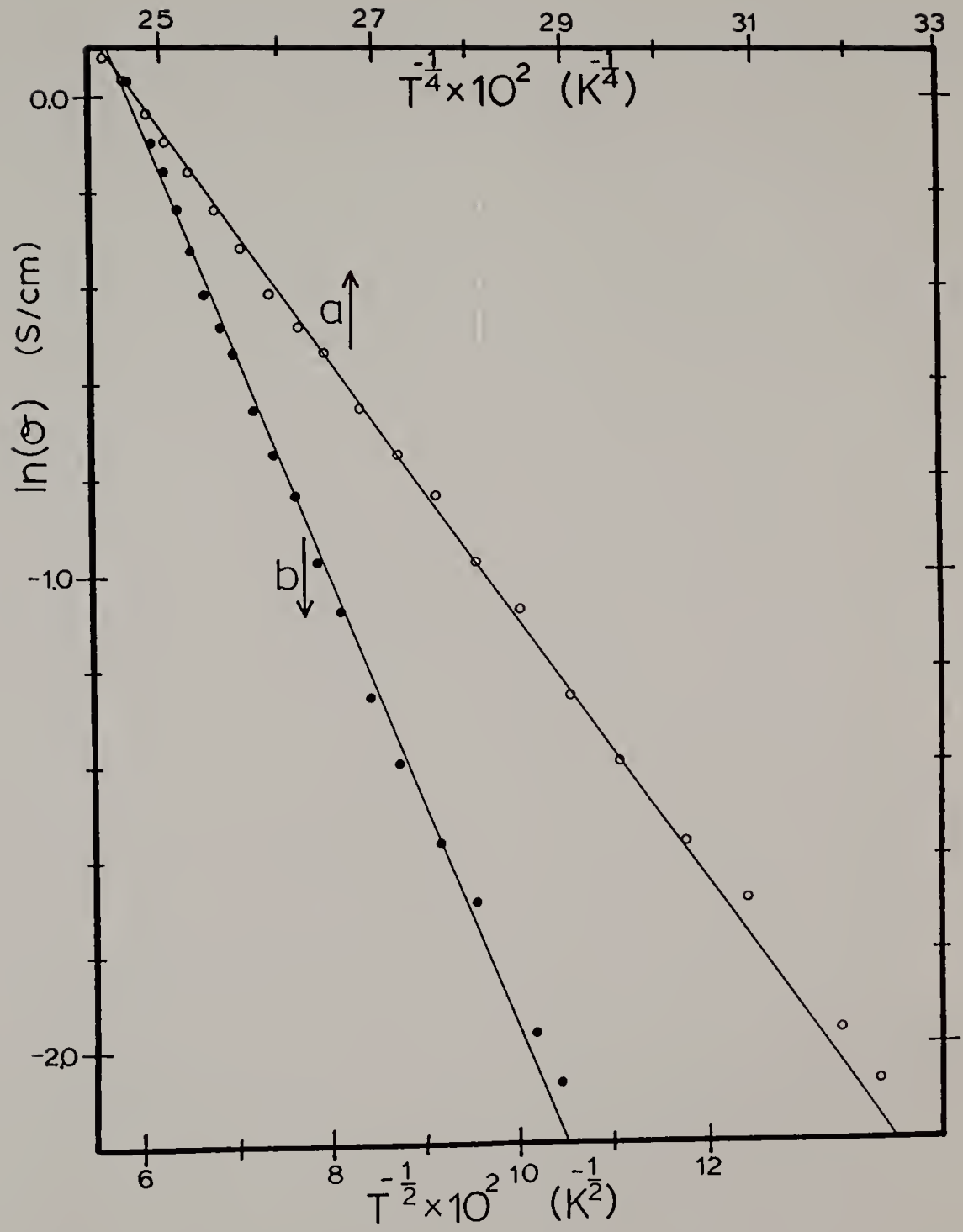
(b) Temperature$^{-\frac{1}{2}}$.

Figure 6.10. Natural log of the conductivity of oriented PPV (λ = 11.5) plotted against (a) Temperature$^{-\frac{1}{4}}$ and (b) Temperature$^{-\frac{1}{2}}$.
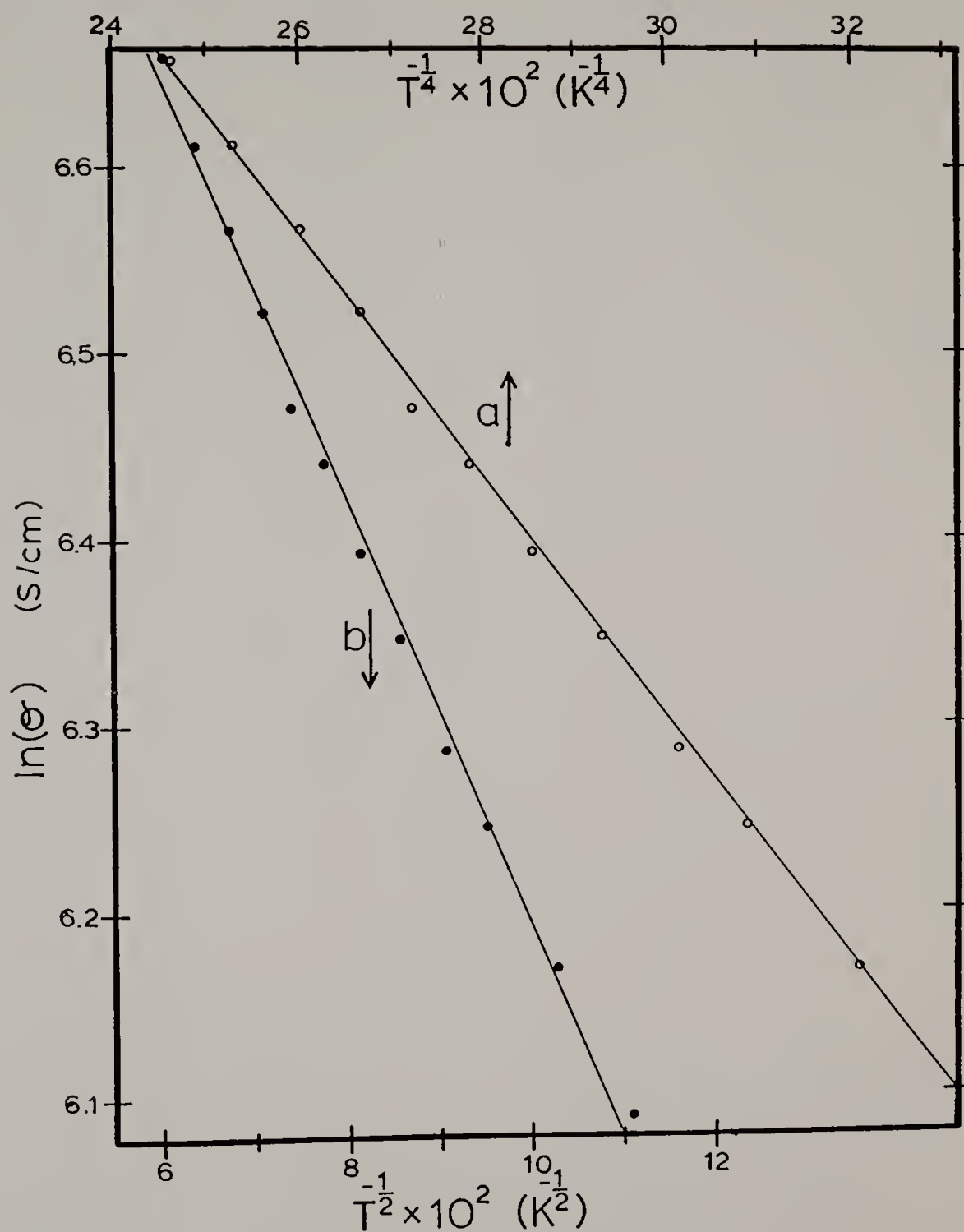
fit the $T^{-\frac{1}{4}}$ dependence slightly better than it does to the $T^{-\frac{1}{2}}$ dependence. The oriented sample had an even weaker temperature dependence, although it could be argued that the data also fit the $T^{-\frac{1}{4}}$ plot best. Obviously, an area that requires future work is the theoretical modeling of charge transport in the highly oriented conducting polymers now available by the precursor route.

Chapter Summary

In this chapter it has been shown by the positive dependence of conductivity upon increasing conjugation length that the electrical conductivity must involve both intrachain and interchain charge transport phenomenon. That is; high molecular weight is not necessary for high conductivity as long as the intermolecular order is very high. However, in polymers, where the degree of intermolecular order is relatively low, a longer conjugation length increases the probability of having sites with good interchain π-oribital overlap, thus facilitating interchain charge transport. The importance of intrachain transport was reinforced by the conductivity anisotropy displayed in the oriented samples, which became greater with increasing draw ratio. Finally, the temperature dependent conductivity data for highly oriented PPV showed that the activation energy for charge transport was decreased by a factor of 3.7 relative to that in unoriented samples, thus further demonstrating that the alignment and the improved lateral packing of the conjugated chains significantly increased the efficiency of charge transport.

CHAPTER VII

OTHER POLY(ARYLENE VINYLENES)

This chapter is a survey of the preliminary results obtained from studies of the effect which phenyl ring substitution, or replacement of the phenyl ring with a naphthalene ring, has upon the conductivity. The organization of this chapter follows that of Chapters II through VI in that it begins with the motivation behind the study, discusses the synthetic preparation and characterization methods, and then concludes with a presentation of conductivity data and its relation to the chemistry and structure of the material.

Motivation

The sulfonium salt precursor route to highly conjugated poly(arylene vinylene)s has great synthetic versatility. Because of the mild conditions required for the initial bis-sulfonium salt formation and the precursor polymerization, the sulfonium route permits its use even in the presence of a large variety of functional groups. This method is also applicable to the polymerization of aromatic vinylenes such as 1,4-naphthalene vinylene and 2,6-naphthalene vinylene. Its versatility, therefore, opens the door to the preparation of a whole series of analogous conducting polymers from which the polymer electronic and morphological structure can be investigated relative to the conductivity.

211

Conductivity depends both upon the ability for the conjugated polymer to be doped (i.e., the number of charges) and upon the ability for the charge carriers to move through the material. The objective for studying a series of phenyl-substituted PPV's was to try to separate these two factors. The ability for a conjugated polymer to be doped (i.e., to support a charge carrier) depends upon the electron density along the backbone. The conductivity limiting charge transport process depends upon interchain interaction, which is affected by interchain packing. Thus, phenyl substitution with groups having differing electron withdrawing or donating characteristics, but which have nearly the same bulkiness, will affect the electronic nature of the backbone without the overlapping effect of chain packing modification. Whereas phenyl substitution with a series of groups of equal electronegativity, but of differing sizes, will affect interchain packing without changing the electron density along the backbone.

2,5-dimethoxy-PPV and 2,5-diethoxy-PPV fulfill the requirements for the study of this second point. They are both nearly equal in the electron donating ability of their oxygens, but they differ in size by an extra methyl group. It is more difficult to realize the criteria of the first point which requires equal size but differing electro-negativity. However, 2,5-dimethyl-PPV and 2-bromo-5-methyl-PPV have been synthesized and may provide a starting point for future studies of this point.

Poly(1,4-naphthalene vinylene), 1,4-PNV, was prepared in an attempt to lower the energy difference between the arylene vinylene and the quinoid resonance structures, based upon a concept first proposed by

Wudl[127] (Figure 7.1). The decrease in energy difference is due to the
fact that the 1,4-naphthalene vinylene quinoid resonance structure, b,
has not completely lost its aromaticity as does the PPV resonance
structure, d. In Wudl's study of poly(isothianaphthene), PITN, and
poly(thiophene), PT, (structures e and g of Figure 7.3) he observed
that the uv/vis/nir absorption edge of 1240 nm (1 eV) in PITN was a
full 1 eV lower than that of PT (620 nm). He attributed this decrease
to an increased contribution of structure f to the overall resonance
structure of PITN which lowers the $\pi-\pi^*$ transition energy. Thus,
delocalization of doped charges should be improved in PITN and
consequently so should the ease of doping and the stability of the
doped polymer.

Poly(2,6-naphthalene vinylene), 2,6-PNV, shown in Figure 7.2 was
also prepared because of an expected increase in delocalization, but
for a different reason. If two repeat units are considered together,
the quinoid resonance structure, b can be visualized as covalently
overlapping 6 unit long trans-polyacetylene chains. Obviously this
reasoning is somewhat simplistic in that it ignores the length
differences between the aromatic and vinylene bonds which would
increase the energy differences between a and b more than this model
suggests. But it did seem like an interesting and somewhat logical
extension of the PPV analog series to prepare.

Figure 7.1. Resonance structures of (a,b) 1,4-poly(naphthalene

vinylene), (c,d) poly(phenylene vinylene), (e,f)

poly(isothianaphthene), and (g,h) poly(thiophene).

(a)   1,4-PNV   (b)

(c)   PPV   (d)

(e)   PITN   (f)

(g)   PT   (h)
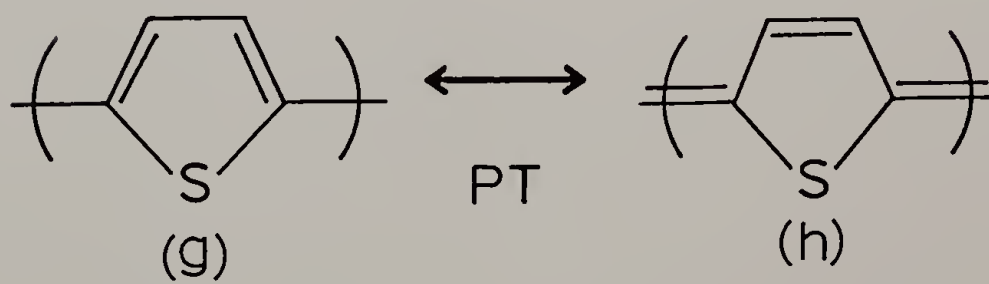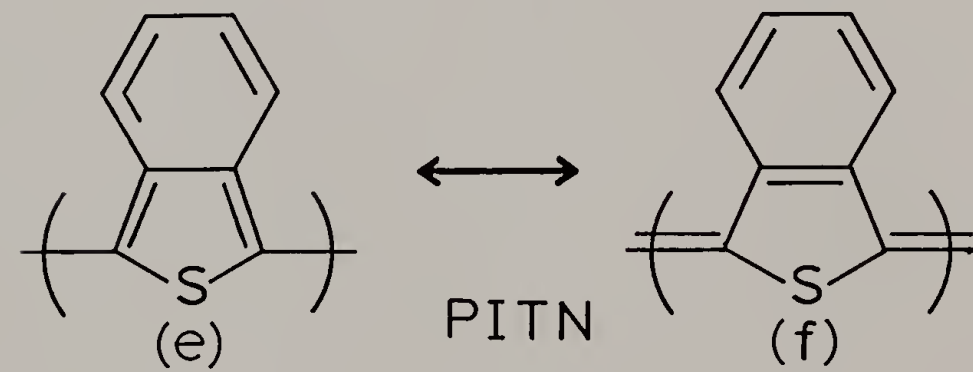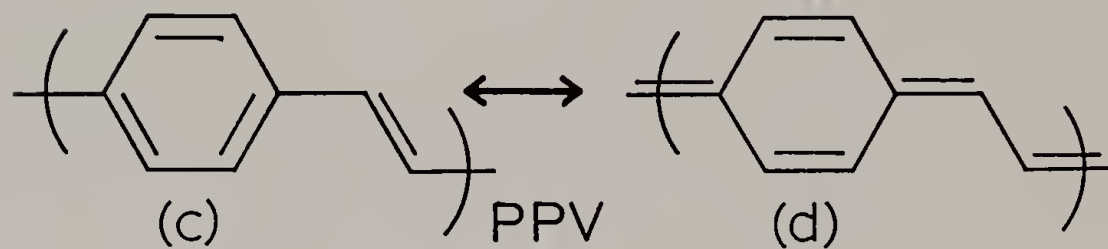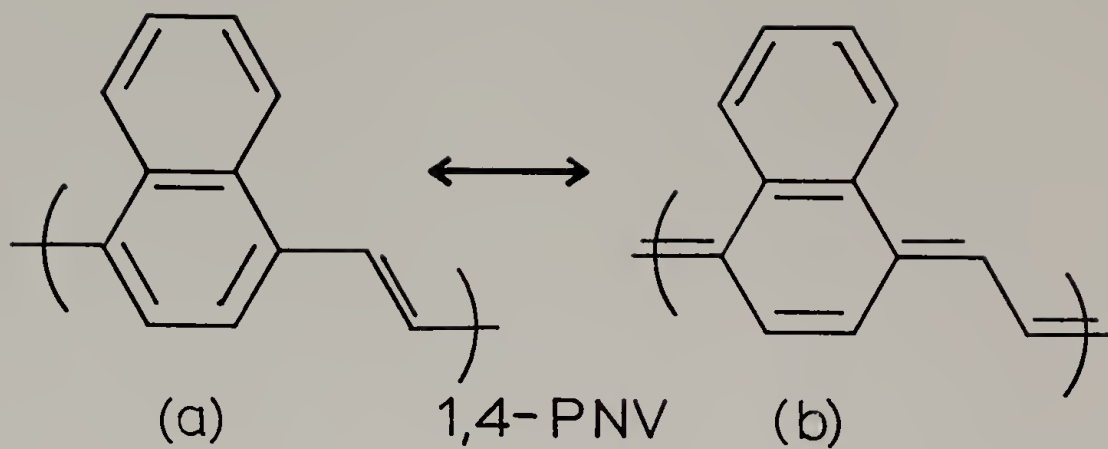
Figure 7.2.   Resonance structures of poly(2,6-naphthalene vinylene).
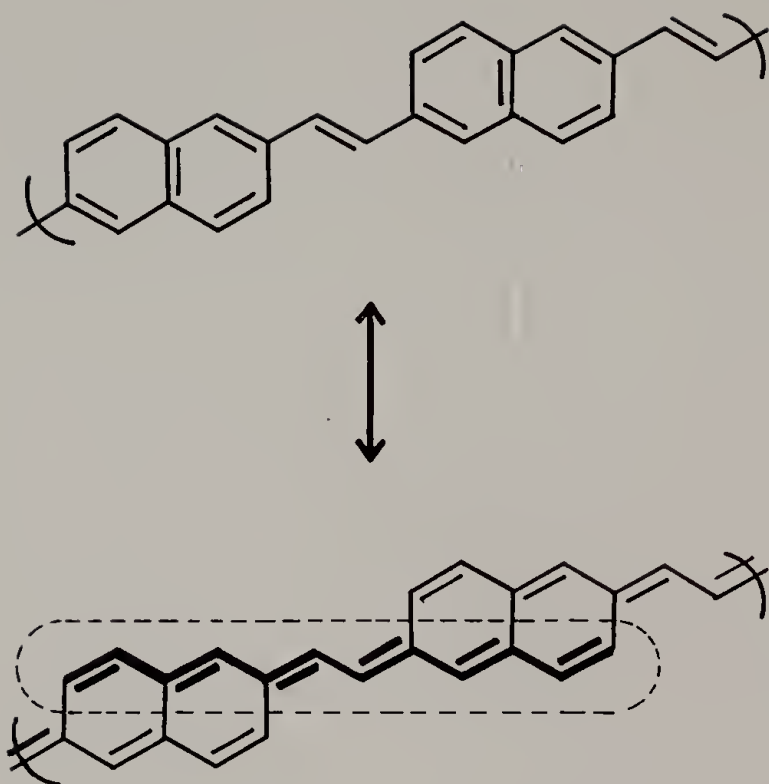
2,6-PNV

Experimental

The polymers synthesized for this study are listed in Figure 7.3.
Naphthalene analogs of PPV were also synthesized in order to study how
the nature of the aromatic ring effects the conductivity; these are
shown in Figure 7.4. All of these polymers were prepared by Dr. S.
Antoun under the direction of Professor R. W. Lenz using the same
procedure as was used to synthesize PPV, except that in some cases the
initial bis(chloromethyl)arylene derivative was not commercially
available and had to be synthesized from other starting materials. The
methods of Wood[128] and Wheland[129] were used for the chloro-
methylation of the appropriate functionalized benzenes. Chlorination
of 1,4-and 1,6-dimethylnaphtalenes was accomplished by reaction with
N-chlorosuccinamide in a refluxing 2:1 CCl_4/benzene solution, to which
a trace of benzoyl peroxide had been added as a radical initiator
following the methods of Brown[130] abd Golden[131].

The bis(sulfonium salt) synthesis, the polymerization, the
elimination, and the doping of these materials were all carried out as
described in Chapter III, except that the elimination temperatures used
varied somewhat due to the differences in the sulfonium stability of
these substituted poly(arylene vinylene)s.

Results and Discussion

Synthesis

The substituted phenylene-bis(sulfonium salt) monomers were found

Figure 7.3. Chemical structures of phenyl substituted PPV's:
(a) poly(2,5-dimethoxy-PPV), (b) poly(2,5-diethoxy-
PPV), (c) poly(2,5-dimethyl-PPV), and (d) poly(2-bromo-
5-methyl-PPV).

(a)

(b)

(c)

(d)
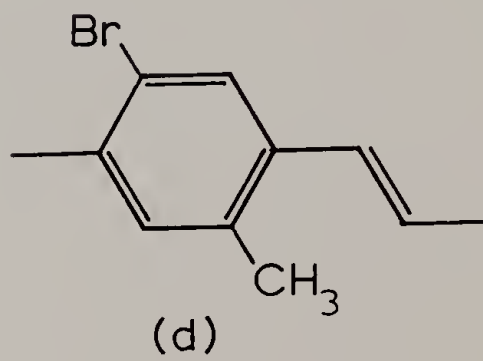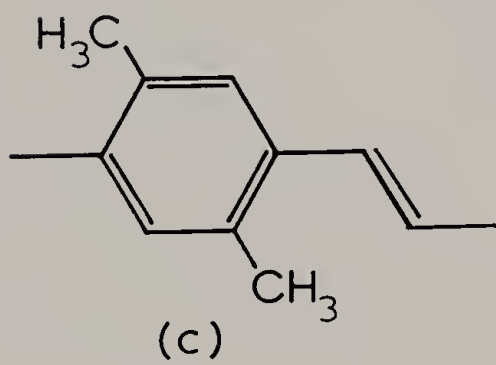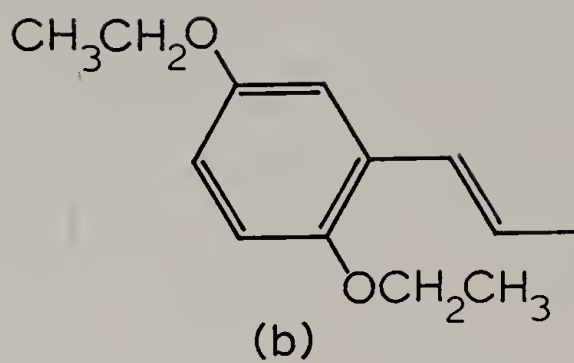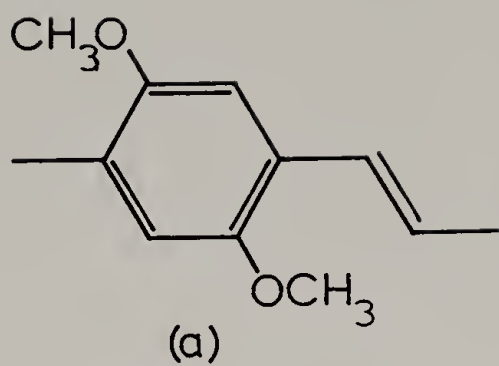
Figure 7.4. Chemical structure of (a) poly(1,4-naphthalene
vinylene) and (b) poly(2,6-naphthalene vinylene).
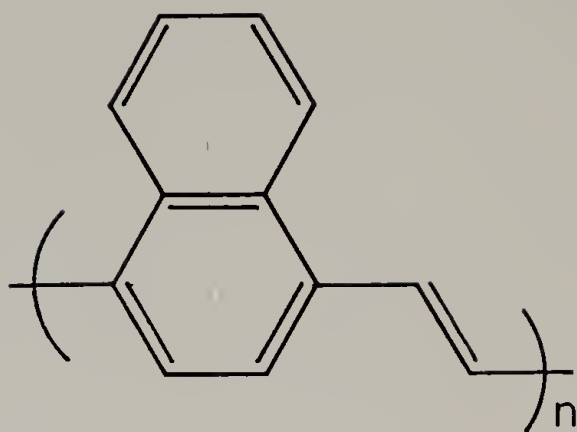
(a)
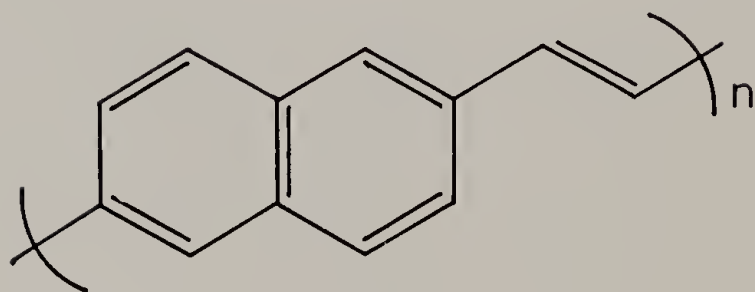
(b)

to be more stable at room temperature than were the naphthalene-bis(sulfonium salts),[132] although all were stable enough to be isolated in high yields (70-90%) and could be polymerized, if used within 1 day of isolation. Again, as with the PPV-bis(sulfonium salt) monomer, refrigeration allowed longer storage times. The synthesis of the polyelectrolytes of the polymers listed in Figures 7.3 and 7.4 were performed under the same conditions as those used for PPV, and resulted in yields of 20-27% (slightly lower than that obtained for PPV). The molecular weight of the precursor polymers were evaluated qualitatively by intrinsic viscosity measurements in a 20/80 methanol/water solvent containing 0.05 M sodium sulfate.

As can be seen in Table 7.1, which shows the yields and intrinsic viscosities of the various PPV derivatives, the PPV precursor itself gave the highest yield and viscosity value. Wessling reported that the preferred sulfonium salt for obtaining the highest molecular weight polyelectrolytes was the 2,5-dimethy-p-xylyene-bis(diethylsulfonium chloride), which was also reported to polymerize 10^3 times faster than the corresponding unsubstituted PPV monomer.[89] As can be seen from Table 7.1, it was found that the 2,5-dimethyl-bis(sulfonium salt) did give the highest viscosity precursor polymer of the substituted series, but that it was not as high as that of the unsubstituted precursor polymer. The reason for the discrepancy between these and Wessling's results may simply be a matter of differing total reactant concentrations, and that this reaction used the dimethylsulfonium salt, where as Wessling uses the diethylsulfonium salt which is a better

Table 7.1. Precursor polymer percent yield and intrinsic viscosity, [η], listed for the PPV derivatives designated according to the chemical formula shown.
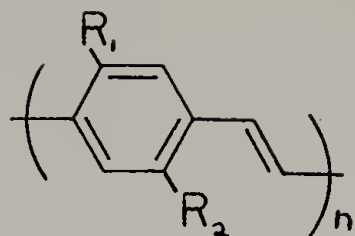
Monomer		Precursor Polymer	$[\eta]$
R_1	R_2	Yield (%)	(dl/g)
H	H	30	2.5
OCH_3	OCH_3	22	1.4
OC_2H_5	OC_2H_5	20	1.3
CH_3	CH_3	27	2.2
Br	CH_3	23	1.7
1, 4-PNV		20	1.4
2, 6-PNV		21	----

leaving group and thus probably decomposes to the quinoid monomer faster. A common observation however, was that the second sulfonium elimination of the precursor in the polymerization solution to give 2,5-dimethyl-PPV units was much slower than that of the PPV precursor for any of the other substituted precursors with the exception of the 2-Br-5-methyl-PPV precursor. The reason for this is not yet clear. The sulfonium group of the naphthalene precursor polymers was the most labile, and significant elimination occurred in solution, especially during the casting step.

Elimination

The elimination transition temperatures for films of 1,4-PNV, 2,5-diMe-PPV and 2,5-diMeO-PPV precursor films were studied by TGA/MS as was done for PPV in Chapter IV. The MS intensities for each of the major elimination components of these precursor polymers and of PPV are plotted in Figure 7.5. Besides slight shifts in the temperatures of the transitions, all these precursors had profiles similar to PPV except that the 2,5-diMeO-PPV showed the loss of most of its CH_3SH at a lower temperature of about $155^{o}C$.

The 2,5-diMeO-PPV precursor film sample showed two major weight loss maxima at 90° and $400^{o}C$. Nearly all of the chlorine and sulfur containing products were released in the low temperature region ($\sim 100^{o}C$). Small amounts of CH_3SH and H_2S were evolved around $330^{o}C$. Although not shown in Figure 7.5, there was also evidence of the possibility that a small amount of CH_3OH was released at a temperature of approximately $110^{o}C$. At this time, the elimination of CH_3OH has not

Figure 7.5. Mass spectral ion intensities for (a) HCl, (b) CH_3SCH_3,
(c) CH_3Cl, and (d) CH_3SH from the precursor polymers
designated within each set of traces as (1) PPV, (2)
2,5-diMeO-PPV, (3) 2,5-diMe-PPV and (4) 1,4-PPV.
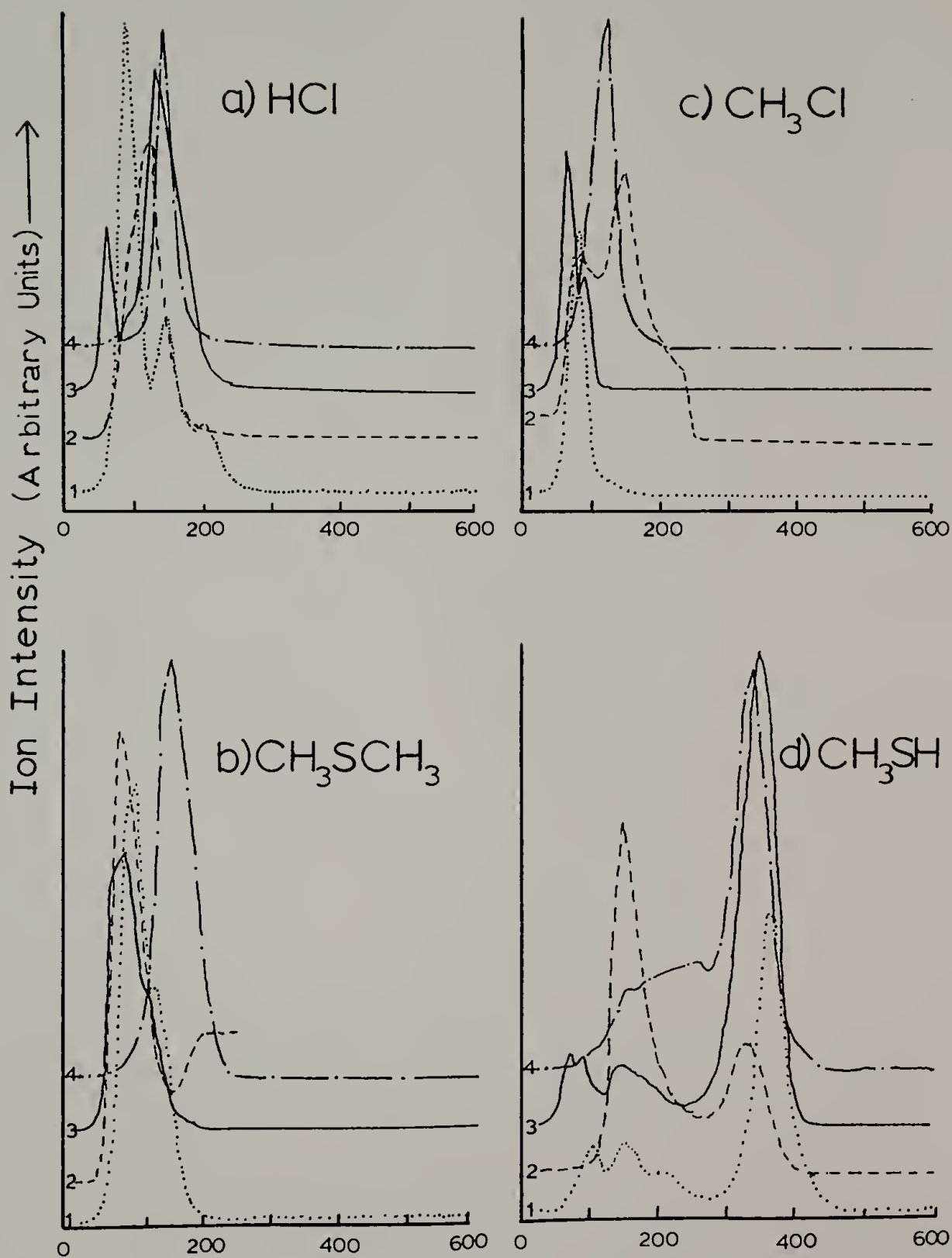
been confirmed; but if this signal was real, it could indicate that some acid induced decomposition of the methoxy substituent occurred, since the HCl also was detected near this temperature. The unconfirmed evolution of CH_3OH is puzzling however, because phenyl ethers are generally quite stable, and when they do decompose, the alkyl-oxygen bond is usually the weakest point, thus methyl chloride would be expected to evolve leaving a phenol compound. Decomposition of the backbone occurred at about $380^{\circ}C$ and was marked by the evolution of expected components such as $(CH_3O)_2-C_6H_3-C_2H_5$ and $(CH_3O)_2-C_6H_3-CH_3$. The $380^{\circ}C$ degradation temperature was about $30^{\circ}C$ lower than the degradation temperature of the other substituted PPV's and was about $100^{\circ}C$ lower than the onset of PPV degradation.

The 1,4-PNV precursor film sample showed three major weight loss maxima at $140^{\circ}C$, $330^{\circ}C$ and $440^{\circ}C$. All of the chlorine products were released during the first transition; and the major sulfur containing product, $(CH_3)_2S$ was released at its maximum rate at $155^{\circ}C$. No unusual products, other than those characteristic of the sulfonium elimination seen in the other precursors, were detected. The maximum rate of main chain degradation occurred around $440^{\circ}C$ with an onset near $400^{\circ}C$, evolving naphthalene, methylnaphthalene, methylethylnaphthalene, and dimethylnaphthalene.

The 2,5-diMe-PPV precursor film sample showed two major weight loss maxima at $90^{\circ}C$ and $410^{\circ}C$; the latter maxima also had a small but significant shoulder at about $330^{\circ}C$. All the chlorine containing products and at least two thirds of the sulfur containing products were released during the first transition around $90^{\circ}C$. The 2,5-diMe-PPV

backbone degradation at 410°C and was characterized by the evolution of dimethylethylbenzene and trimethylbenzene.

X-ray Diffraction

As in the case of PPV films, the x-ray diffraction patterns of the substituted, unoriented PPV's showed only diffuse, low intensity reflections which were interpreted as most probable packing distances or as reflections from extremely small crystallites. Since only 1 to 3 reflections could be discerned for these polymers, and since insufficient quantities of these polymers had been made to optimize the stretching process, it was not possible to index a crystallographic unit cell. The d-spacings of these polymers were measured from the flat film x-ray patterns and are listed in Table 7.2. Not unexpected was that the unsymmetrical 2-Br-5-Me-PPV was the least ordered. Its x-ray diffraction pattern showed only a broad amorphous halo centered at about 3 $\overset{\circ}{A}$.

Conductivity

Table 7.3 lists the conductivities of the various PPV analogs, along with the pertinent sulfur elemental analyses and the maximum absorption wavelengths of their electronic spectra. The sulfur weight percent analysis for each of these materials, except the 2-Br-5-Me-PPV, was low enough so that the conjugation length should be in the regime where the conductivity was insensitive to further elimination. The undoped conductivities for the electron-rich analogs (the alkoxy-PPV's and the PNV's) were higher than that of PPV as expected.

Table 7.2. d-Spacings for 2,5-diMeO-PPV; 2,5-diEtO-PPV; 2,5-diMe-
PPV; 2-Br-5-Me-PPV and 1,4-PNV measured from flat film
wide angle x-ray diffraction patterns.

Polymer	Spacings ($\overset{\circ}{A}$)
2, 5-diMeO-PPV	8.9 (broad, very weak) 6.1 4.4 (broad halo, weak)
2, 5-diEtO-PPV	6.3 4.0 (very broad halo)
2, 5-diMe-PPV	7.7 (very weak) 5.9 3.6
2-Br-5-Me-PPV	ca. 3.0 (very broad halo)
1, 4-PNV	7.1 6.3 3.7

Table 7.3. Sulfur weight percent, undoped color, uv/vis maximum
absorption wavelength (λ_{max}), undoped conductivity, AsF_5
doped conductivity, and iodine doped conductivity for
various PPV derivatives, 1,4–PNV and 2,6–PNV.
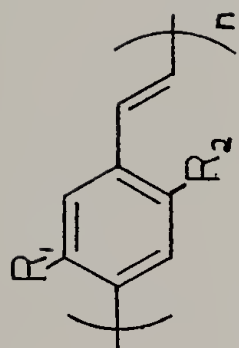
R_1	R_2	S (wt %)	color	λ_{max}	(eV)	$\sigma(S/cm)_{undoped}$	$\sigma(S/cm)_{AsF_5}$	$\sigma(S/cm)_{I_2}$
H	H	<0.01	orange	512	(2.4)	$2 * 10^{-11}$	8.0	no rxn.
OCH_3	OCH_3	0.57	red	620	(2.0)	$1 * 10^{-8}$	1.8	18.0
OC_2H_5	OC_2H_5	0.06	red	620	(2.0)	$6 * 10^{-9}$	0.9	---
CH_3	CH_3	0.93	yellow	475	(2.6)	$4 * 10^{-11}$	$1 * 10^{-6}$	no rxn.
Br	CH_3	3.65	yellow	---	---	$6 * 10^{-11}$	$5 * 10^{-6}$	no rxn.
1,4-PNV		<0.01	red	620	(2.0)	$2 * 10^{-10}$	$3.2 * 10^{-6}$ [a]	$1.6 * 10^{-5}$
2,6-PNV		<0.01	red	620	(2.0)	$1 * 10^{-9}$	3.5	---

The 2,5-diMe-PPV and the 2-Br-5-Me-PPV samples had undoped conductivities only slightly higher than PPV, although the differences were probably within experimental error.

The undoped room temperature conductivities for PPV and for 2,5-diMeO-PPV were reported by Haertel et al., as 2×10^{-14} S/cm and 3×10^{-10} S/cm respectively.[133] These measurements were made on pressed pellets of oligomeric powders which had been synthesized by Wittig condensation. Thus, the lower conductivity of the pellets relative to the precursor synthesized films may be due to either the low molecular weight or the grain/grain contacts of the powder. Gourley et al., reported AsF_5 doping of 2,5-dimethoxy-PPV oligomers, prepared by dehydrohalogenation, to a maximum conductivity of only 4×10^{-4} with an AsF_5 mole ratio of 43%[60]. Although these workers expected to achieve at least as high a conductivity as PPV, due to the electron stabilization of the cation charge carriers, they reasoned that AsF_5 formed an oxonium complex with the methoxy oxygen rather than efficiently doping the backbone. They also reported that other dopants such as iodine were ineffective. The other PPV derivatives and the PNV polymers had not been prepared previously by either the Wittig or dehydrohalogenation methods.

AsF_5 doping of the 2,5-diMe-PPV and 2-Br-5-Me-PPV polymers resulted in a small increase in conductivity to rather low values of 1×10^{-6} S/cm and 5×10^{-6} S/cm respectively.[134] These polymers did not show any evidence of reactivity towards iodine, that is there was no change in color or conductivity after 72 hours exposure to I_2 vapor. One of the possible reasons for these low conductivities was the poor

molecular order evidenced by their x-ray diffraction patterns (Table 7.2). The 2,5-diMe-PPV did show three weak reflections, but the spacing of each ring was about 2 Å greater than that of the rings seen in PPV, possibly indicating larger interchain packing distances which could account for the low conductivity. In the case of 2-Br-5-Me-PPV there was no crystallographic order; only an amorphous halo centered at about 3 Å was observed in the x-ray pattern.

The electron withdrawing inductance of the bromine substituent would also be expected to lower the reactivity towards oxidation of the backbone by AsF_5, and to decrease electron delocalization an stability of the resulting cation.

The 1,4-PNV[135] and 2,6-PNV films were a deep red color with a maximum visible absorption wavelength of 620 nm corresponding to an optical $\pi-\pi^*$ excitation energy (band gap) of 2.0 eV. This is about 0.4 eV lower than that of PPV. Based upon the concepts discussed at the beginning of this Chapter, this decrease in the excitation energy relative to PPV was as expected. AsF_5 doping of the 1,4- and 2,6-PNV's resulted in conductivities of 3.2×10^{-2} S/cm and 3.5 S/cm respectively. One explanation of this difference might be that the fused phenyl ring of the 1,4-PNV provided a site for the charge carrier to be localized, thus decreasing its mobility relative to that observed in the 2,6-PNV where the phenyl rings were all in the main chain.

The 1,4-PNV could be doped by iodine to a conductivity of 1.6×10^{-5} S/cm. The reactivity to iodine indicates that the additional electron delocalization induced by the phenyl ring fused to the PPV backbone, also lowered the ionization potential. The fact

that a milder dopant was effective may also mean that the created cationic charge carrier might also be less reactive, and hence more stable to atmospheric oxygen and moisture than was AsF_5 doped PPV. The data shown in Figure 7.6 confirms this supposition and showed that the conductivity drops from the initial 1.6×10^{-5} S/cm value (in vacuum) to a value only 4 times less, over a five week period in air. AsF_5 doped PPV and its analogs generally showed conductivity decreases of 4-5 orders of magnitude within a few days in air.

The 2,5-diMeO-PPV and 2,5-diEtO-PPV films were the same color and displayed the same maximum optical absorption wavelength of 620 nm for the $\pi-\pi^*$ transition as did the PNV films.[134] Therefore, the non-bonded electrons of the alkoxy oxygens do contribute to the electron density along the backbone, relative to the electron density of PPV. Contrary to the findings of Gourley et al., for oligomeric powders of 2,5-diMeO-PPV, AsF_5 doping of these films gave conductivities nearly as high as PPV. It was tempting to attribute the difference between the AsF_5 doped conductivities for the 2,5-di-MeO-PPV of (1.8 S/cm) and the 2,5-diEtO-PPV (0.88 S/cm) to expected differences in interchain packing distances, since there should not be a difference in the backbone electronic structure. But the poor quality and lack of information in the x-ray diffraction patterns does not allow this conclusion to be drawn at this time.

Again, contrary to findings on the oligomeric powder, this film of 2,5-diMeO-PPV could also be successfully doped with iodine to a surprisingly high conductivity of 18 S/cm. It is unknown at this time, why there should be such a large disparity between these results and

Figure 7.6. Conductivity of iodine doped 1,4-PNV plotted as a
function of air exposure time.
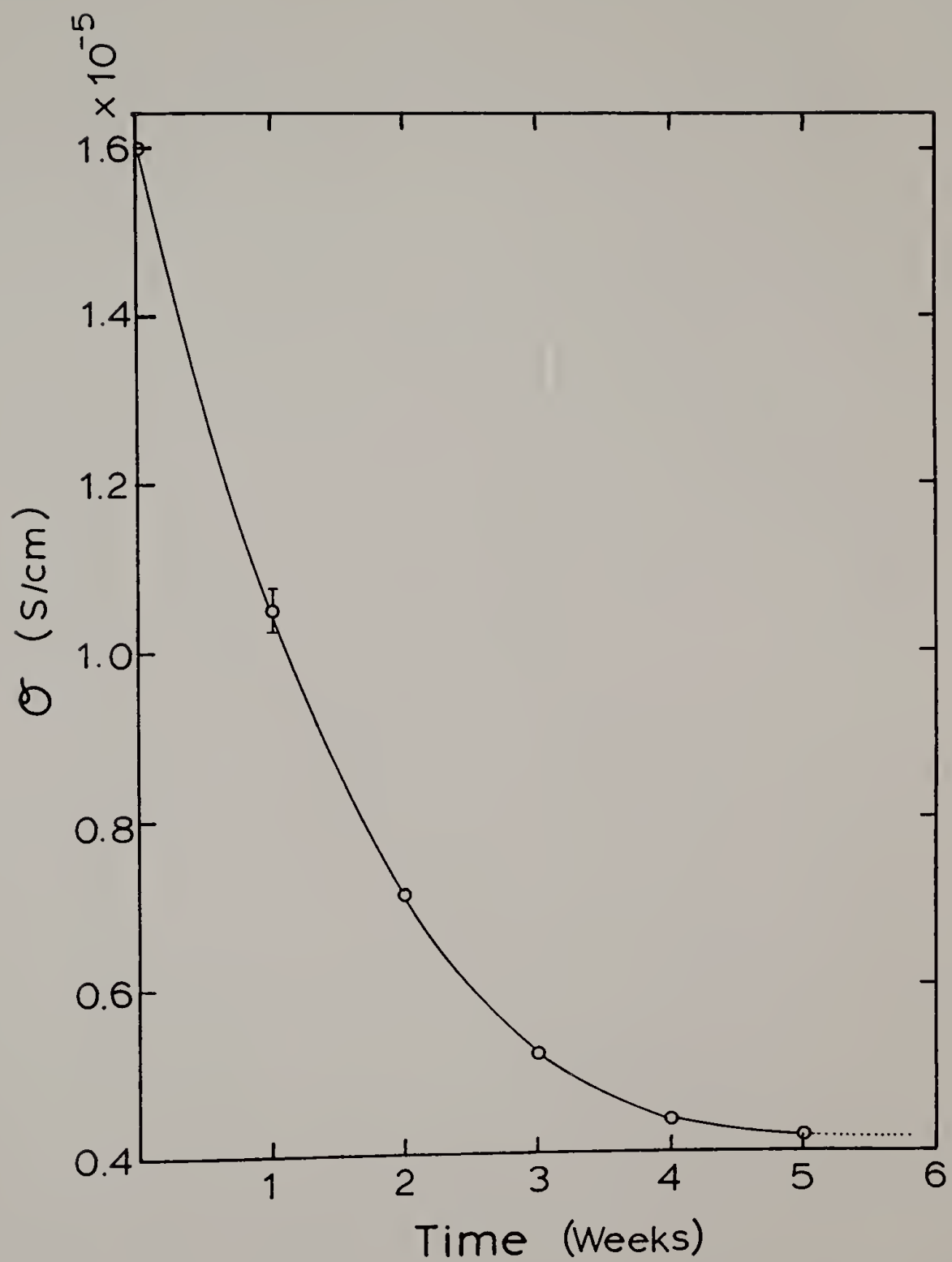
those of Gourley et al. Iodine doping of this material has also been reported by Ohnushi et al.,[136] to a conductivity of 100 S/cm; but again as in their work on iodine doping of PPV films, the numbers they report are suspect because the excess adsorbed iodine was not removed by vacuum prior to their measurements.[113]

The most remarkable result obtained for the iodine doped 2,5-diMeO-PPV (Figure 7.7) was that upon exposure of the sample to air for 5 weeks, the conductivity decreased only by a factor of 0.6 to a nearly stable conductivity of 11 S/cm. This stability of a processable conducting polymer with such a high conductivity is exciting in that it opens the door to a wide range of possible applications. Certainly, this material should be one of the foci of interest for future work on PPV analogs.

Figure 7.7. Conductivity of iodine doped 2,5-diMeO-PPV plotted as

a function of air exposure time (top curve, right

ordinate), superimposed upon the data of Figure 7.6

(bottom curve, left ordinate).
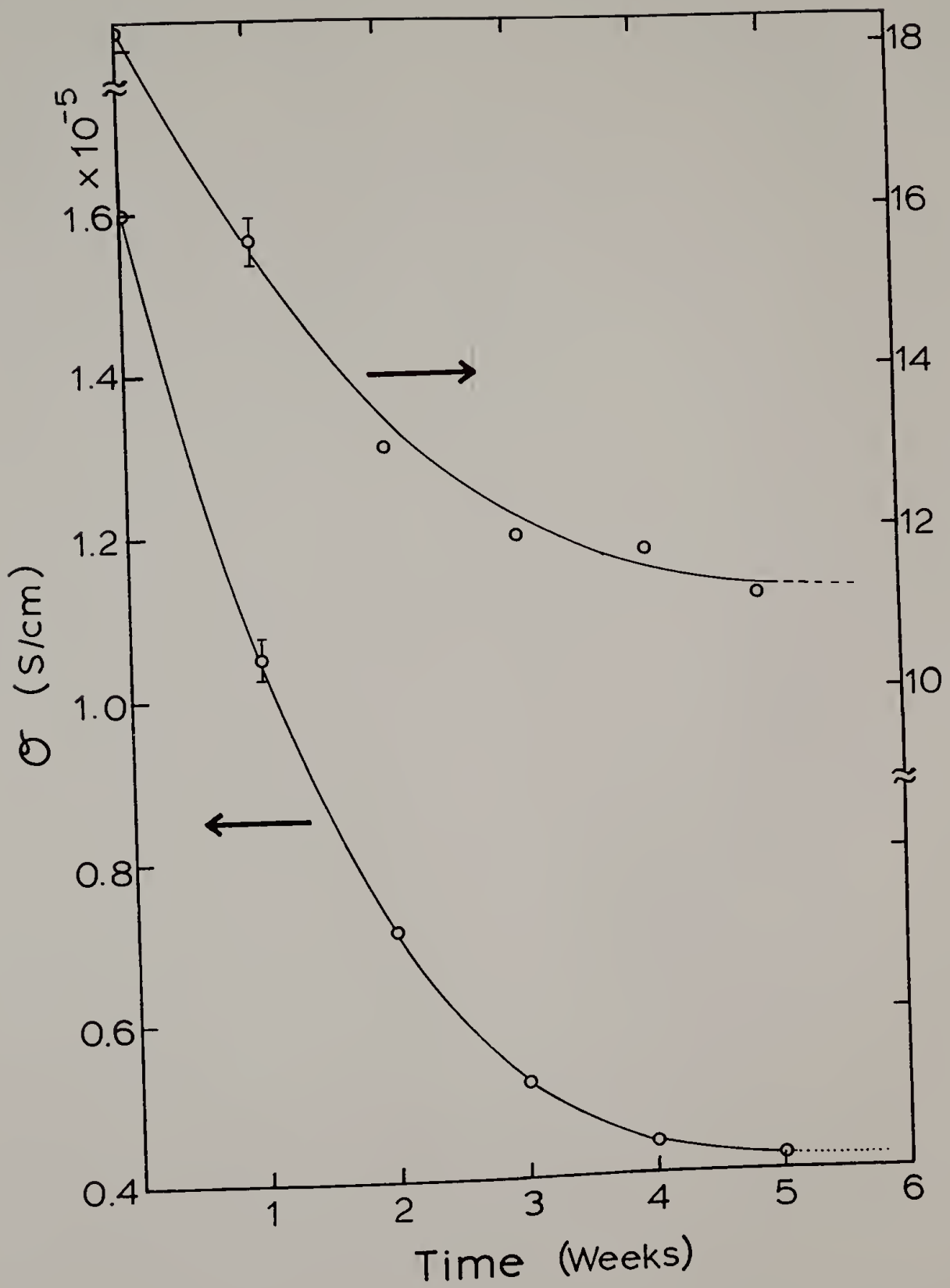
CHAPTER VIII

CONCLUSIONS AND FUTURE WORK

The primary objectives of this dissertation have been to understand the synthesis and conversion chemistry of the precursor polymer to PPV as a basis from which to optimize the rational modification of the morphology of PPV films; to characterize this resulting morphology in terms of the molecular orientation and crystal structure; and then by measuring the electrical conductivity of these PPV films, after doping, to begin to gain some insight into the charge propagation in terms of the chemical and morphological structure of the polymeric matrix. In this final chapter, the experimental results which were obtained and the techniques which were devised towards fulfilling these objectives, will be summarized. The chapter concludes with some suggestions for the future extension of this study to more fully probe the conduction transport mechanisms, and to take advantage of the synthetic and processing versatility of the precursor technique for the preparation of materials which may have interesting properties and applications.

Summary of Results

Chemistry and Processing

Looking back upon the initial results of this research, the mere reduction of the base to bis(sulfonium) monomer stoichiometry to equimolar, rather than the use of the equinormal stoichiometry

specified by Wessling and Zimmerman, seems almost trivial. However, it is this simple procedure which has made possible the attainment of a high molecular weight precursor polymer, which has further enabled the casting of the strong, coherent films having a low degree of premature base induced sulfonium elimination, that were absolutely necessary for thermal stretch processing. The other conditions which were important for successful polymerization were the rigorous exclusion of oxygen from the reaction mixture to insure high molecular weight, and the use of low reaction temperatures (less than $0^{o}C$) to further reduce premature sulfonium elimination. A monomer concentration less than 0.3 molar was also found to be necessary to prevent gelation of the solution so that stirring was effective in maintaining solution homogeneity.

The mechanism proposed for p-xylene-bis(dimethylsulfonium chloride) polymerization was the free radical addition reaction of an α-sulfonium quinoid type intermediate produced by the reaction of base, and initiated by the diradical resonance conjugate of the quinoid monomer. This radical mechanism was supported by the fact that a molecular weight of greater than 5×10^5 daltons was achieved even though the polymer yield was less than 30%. Additional support came from the observation that addition of a water soluble radical initiator increased the rate of reaction, and that in the presence of oxygen, only low molecular weight oligomers resulted. The significance of this mechanism is that the success of the future utilization of the sulfonium precursor route for preparation of various substituted PPV's

and analogs of PPV will depend upon avoiding functional groups which might interfere in the free radical chemistry.

The elimination reaction of the sulfonium group from the precursor polymer film was studied using uv/vis spectroscopy, elemental analysis, and TGA/mass spectroscopy in an attempt to understand the factors which affected the preparation of partially eliminated films, stretched films, and fully eliminated PPV films. What was discovered, was that the elimination of the α-dimethylsulfonium chloride and the β-hydrogen did not occur just by the simple E1cB mechanism of methylsulfide and HCl elimination observed at approximately 105°C. There was also the dealkylation side reaction of the sulfonium group which liberated methyl chloride at approximately 105°C which left an α-thiomethyl ether pendant group on the poly(p-xylylene) backbone. The final quantitative conversion to PPV occurred at approximately 360°C by homolytic cleavage of the benzylic carbon-sulfur bond and abstraction of the β-hydrogen liberating methylmercaptan, dimethyldisulfide and dimethyltrisulfide. The TGA/MS experiment also demonstrated that PPV was quite thermally stable in an inert environment, since it only decomposed above 500°C.

Stretching of the precursor film was only possible during the thermal elimination step because of the plasticizing effect of the volatiles which were produced. Thus by understanding the temperature dependence of the elimination process, the draw process was optimized. The important draw variables were found to be the initial degree of elimination, which determined the overall concentration of plasticizing volatiles available; and the temperature of drawing, which determined the rate of the plasticizing volatile evolution. The optimum starting

material had a 2:1 ratio of uneliminated to eliminated polymer repeat units, and was stretched at a temprature between the initial elimination temperature of approximately 110°C and 180°C. Above 180°C the volatile production was so rapid that bubbles formed in the film. This last point was interesting, because PPV foam could be made by performing the elimination of films by rapid heating above 180°C, (i.e., by immersion in a hot fluidized sand bath). A zone drawing technique was devised to stretch the precursor films and was shown to be the most facile method for utilizing the short lived plasticization, afforded by the elimination reaction, to obtain high and uniform orientation.

Structural Characterization

A remarkable amount of molecular orientation was imparted to the PPV films by the stretching process. Wide angle x-ray diffraction and especially electron diffraction patterns showed well developed fiber patterns consisting of up to 7 equatorial reflections and 7 layer lines. Only the first layer line showed any evidence of 3-dimensional order, all other layer lines consisted of diffuse streaks perpendicular to the meridian indicating a high degree of axial translational disorder. An important and interesting piece of information was that the reflections on the first layer line arose only from molecular correlations within the (0kℓ) plane, thus in the (h00) direction there was effectively complete axial translational disorder. So the crystal structure of oriented PPV could be described as randomly axially dispaced sheets of parallel chains. The monoclinic unit cell was

indexed as having the following parameters: a = 7.90$\mathring{A}$, b = 6.05$\mathring{A}$, c = 6.58$\mathring{A}$ (chain axis), α = 123°, and a setting angle of the planar chains in the (hk0) plane of about 56°. The unit cell contained 2 repeat units and had a calculated density of 1.283 g/cm^{3}.

Characterization of the molecular orientation of PPV samples, stretched to draw ratios up to 10 times the original length, was performed by wide angle x-ray diffraction of the (110) equatorial reflection and by infrared dichroism of the trans-vinyl CH bending mode at 963 cm^{-1}. Even at a low draw ratio of 1.2, a relatively high Hermans orientation function of 0.58 was measured which was shown to increase rapidly to a value of 0.95 at a draw ratio of 6. Further stretching did not seem to induce significant additional orientation.

An approximation of the crystallite diameter perpendicular to the fiber axis was made from 2θ x-ray scans of the (210) reflection. The unoriented film gave a diameter of about 87$\mathring{A}$ which increased to about 121$\mathring{A}$ at a draw ratio of 6. Thus there was a much less significant effect upon the crystallite size by stretching than there was upon the molecular orientation. The small crystallite size was also reflected by the optical clarity of the stretched films, thus birefringence measurements of orientation might be useful in the future.

Electrical Characterization

PPV films were p-doped in this study using the vapors of perchloric acid, sulfuric acid, and arsenic pentafluoride to conductivities of 0.3 S/cm, 125 S/cm, and 8 S/cm respectively. The conductivity of the acid doped samples, however was partially ionic in nature, while that of the

arsenic pentafluoride doped samples was purely electronic. Iodine, a common dopant for polyacetylene, was found to be ineffective either in solution or as a vapor. N-doping was performed by immersing a PPV film in a THF solution of sodium napthalide. After washing and drying the sample had a conductivity of 2×10^{-4} S/cm, but was extremely unstable to the atmosphere.

An open system method for AsF_5 doping was devised which allowed the doping to be performed simultaneous with the removal of the AsF_3 by-product and any volatile impurities in the system. An experiment was also designed, which allowed the measurement of dopant weight uptake using a sensitive fused quartz spring balance while measuring conductivity at the same time.

The electrical conductivity was shown to have a strong dependence upon the chemical and molecular structure of the PPV chains. Isotropic films of PPV were prepared with a range of conjugation lengths by varing the degree of elimination. The log of the maximum conductivities of these films, after AsF_5 doping, varied approximately with the 5.8 power of the average conjugation length, until a conjugation length of about 6 units was reached. Above this length there was no further effect of the conjugation length upon the measured conductivity. Since the dopant weight uptake was about the same for all of these samples, it seemed that the conjugation length affected more than just the stability of the charges, but that the mobility of the charges was also increased at higher conjugation lengths.

AsF_5 doped PPV samples, oriented by stretching to draw ratios of 14 times the original length, displayed a conductivity measured parallel

to the stretch direction of 2500 S/cm which was over 2 orders of magnitude higher than the unoriented films and was comparable to the highest conductivity measured for doped polyacetylene. The log of the parallel conductivity was a strong positive function of the orientation function over the draw ratio range less than about 8. Above this draw ratio, the conductivity continued to increase (although at a slower rate) while the orientation function showed little change. Measurements of conductivity perpendicular to the fiber axis showed a decrease in conductivity with orientation by a factor of about 0.25. Temperature dependant conductivity measurements, which were made for both the oriented and unoriented doped samples, showed that the Arrhenius activation energy for charge carrier transport was about 3-4 times lower for parallel conductivity in highly oriented samples than it was for conductivity in unoriented PPV samples.

In order to explain this data, it was proposed that the conductivity in AsF_5 doped PPV was due to charge carrier transport both along the polymer backbone and between the polymer chains. The dramatic increase in conductivity parallel to the chain axis and the decrease in conductivity perpendicular to the chains indicated that the interchain charge transport was the limiting step of the charge mobility; and that, relative to the energy of interchain mobility, the intrachain mobility was very high. Since the ease of interchain charge transport depends upon the $\pi - \pi$ orbital overlap between the chains, the effect of increasing conjugation length was to increase the probability of having sites with sufficient overlap. Orientation also increased the quality of chain packing, but because of the highly translationally

disordered crystal structure of the chains, there were still probably only a small number of sites with good interchain $\pi-\pi$ overlap. Thus with an applied electric field along the stretch direction, the charge moved more easily along the backbone, and only hopped to an adjacent chain when it reached a chain end or other defect which interrupted the conjugation. On the other hand, when the field was applied in the direction perpendicular to the orientation direction, all transport in this direction had to occur by interchain transport. This picture explained the observed mobility anisotropy.

Future Studies

The above proposal for the conductivity charge transport process is a qualitative simplification of a quite complex process. Thus, there is room for a significant amount of refinement and quantification of this model, and there are many further experiments which should be performed. One of the most important of these experiments would be to measure the charge carrier mobility and mobility anisotropy directly using Hall effect measurements parallel and perpendicular to the stretch direction. Another would be to address the effect of dopant concentration upon conductivity, especially at low dopant concentrations. It would be interesting to see if the semiconductor-to-metal transition, demonstrated in AsF_5 doped polyacetylene by Warakomski,[116] appears in the parallel direction at a lower dopant concentration than in the perpendicular direction.

Since the molecular structure of undoped oriented PPV films has now been determined, the next step should be to investigate the fundamental question of "where is the dopant?" The charge transport concept proposed here cannot differentiate between an interchain hopping which relies on an intercalated doped structure or one which does not require a regular doped structure. But with the well oriented films now available, x-ray and electron diffraction studies of the doped polymer should be relatively straightforward.

The nature of the charge carrier in p-doped PPV should be studied using electron paramagnetic resonance and ultraviolet/visible/near infrared spectroscopy, following the approach of Bredas et al., applied to polypyrrole.[137] It is expected that initial doping produces cation-radicals (termed polarons by physicists) and with further doping the radicals combine to produce a divalent cation (or bipolaron) delocalized along some length of the polymer backbone and which is the actual charge carrier for conduction. Preliminary evidence for polaronic and bipolaronic doping has already been obtained by the electrochemical doping of PPV within the sample compartment of the uv/vis/nir spectrophotometer.[138]

The reason for the continued increase in the parallel conductivity of AsF_5 doped PPV above a draw ratio of 6, in the light of the fact that the Hermans orientation function has leveled off, is not very well understood at this point. X-ray diffraction of these thin films and infrared dichroism measurements enabled only a second order orientation function to be measured, higher order orientational measures should be used to determine if it was just that the second

order techniques used were too insensitive. Also, since the oriented precursor films were fully converted to PPV at 370°C without constraining the ends of the films, it might be possible to increase the molecular orientation and the 3-dimensional crystallographic order within the films further by performing the final elimination of the films under conditions of uniaxial stress.

Other ideas for the processing of the precursor polymer include: adapting the zone drawing technique to an Instron tensile machine by gearing the heat zone to move along the film at a fraction of the crosshead speed, thus producing a draw ratio inverse to that fraction; extruding fibers of PPV precursor from the solution or polymerizing the monomer at high a concentration within the die in a type of reaction extrusion process, this process has already been shown to be viable;[139] and stretching films of the substituted PPV's, especially the alkoxy-PPV's which showed environmental stability after iodine doping.

There are an almost infinite number of possible ideas for variation of the chemical structure and for utilization of the exceptional synthetic versatility of the sulfonium precursor polymers. For instance, copolymers of all types including graft, block, and random copolymers could be prepared. Some of the targets for this approach might be the substitution of side-chain liquid crystalline mesogens onto the PPV backbone which may result in advantageous ordering in the cast films. The use of highly polarizable side groups might lead to some interesting non-linear optical properties which could be modified by the conductivity of the matrix. Block copolymers would lead to

phase separated morphologies, possibly of conducting and insulating

phases similar to what has been observed in the poly(2-vinyl

pyridine)-block-polystyrene or block-polybutadiene systems,[140,141]

and this may also lead to post-processability after the final

conversion of the precursor to PPV. The use of side group substituents

on the phenyl ring which can be complexed with iodine or other reagents

to give charge transfer salts may give a system which can be doped

"twice" and lead to interesting properties.

The chemistry of the sulfonium elimination can also be utilized.

One of the problems with the use of dimethylsulfonium salts is that the

loss of methylchloride predicates the necessity to carry out the final

elimination at above 360°C to remove the residual thiomethyl ether side

group. Recent work by Han and Machado[142] has shown that the use of

tetrahydrothiophene as the alkyl sulfide removes the possibility for

the dealkylation side reaction, and that PPV can be obtained

quantitatively at 250°C from the tetrahydrothiophene sulfonium

precursor polymer. The less severe requirements of a lower elimination

temperature increases the possible choices of phenyl substituents.

Another way to modify the sulfonium chemistry would be to use a

sulfonium counterion which forms a protonic acid upon elimination that

could dope the sample concurrent with the elimiantion reaction. Antoun

attempted this by preparing the bis(sulfonium perchlorate) monomer, but

when this monomer exploded in the melting point capillary during

analysis, further work on this approach was suspended.[143] The use of

sulfonate or similar counterions should be safer.

Conclusion

If measured by the number of ideas generated and by the potential which has become apparent for this precursor route to conjugated polymers, this dissertation research has been quite successful. It has been demonstrated that the sulfonium precursor route to PPV can yield chemically high quality material from a well characterized thermal conversion step, and that highly conjugated PPV could be obtained with a wide variety of morphological forms and chemical compositions. The crystal structure and the degree of molecular order of uniaxially stretched films has been characterized in detail, and this characterization has been shown to provide a basis for the understanding of the anisotropic electrical behavior of these doped films of conducting PPV.

REFERENCES

1. C. K. Chaing, C. R. Fincher, Y. W. Park, A. J. Heeger, H. Shirakawa, E. J. Louis, S. C. Gau and A. G. MacDiarmid, Phys. Rev. Lett., 39, 1098 (1977).

2. G. Wegner, Angew. Chem. Int. Ed. Engl., 20, 361 (1981).

3. K. Seeger, Die Angew. Makro. Chemie 109/110, 227 (1982).

4. W. J. Feast, Chem. Ind. L., (8) 263 (1985).

5. W. Hayes, Contemp. Phys., 26(5), 421 (1985).

6. R. B. Seymore, (Ed.), Conducting Polymers, Plenum Press, New York, 1981.

7. D. A. Seanor, Electrical Properties of Polymers, Academic Press, New York, 1982.

8. J. Mort and G. Pfister, Electronic Properties of Polymers, J. Wiley & Sons, New York, 1982.

9. J. C. W. Chien, Polyacetylene, Academic Press, New York, 1984.

10. T. A. Skotherm, (Ed.) Handbook of Conducting Polymers, Vols. I and II, Marcel Dekker, Inc., New York, 1986.

11. S. B. Mainthia, P. L. Kronick and M.M. Labes, J. Chem. Phys., 41, 2206 (1964).

12. W. E. Hatfield, Molecular Metals, Plenum Press, New York, 1979.

13. G. Wegner, Makromol. Chem. (Symp.), 1, 151 (1986).

14. P. Pfluger, U. M. Gubler and G. B. Street, Solid State Comm., 49, 911 (1984).

15. V. Enkelmann, K. Goeckelmann, G. Wieners and M. Monkenbusch, Mol. Cryst. Liq. Cryst., 50, 235 (1979).

16. L. W. Shaklette, et al., Synthetic Metals, 1, 307 (1979).

17. A. Boloynesi, M. Catellani, S. Destri and W. Porzio, Polymer, 26, 1628 (1985).

18. H. T. Chiu, T. Tsutsui and S. Saito, Polymer Comm., 26, 61 (1985).

19. C. R. Fincher, P. L. Peebles, A. J. Heeger, M. A. Druy, Y. Matsumura, A. G. MacDiarmid, H. Shirakawa and S. Ikeda, Solid State Comm., 27, 489 (1978).

20. G. Lugli, U. Pedretti and G. Perego, Mol. Cryst. Liq. Cryst., 117, 43 (1985).

21. G. Leising, R. Vitz, B. Ankele, W. Ottinger and F. Stelzer, Mol. Cryst. Liq. Cryst., 117, 327 (1985).

22. H. Shirakawa and S. Ikeda, Polymer J., 2, 231 (1971).

23. T. Ito, H. Shirakawa and S. Ikeda, J. Polym. Sci. (Chem), 12, 11 (1974).

24. F. E. Karasz, J. C. W. Chien, R. Galkiewicz, G. E. Wnek, A. J. Heeger and A. G. MacDiarmid, Nature, 282, 286 (1979).

25. P. Kovacic and A. Kyriakis, J. Amer. Chem. Soc., 85, 454 (1963).

26. T. Yamamoto, Y. Hayashim and A. Yamamoto, Bull. Chem. Soc. Jpn. 51, 2091 (1978).

27. R. N. McDonald and T. W. Campbell, J. Amer. Chem. Soc., 82, 4669 (1960).

28. H. H. Hoerhold and J. Opfermann, Makromol. Chem., 131, 105 (1970).

29. M. Salmon, A. F. Diaz, A. J. Logan, M. Krounbi and J. Bergon, Mol. Cryst. Liq. Cryst., 83, 265 (1982).

30. G. Tourillon and F. Garnier, J. Polym. Sci. (Phys.), 22, 33 (1984).

31. Y. W. Park, M. A. Druy, C. K. Chaing, A. G. MacDiarmid, A. J. Heeger, H. Shirakawa and S. Ikeda, J. Polym. Sci. (Lett.), 17, 195 (1979).

32. H. Shirakawa and S. Ikeda, Synth. Metals, 1, 175 (1979/80).

33. W. H. Meyer, Synth. Metals, 4, 81 (1981).

34. W. H. Meyer, Mol. Cryst. Liq. Cryst., 77, 137 (1981).

35. H. Kiess, D. Bacriswyl and G. Harbeke, Mol. Cryst. Liq. Cryst., 77, 147 (1981).

36. J. C. W. Chien, F. E. Karasz, M. A. Schen and Y. Yamashita, Makromol. Chem (R. C.), 4, 5 (1983).

37. T. Woerner, A. G. MacDiarmid and A. J. Heeger, J. Polym. Sci. (Lett.), 20, 305 (1982).

38. T. Woerner, A. G. MacDiarmid, A. Feldblum and A. J. Heeger, J. Polym. Sci. (Lett.), 22, 119 (1984).

39. M. Ozaki, Y. Ikeda and T. Arakawa, J. Polym. Sci (Lett.), 21, 989 (1983).

40. M. Ozaki, Y. Ikeda and T. Arakawa, Mol. Cryst. Liq. Cryst., 117, 39 (1985).

41. J. H. Edwards and W.J. Feast, Polym. Comm., 21, 595 (1980).

42. K. Harper and P. G. James, Mol. Cryst. Liq. Cryst., 117, 55 (1985).

43. G. Leising, F. Stelzer and H. Kahlert, J. dePhysique, 44, C3-139 (1983).

44. P. Foot, P. Calvert, M. Ware and N. Billingham, Mol. Cryst. Liq. Cryst., 117, 47 (1985).

45. D. C. Bott, C. S. Brown, J. H. Edwards, W. J. Feast, D. Parker and J. N. Winter, Mol. Cryst., 117, 9 (1985).

46. K. P. J. Williams, D. L. Gerrard, D. C. Bott and C. K. Chai, Mol. Cryst. Liq. Cryst., 117, 23 (1985).

47. M. E. Horton, D. D. C. Bradley and R. H. Friend, Mol. Cryst. Liq. Cryst., 117, 51 (1985).

48. W. Ottinger, G. Leising and H. Kahert, to be published in Springer Series in Solid State Sciences, Vol. 61, 1985.

49. D. White and D. C. Bott, Polym. Comm., 25, 98 (1984).

50. G. Leising, Polym. Comm., 25, 201 (1984).

51. H. Kahlert, G. Leising, O. Leitner, R. Vitz and F. Stelzer, Proc. ICPS, San Francisco, 1984.

52. D. C. Bott, N. S. Walter, D. White, R. H. Friend and P. D. Townsend, Mol. Cryst. Liq. Cryst., 117, 95 (1985).

53. R. A. Wessling and R. G. Zimmerman, a) U. S. Pat. #3,401,152 (1968); b) U. S. Pat #3,706,677 (1972).

54. H. Kalhert and G. Leising, Mol. Cryst. Liq. Cryst., 117, 1 (1985).

55. H. H. Hoerhold and R. Bergmann, Advances in the Chemistry of Thermally Stable Polymers, Warzawa, 1977 p. 29.

56. G. E. Wnek, J. C. W. Chien, F. E. Karasz and C. P. Lillya, Polymer, 20, 1441 (1979).

57. G. E. Wnek, et al., in Conducting Polymers, R. B. Seymore (Ed.), Plenum Press, New York, 1981, p. 183.

58. K. D. Gourley, J. R. Reynolds, J. C. W. Chien, C. P. Lillya and F. E. Karasz, Proc. 26th IUPAC Macromolecular Symp., July, 1982, p. 439.

59. J. R. Reynolds, F. E. Karasz, J. C. W. Chien, K. D. Gourley and C. P. Lillya, J. dePhysique, _44_, C3-693 (1983).

60. K. D. Gourley, C. P. Lillya, J. R. Reynolds and J. C. W. Chien, Macromolecules, _17_, 1025 (1984).

61. M. Kanbe and M. Okawara, J. Polym. Sci (A-1), _6_, 1058 (1968).

62. J. D. Capistran, D. R. Gagnon, S. A. George, R. W. Lenz and F. E. Karasz, ACS Polym. Preprints _25(2)_, 282 (1984).

63. D. R. Gagnon, J. D. Capistran, F. E. Karasz and R. W. Lenz, ACS Polym. Preprints, _25(2)_, 284 (1984).

64. D. R. Gagnon, J. D. Capistran, F. E. Karasz and R. W. Lenz, Polym. Bull., _12_, 293 (1984).

65. G. Drefahl, R. Kuehmstedt, H. Oswald and H. H. Hoerhold, Die Macromol. Chemie, _131_, 89 (1970).

66. _X-ray Powder Data File_, Sets 1-10, American Society for Testing Materials, Philadelphia, PA, 1960.

67. M. Kakudo and N. Kasai, _X-ray Diffraction by Polymers_; Elsevier Publishing Co., New York, 1972.

68. B. E. Read, _Structure and Properties of Oriented Polymers_, Chpt. 4, I. M. Ware (Ed.), John Wiley & Sons, New York, 1975.

69. A. R. Stokes, Proc. Phys. Soc. (London), _A61_, 382 (1948).

70. B. E. Warren, Phys. Rev., _59_, 693 (1941).

71. A. Guthrie, _Vacuum Technology_, John Wiley & Sons, Inc., New York, 1963.

72. T. C. Clark, K. K. Kanazawa, V. Y. Lee, J. F. Rabolt, J. R. Reynolds and G. B. Street, Chemica Scripta 17, 169, (1981).

73. F. K. Harris, Electrical Measurements, John Wiley & Sons, Inc., New York, 1952.

74. J. Oesterholm and P. Passiniemi, Chem. & Eng. News, February 10, 1986, p. 2.

75. A. Olefe, Ann. Chem. Pharm., 132, 82 (1864).

76. J. Goerdeler, in Methoden der Organishen Chemie, W. Houben, (Ed.), Vol. IX, Georg Thieme Verlag, Stuttgart, 1955, pp. 175–187.

77. E. E. Reid, Chemistry of Bivalent Sulfur, Vol. I-VI, Chemical Publishing Co., New York, 1958–65.

78. C. C. Price and S. Oae, Sulfur Bonding, Ronald Press, New York, 1962.

79. B. M. Trost and L. S. Melvin, Jr., Sulfur Ylides, Emerging Synthetic Intermediates, Academic Press, London, 1975

80. J. P. Marino, in Topics in Sulfur Chemistry, Vol. I, (A. Senning, Ed.), Georg Thieme Verlag, Stuttgart, 1976, pp. 1–110.

81. C. J. M. Stirling, in Organic Chemistry of Sulfur, S. Oae, (Ed.) Plenum Press, New York, 1977, pp. 473–525.

82. P. A. Lowe, in The Chemistry of the Sulfonium Group, pt. 2, C. J. M. Stirling, (Ed.), John Wiley & Sons, New York, 1981, pp. 267–312.

83. M. J. Hatch, J. Org. Chem., 34, 2133 (1969).

84. C. R. Hauser, S. W. Kantor and W. R. Brasen, J. Amer. Chem. Soc., 75, 2660 (1953).

85. A. J. Speziale, C. C. Tung, K. W. Ratts and A. Yao, J. Amer. Chem. Soc., 87, 3460 (1965).

86. G. B. Rayne, J. Org. Chem. 32, 3351 (1967).

87. Y. Hayashi and H. Nozaki, Bull. Chem. Soc. Jpn., 45, 198 (1972).

88. D. Van Ooteghem, R. Deveux and E. J. Goethals, Int. J. Sulfur Chem., 8, 31 (1973).

89. R. A. Wessling, J. Polym. Sci. (Symp.), 72, 55 (1985).

90. C. G. Swain and E. R. Thorton, J. Amer. Chem. Soc., 83, 4033 (1961).

91. I. Rothberg and E. R. Thorton, J. Amer. Chem. Soc., 85, 1704 (1963).

92. I. Rothberg and E. R. Thorton, J. Amer. Chem. Soc., 86, 3302 (1964).

93. W. B. DeMore, H. O. Pritchard and N. Davidson, J. Amer. Chem. Soc., 81, 5874 (1959).

94. G. Holzworth, L. Soni and D. N. Schulz, Macromolecules, 19, 422 (1986).

95. R. Hosemann and S. N. Bagchi, Direct Analysis of Diffraction by Matter, North Holland Press, Amsterdam, 1962.

96. A. Blumstein, Liquid Crystalline Order in Polymers, Academic Press, New York, 1978.

97. A. Rich and F. H. C. Crick, Nature, 176, 593 (1955).

98. R. S. Bear and H. F. Ruzo, Proc. N. Y. Acad. Sci., 33, 627 (1955).

99. C. Cohen and C. C. Holmes, J. Mol. Biol., 6, 423 (1963).

100. E. D. T. Atkins, D. H. Issac, A. Keller and K. Miyasaka, J. Polym. Sci. (Phys.), 15, 211 (1977).

101. K. Suchiro, Y. Chatani and H. Tadokoro, Polymer J., 7, 352 (1975).

102. J. Blackwell and G. Gutieriez, Polymer, 63, 617 (1982).

103. E. J. Roche, T. Takahashi and E. L. Thomas, ACS Symposium Series No. 141, Fiber Diffraction Methods, American Chemical Society, 1980, p. 303.

104. J. Minter, Ph.D. Dissertation, Polymer Science and Engineering, University of Massachusetts, 1982.

105. C. J. Finder, M. G. Newton and N. L. Allinger, Acta Cryst., B30, 411 (1974).

106. B. K. Vainshtein, Diffraction of X-rays by Chain Molecules, Elsevier Press, London, 1964.

107. N. Norman, Acta Cryst., 7, 462 (1954).

108. B. E. Read and R. S. Stein, Macromolecules, 1, 116 (1968).

109. H. Shirakawa, E. J. Louis, A. G. MacDiarmid, C. K. Chaing and A. J. Heeger, J. Chem. Soc. Chem. Comm., 578 (1977).

110. C. K. Chaing, M. A. Druy, S. C. Gau, A. J. Heeger, E. J. Louis, A. G. MacDiarmid, Y. W. Park and H. Shirakawa, J. Amer. Chem. Soc. 100, 1013 (1978).

111. A. G. MacDiarmid, R. J. Mammone, R. B. Kaner and S. J. Porter, to be published.

112. I. Murase, T. Ohnishi, T. Noguchi and M. Hirooka, Polym. Comm., 25, 327 (1984).

113. Personal Conversation with T. Ohnushi, August 1985.

114. S. C. Gau, J. Milliken, A. Pron, A. G. MacDiarmid and A. J. Heeger, J. Chem. Soc. Chem. Comm., 662 (1979).

115. C. K. Chaing, C. R. Fincher, Y. W. Park, A. J. Heeger, H. Shirakawa, E. J. Louis, S. C. Gau and A. G. MacDiarmid, Phys. Rev. Lett., 39, 1098 (1977).

116. J. M. Warakomski, Ph.D. Dissertation, Polymer Science and Engineering, University of Massachusetts, 1984.

117. W. J. Weast, Ed., 60th Edition, CRC Handbook of Chemistry and Physics, CRC Press, Boca Raton, Florida, 1980, p. D-199.

118. H. D. Fritz, H. Gebauer, P. Friedrich, P. Ecker, R. Artes and U. Schubert, Z. Naturforschg., B33, 498 (1978).

119. S. L. Hsu, A. J. Signorelli, G. P. Pez and R. H. Baughman, J. Chem. Phys., 69, 106 (1978).

120. M. Monkenbusch, B. S. Morra and G. Wegner, Makromol. Chem., Rapid Comm., 3, 69 (1982).

121. K. Shimamura, F. E. Karasz, J. C. W. Chien and J. A. Hirsh, Makromol. Chem. Rapid Comm. 3, 269 (1982).

122. J. C. W. Chien, F. E. Karasz and K. Shimamura, Macromolecules, 15, 1012 (1982).

123. R. H. Geiss, G. B. Street, W. Volksen and J. Economy, IBM. J. Res. Dev., 27, 321 (1983).

124. K. Soga and M. Nakamaru, J. Chem. Soc. Chem. Comm., 1495 (1983).

125. S. I. Yaniger, M. J. Kletter and A. G. MacDiarmid, ACS Polym. Preprints, 25, 264 (1984).

126. F. E. Karasz, J. D. Capistran, D. R. Gagnon and R. W. Lenz, Mol. Cryst. Liq. Cryst., 118, 327 (1985).

127. F. Wudl, M. Kobayashi, N. Iolaneri, M. Boysel and A. J. Heeger, Mol. Cryst. Liq. Cryst., 118, 199 (1985).

128. J. H. Wood and E. Gibson, J. Amer. Chem. Soc., 71, 393 (1949).

129. R. C. Wheland and E. L. Martin, J. Org. Chem., 40, 3101 (1975).

130. H. S. Brown, C. D. Muenchausen and L. R. Sousa, J. Org. Chem., 45, 1682 (1980).

131. J. H. Golden, J. Chem. Soc. (London), 3741 (1961).

132. S. Antoun, D. R. Gagnon, F. E. Karasz and R. W. Lenz, ACS Polym. Preprints, 27(1), 116 (1986).

133. M. Haertel, G. Kossmehl, G. Manecke, W. Wille, D. Woehrle and D. Zerpner, Die Angew. Makromol. Chemie, 29/30, 307 (1973).

134. S. Antoun, D. R. Gagnon, F. E. Karasz and R. W. Lenz, Polym. Bull. 15, 181 (1986).

135. S. Antoun, D. R. Gagnon, F. E. Karasz and R. W. Lenz, J. Polym. Sci. (Lett.), in press.

136. T. Ohnushi, I. Murase, T. Noguchi and M. Hirooka, Abstracts of 30th IUPAC Symposium on Macromolecules, 440 (1985).

137. J. L. Bredas and G. B. Street, Acc. Chem. Res., 18, 309 (1985).

138. J. Obrzut and F. E. Karasz, unpublished results, 1986.

139. J. Machado and F. E. Karasz, unpublished results, 1986.

140. M. Moeller, J. Capistran and R. W. Lenz, ACS Polym. Prepr. 24(2), 342 (1983).

141. R. Stankovich and R. W. Lenz, unpublished results, 1985.

142. C. C. Han, J. Machado, F. E. Karasz and R. W. Lenz, unpublished results, 1986.

143. S. Antoun, and R. W. Lenz, unpublished results, 1985.